Ionic liquid based gel polymer electrolyte for all quasi solid state supercapacitors and lithium-ion batteries

A thesis submitted towards partial

fulfilment of the requirements for the degree of

Master of Technology in

Nano Science and Technology

Submitted by

Aritra Mukherjee

Roll No: 002230701007

Exam Roll No: M4NST24007

Registration No.: 163812 of 2022-2023

Under the guidance of

Prof. (Dr.) Kalyan Kumar Chattopadhyay
Department of Physics &
School of Materials Science and Nanotechnology
Jadavpur University

Jadavpur University

Kolkata-700032
India 2024

CERTIFICATE OF RECOMMENDATION

This is to clarify that the thesis entitled **"Ionic liquid based gel polymer electrolyte for all quasi solid state supercapacitors and lithium-ion batteries''** is a bonafide work carried out by ARITRA MUKHERJEE under our supervision and guidance for partial fulfilment of the requirement of Master of Technology (Nano Science and Technology) in School of Materials Science and Nanotechnology, during the academic session 2022-2024.

SUPERVISOR
Prof. (Dr.) Kalyan Kumar Chattopadhyay
Department of Physics
Jadavpur University, Kolkata-700032

DIRECTOR
Dr. Mahua Ghosh Chaudhuri
School of Materials Science and Nanotechnology Jadavpur University, Kolkata-700032

DEAN
Faculty Council of Interdisciplinary Studies,
Law and Management (FISLM)
Jadavpur University, Kolkata-700032

CERTIFICATE OF APPROVAL**

This forgoing thesis is hereby approved as a credible study of an engineering subject carried out and presented in a manner satisfactorily to warranty its acceptance as a prerequisite to the degree for which it has been submitted. It is understood that by this approval the undersigned do not endorse or approve any statement made or opinion expressed or conclusion drawn therein but approve the thesis only for purpose for which it has been submitted.

Committee of final examination for evaluation of thesis

** Only in case the thesis is approved.

ACKNOWLEDGEMENT

In the first place, I would like to express my profound gratitude to my supervisor **Prof (Dr). Kalyan Kumar Chattopadhyay** for his advice and guidance from the very early stage of this research as well as giving me extraordinary experiences throughout the work. Above all and the most needed, he provided me constant encouragement and support in various ways. Thank you also for the amicable environment conducive to extensive research work at Thin Film and Nanoscience Lab, in which you have welcomed me. All these provided me great support, helping me to confront the difficult periods of my project, which I do not think I would have completed it otherwise.

I want to extend my gratitude to my co-supervisor Pulak Pal for his advices, guidance, and crucial contribution throughout my work. His involvement with his originality has triggered and nurtured my scholarly development that I will benefit from, for a long time to come. I really cannot value his support and generous cooperation. He has been like an elder brother to me always by my side whenever needed him.

I would also like to express my sincere thanks to Prof. Sourav Sarkar, Prof. C.K. Ghosh, Dr. Mahua Ghosh Chowdhury for their help, support, encouragement, suggestion and advice during the course of the research. Their enthusiasm provided me a helpful and effective way of learning which in turn inspired me to follow the research project with great enthusiasm.

I would also really like to thank all the staff members of School of Materials Science and Nanotechnology and Department of Physics for carrying out the critical characterization parts of the synthesized samples that composed a very important part of the thesis.

I extend my heartiest thanks to all my seniors of 'Thin Film & Nano Science' lab especially, Abhirup, Sreya, Shuvankar, and everyone in this lab for extending their helping hands. I would also like to thank all my friends Kingshuk, Ankita, Prasanjit, for their encouragement and cooperation.

Finally, I express my special gratitude to my parents and all my well-wishers for their wholehearted support, love and encouragement.

ABSTRACT

The work described in the thesis has been conducted with an objective to develop Gel Polymer Electrolyte based Lithium-ion batteries and Supercapacitors. Extensive literature survey has been performed on this subject. We have gone through the history, basic working principle, properties and what could be the possible future of this technology. While reviewing the literature many research papers and scientific documents were examined in order to find the current status of research in the field of Gel Polymer based Lithium-ion batteries and also Electrochemical Double layer capacitors.

Li-ion batteries have been widely used in electronic devices, electrical vehicles, and large-scale charge-storage systems due to their relatively long cycling life, high energy density, low self-discharge. Lithium ions participate in the energy-storage process in Li-ion batteries. Generally, graphite materials having good anion intercalation properties and different alloy-type materials have been used, respectively, as cathodes and anodes. The Li metal has been also used as the anode material due to its high theoretical capacity and ability to provide for high energy density. Covalent organic frameworks (COFs) are used to enhance different properties of Li-ion Batteries and Supercapacitors.

Analysis and study of energy storage materials is a promising field of research for the design of electrochemical charge storage devices such as batteries and supercapacitors. It has been reported that the output power and cycling time for batteries are low, while supercapacitors provide high power density, long cycle life, superb intrinsic safety, etc. The supercapacitors store charge electrostatically or electrochemically by charge transfer mechanisms. One of the major drawbacks of supercapacitors is their low energy density. The specific capacity plays an important role in the charge storage process that depends on the electrode materials and electrolytes. The choice of proper electrolytes is essential to design supercapacitors with high energy density. Currently, ionic liquids (ILs) have received a great attention as novel electrolytes or electrolyte components due to their high ionic conductivity, nonvolatility, nonflammability, and wide range of potential stability window. The IL incorporated gel polymer electrolytes (GPEs) are suitable alternative option to replace the liquid electrolyte. Similarly, aliphatic dinitrile, has recently received great attention as a plasticizer for lithium-ion batteries and supercapacitors electrolytes due to its inexpensive cost, superior thermal stability, strong ion salvation power, high boiling point, low vapor pressure, excellent electrochemical oxidation tolerance, and specific electrochemical properties.

The above advantages open the gateway for further research in the field of Li ion batteries and Supercapacitors.

CONTENTS

CHAPTER 1: INTRODUCTION AND OBJECTIVE **PAGE NUMBER**

1.1 Preface 1
1.2 Nanotechnology and its Applications 2-3
1.3 Electrochemical Energy Storage Devices 4
1.3.1 Battery 5-10
1.3.2 Supercapacitors 10-12
1.4 Polymer Electrolytes 12-15
1.5 Polymer Matrix 16-18
1.6 Solvent 19-20
1.7 Ionic liquids 20-23
1.8 Covalent Organic Frameworks (COFs) 24-29
1.9 Objectives 30
1.10 References 31

CHAPTER 2: REVIEW OF PAST WORK

2.1 Literature review of past work 32-39
2.2 References 40

CHAPTER 3: INSTRUMENTS AND APPARATUS

3.1 Morphological Analysis
3.1.1 FESEM 42-46

3.2 Crystal Structure Analysis
3.2.1 XRD 47-50

3.3 Absorbance Spectra Analysis
3.3.1 FTIR 51

3.4 Thermal Analysis
3.4.1 Thermogravimetric Analysis (TGA) 57-58
3.4.2 Differential Scanning Calorimetry (DSC) 59-61

3.5 Electrical and Electrochemical Analysis
3.5.1 DC Conductivity 62-63
3.5.2 Electrochemical Impedance Spectroscopy (EIS) 64
3.5.3 Cyclic Voltammetry (CV) 65-67
3.5.4 Galvanostatic Charge Discharge Studies (GCD) 67-72
3.5.5 Lithium-ion transference number measurement 73-74
3.6 References 75

CHAPTER 4: SAMPLE PREPARATION AND FABRICATION

4.1 Introduction 76-77

4.2 Sample Preparation
- 4.2.1 Preparation of Electrolyte 77-83
- 4.2.2 Preparation of Electrode 84-85

4.3 Fabrication of Energy storage Devices
- 4.3.1 Electrochemical Double Layer Capacitor 86
- 4.3.2 Full cell Lithium-ion battery (CR 2032) 87-89

4.4 References 90

CHAPTER 5: CHARACTERIZATION RESULTS AND DISCUSSION

5.1 Introduction 91-93

5.2 Results and Discussion

- 5.2.1 Crystal Structure Characterization
  - XRD 94
- 5.2.2 Morphological Characterization
  - SEM 95
- 5.2.3 Thermal Characterization
  - Differential Scanning Calorimetry (DSC) 96-97
  - Thermogravimetric Analysis (TGA) 97-98
- 5.2.4 Absorbance Spectra Characterization
  - FTIR 98-99
- 5.2.5 Electrical Characterization
  - AC Conductivity and Ionic Conductivity 99-102
- 5.2.6 Electrochemical Characterization
  - Cyclic Voltammetry (CV) 103-104
  - Electrochemical potential stability window (EPSW) 107
  - Galvanostatic Charge Discharge (GCD) 108-111
  - Ragone Plot 112-113
  - Electrochemical Impedance Spectroscopy (EIS) 114-115
- 5.2.7 Functionality of Lithium-ion coin cell (CR 2032)
  - Lithium-ion transference number 116-117
  - Charge Discharge Characteristics 117-118

5.3 Bibliography 119-121

CHAPTER 6: CONCLUSIONS AND FUTURE SCOPE OF WORK

6.1 Conclusions 123

6.2 Future scope of work 124-125

LIST OF FIGURES

- Fig 1.1 Simplified representation of density of states in semi-conductor
- Fig 1.2 General Ragone Plots for supercapacitor and batteries
- Fig 1.3 Parts of Lithium-ion battery
- Fig 1.4 Lithium-ion battery during charging
- Fig 1.5 Lithium-ion battery during discharging
- Fig 1.6 Lithium classification of supercapacitors
- Fig 1.7 Classification of polymer electrolytes based on structure and components
- Fig 1.8 Commonly used polymer matrix
- Fig 1.9 3 D structure of P(VdF-HFP)
- Fig 1.10 3 D structure of PMMA
- Fig 1.11 Unit cell of semicrystalline PEO
- Fig 1.12 Structure of some commonly used solvents
- Fig 1.13 Categories of ionic liquids and their applications
- Fig 1.14 Cations and anions in ionic liquid
- Fig 1.15 Structure of EMIMTFSI ionic liquid
- Fig 1.16 Physiochemical properties of ionic liquids
- Fig 1.17 Covalent Organic Frameworks (COFs)
- Fig 1.18 Increased conductivity in 2D COF material
- Fig 3.1 Schematic of signals generated during SEM
- Fig 3.2 Schematic diagram of SEM
- Fig 3.3 Experimental setup of SEM

- Fig 3.4 Bragg's equation deduction
- Fig 3.5 Schematic of Bragg's Brentano geometry
- Fig 3.6 Schematic of Parallel Beam geometry
- Fig 3.7 Experimental setup of X-Ray Diffractometer
- Fig 3.8 Different parts of FTIR spectrometer
- Fig 3.9 Schematic diagram of FTIR spectrometer
- Fig 3.10 Electromagnetic spectrum for infrared spectroscopy
- Fig 3.11 Schematic diagram representing light source and output of interferometer
- Fig 3.12 Band deconvolution of FTIR spectrum
- Fig 3.13 Experimental setup of FTIR spectrometer
- Fig 3.14 Schematic representation of TGA setup
- Fig 3.15 Schematic representation of DSC measurement technique
- Fig 3.16 DSC curve of polymer electrolyte sample at different temperature
- Fig 3.17 Simple schematic of potentiostat
- Fig 3.18 Setup of three electrode electrochemical cell
- Fig 3.19 Cyclic voltammetry of ideal and real supercapacitor
- Fig 3.20 Charge discharge behaviour of ideal and real supercapacitor
- Fig 4.1 Host polymer used for study
- Fig 4.2 Schematic of Solution Cast technique
- Fig 4.3 GPE-1 polymer film after casting
- Fig 4.4 GPE-2 polymer film after casting
- Fig 4.5 Structure and XRD of DAAQ-TEP COF

- Fig 4.6 Structure of DAAQ monomer
- Fig 4.7 Schematic showing conduction
- Fig 4.8 GPE-3 polymer after casting
- Fig 4.9 Electrodes for EDL capacitor
- Fig 4.10 Schematic diagram of EDL capacitor
- Fig 4.11 Schematic diagram of coin cell type full cell lithium battery.
- Fig 4.12 Different components of CR2032 coin cell
- Fig 4.13 Glove box for fabrication
- Fig 5.1 XRD of pure P(VdF-HFP), GPE-1, GPE-2, GPE-3
- Fig 5.2 SEM images of GPE-1, GPE-2, GPE-3
- Fig 5.3 DSC traces of P(VdF-HFP), GPE-1, GPE-2, GPE-3
- Fig 5.4 TGA of P(VdF-HFP), GPE-1, GPE-2, GPE-3
- Fig 5.5 FTIR of P(VdF-HFP), GPE-1, GPE-2, GPE-3
- Fig 5.6 Conductivity spectra of gel polymer electrolytes
- Fig 5.7 Comparison from conductivity spectra for gel polymer electrolytes
- Fig 5.8 Ionic conductivity spectra of gel polymer electrolytes
- Fig 5.9 Temperature dependent ionic conductivity of gel polymer electrolytes
- Fig 5.10 Cyclic voltammetry of different capacitor cells
- Fig 5.11 Specific capacitance from CV
- Fig 5.12 Cyclic voltammetry at constant scan rate
- Fig 5.13 Cyclic voltammetry for EPSW for gel polymer electrolytes
- Fig 5.14 GCD characteristics of Cell-1,Cell-2,Cell-3

- Fig 5.15 Variation of specific capacitance obtained from GCD
- Fig 5.16 Ragone plots for supercapacitor cells
- Fig 5.17 Comparative GCD characteristics study of Cell-1, Cell-2, Cell-3,
- Fig 5.18 Complex impedance plots of cells at room temperature
- Fig 5.19 Variation of specific capacitance with frequency for supercapacitor cells
- Fig 5.20 Current vs time with lithium-ion transference number for GPE-2 and GPE-3
- Fig 5.21 Rate capability of lithium-ion coin cell (CR 2032)
- Fig 5.22 Cyclic performance of specific capacity and coulombic efficiency for coin cell

CHAPTER 1

INTRODUCTION AND OBJECTIVE

1.1 Preface

Energy storage systems have long been recognized for their ability to decouple energy supply from demands, an important feature that offers valuable flexibility in the choice of energy sources. Early cultures stored energy in rocks, water. More advanced forms were not practiced until Industrial Revolution. Our society has grown dependent on available clean energy and as a result ways of storing it has become more and more important.

Recently, solid-state rechargeable lithium-ion batteries (LIB) and electrochemical double layer (EDL) supercapacitors are the most workable option as alternative green energy storage devices [3]. There are some basic differences between Li^+ ion batteries and supercapacitors in their charge storage mechanism. These are as follows (i) supercapacitors do store charge through electrostatic interaction between electrode surfaces and electrolyte charge carriers, whereas Li^+ ion batteries store energy via electrochemical reactions [1], (ii) cycle life of batteries is smaller than that of supercapacitors [5] and (iii) batteries can store more energy than supercapacitors.

Polymer Electrolytes (PE) are macromolecular systems capable of transporting charged species such as ions or protons. Polymer electrolytes are fundamental key components used to prepare highly efficient electrochemical energy storage devices. When used in different energy storage/conversion devices polymer electrolytes have beneficial properties over their liquid counterpart like free from leakage, high energy density and processability. It is essential to optimize the physicochemical properties of polymer electrolytes for preparing better electrochemical energy storage/conversion devices.

Polymer Electrolytes consist of polymer matrix that allows the movement of ions while remaining solid. These materials offer advantages like flexibility, lightweight, and compatibility with various electrode materials. They are a promising avenue for improving the performance of energy storage and conversion devices.

The advantages of Polymer Electrolytes have been extensively used in fabrication of Lithium-ion batteries and Supercapacitors and comparative study was conducted.

1.2 Nanotechnology and its Applications

Nanotechnology refers to the branch of science and engineering devoted to designing, producing and using structures, devices and systems by manipulating atoms and molecules at nanoscale.

The study of extremely small objects and their usage in various scientific disciplines, including biology, physics, chemistry, and materials science, are the subjects of nanoscience and nanotechnology. The word 'Nano' means one billionth of a meter" (From the talk ***There's Plenty of Room at the Bottom***, delivered by Richard P. Feynman at the annual meeting of the American Physical Society).

The concept of nanotechnology was coined for the first time by the eminent physicist Richard Feynman in 1959 in his lecture which was published in 1960 enfranchised 'There's Plenty of Room at the Bottom' [2]. The term 'nano-technology' was first used by Norio Taniguchi in 1974 although it is not very well known to people since centuries. In 1986 inspired by Feynman's concept, K. Eric Drexler used the word 'nanotechnology' in book 'Engines of Creation: The Coming Era of Nanotechnology [3].

Nanoscience is the study of objects that typically range in size from 1 to 100 nm in at least one direction. It is possible to change the mechanical, electric, optical, and magnetic properties of matter if it is broken up into such tiny units [3]. Bulk properties would diminish and nano properties would dominate. Quantum effects due to the size limitation come into play. Nanoscience and Nanotechnology are interdisciplinary topic, crossing the boundaries between physics, chemistry, chemical, electrical, mechanical, and electronics engineering. One of the most significant developments in the previous several decades is thought to be nanoscience. Several basic Newtonian principles do not apply at the nanoscale, necessitating the development of new technologies.

Nanotechnology is thought to be the next Industrial Revolution. Due to the development of novel synthesis pathways and characterisation strategies, nanoscience and nanotechnology have rapidly advanced during the last few decades. Nanoscale structures come in many

different forms, such as nanotubes, nanowires, and nanosheets. Since they are zero dimensional structures; nanoparticles are also frequently referred to as quantum dots. It is nothing but basic physics acting behind the novel properties of the above systems and it has been well explained by quantum mechanical point of view. In order to understand these systems, it is very essential to discuss the density of states (DOS) of quantum dots (0 dimension), quantum wires (1 dimension) and quantum wells (2 dimensions) in brief. The available electron states in a system can be calculated by the well-known Schrödinger equation: $H\psi = E\psi$. Solving this we can finally get the density of states in k-space/ volume.

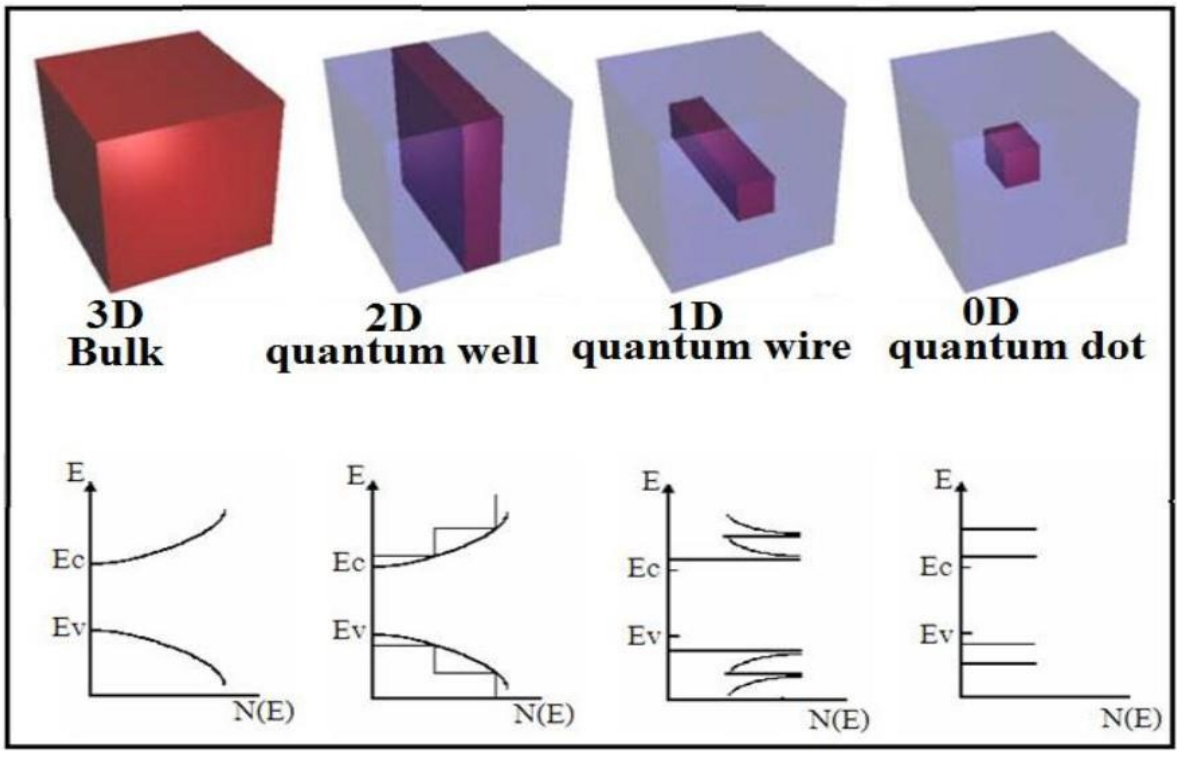


Fig. 1.1 *Simplified representation of the density of states in 3D, 2D, 1D and 0D semiconductor [1]*

.

The ability of solids to conduct current can vary greatly, and this can be shown by comparing the resistivity of good conductors and insulators. At 1K temperature, the electrical resistivity of pure metal is 10–12 ohm-cm. A good insulator has a resistance as high as 1022 ohm-cm and can range as wide as 1032 ohm-cm. Understanding this astounding range is made possible by the presence of electron band energy in materials [4].

1.3 Electrochemical Energy Storage Devices

Research on energy storage devices is a vibrant field encompassing various technologies like batteries, supercapacitors, capacitors. Scientists explore materials, designs, and mechanisms to enhance energy density, lifespan and efficiency. Investigations, include advancements in lithium-ion batteries, solid state batteries EDLC etc. For energy storage devices reactants are sealed in the container and for energy conversion devices oxidant and reductant are fed into the electrochemical cell so that a permanent flow of electricity can be achieved [5]. The rechargeable lithium-ion batteries and supercapacitors are the example of energy storage device

Requirement to study the mapping of power density as a function of energy density (Ragone plot) to gain wide perspective of these devices is essential. Fig. 1.1 [4-5]. User can achieve very high output current at very short time period by using electrochemical double layer supercapacitors. A concise discussion on the structural and working principle of these devices are required for a better understanding of their functionality.

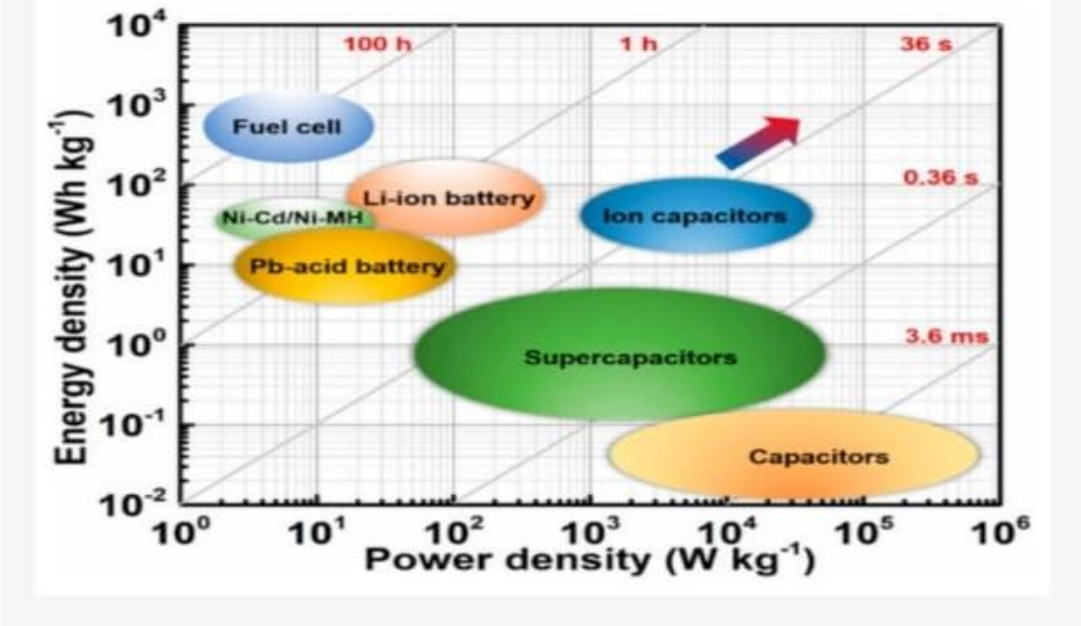


Fig. 1.2 *Ragone plot representing a comparative study of power density and energy density of different electrochemical energy storage/conversion devices [4-5].*

1.3.1 Battery

A battery is a device that stores energy and then discharges it by converting chemical energy into electricity. Typical batteries most often produce electricity by chemical means through the use of one or more electrochemical cells.[2] Many different materials can and have been used in batteries, but the common battery types are alkaline, lithium-ion, lithium-polymer, and nickel-metal hydride. Batteries can be connected to each other in a series circuit or a parallel circuit.

Primary and secondary batteries are essential components in the field of electrical engineering. Primary batteries, also known as non-rechargeable batteries, are designed for single-use applications. They generate electrical energy through chemical reactions and provide a reliable power source until the reactants are depleted. On the other hand, secondary batteries, also known as rechargeable batteries, can be reused multiple times by reversing the chemical reactions through an external power source. This enables the storage and retrieval of electrical energy, making them suitable for portable devices, electric vehicles, and renewable energy systems. Batteries can be classified into two main categories:

Primary Battery: A primary battery refers to a non-rechargeable power source that generates electrical energy through chemical reactions. It is designed for single-use applications and cannot be recharged or reused. Primary batteries typically consist of one or more electrochemical cells that convert stored chemical energy into electrical energy. Once the chemical reactants are consumed or depleted, the battery becomes inactive and cannot be used further. Common examples of primary batteries include alkaline batteries, zinc-carbon batteries. These batteries find applications in portable electronic devices, toys, flashlights, and various other devices where a long-lasting but non-rechargeable power source is required. The features of primary batteries are:

- **Non-rechargeable:** Primary batteries cannot be recharged or restored to their original energy state. Once the chemical reactants are depleted, the battery cannot be reused and must be replaced.

- **Self-contained:** Primary batteries are self-contained power sources, meaning they do not require external devices or power inputs to generate electrical energy. They rely solely on the chemical reactions within the battery itself.

- **Single-use:** Primary batteries are designed for one-time use only. They provide a finite amount of energy until the chemical reactants are fully consumed, after which they become inactive and must be discarded.
- **Long shelf life:** Primary batteries have a relatively long shelf life, meaning they can retain their energy capacity for extended periods without significant loss. This makes them suitable for storage and use in emergency situations or infrequent applications.
- **Simple maintenance:** Primary batteries do not require any maintenance or special procedures. Once the battery is depleted, it can be safely disposed of without any specific considerations.

Secondary Battery: A secondary battery refers to a rechargeable power source that can store and release electrical energy multiple times. Unlike primary batteries, secondary batteries can be recharged by applying an external electrical current that reverses the chemical reactions within the battery. This allows the battery to restore its energy capacity and be reused. Common examples of secondary batteries include lead-acid batteries, lithium-ion batteries, and nickel-metal hydride batteries. Secondary batteries are widely used in applications such as electric vehicles, portable electronics, renewable energy systems, and grid storage, where the ability to recharge and reuse the battery is essential for sustainability and cost-effectiveness. The features of secondary batteries are:

- **Rechargeable:** The primary characteristic of secondary batteries is their ability to be recharged multiple times.
- **Energy storage:** Secondary batteries are capable of storing electrical energy when they are charged.
- **Reusable:** Unlike primary batteries, secondary batteries can be used multiple times, making them a more sustainable and cost-effective choice. They can be discharged and recharged numerous times without significant loss of performance.
- **Energy density:** Secondary batteries can store more energy per unit of weight or volume, resulting in longer operating times for devices and applications.

- **Voltage stability:** Secondary batteries typically provide a stable voltage output throughout their discharge cycle. This allows them to maintain a consistent power

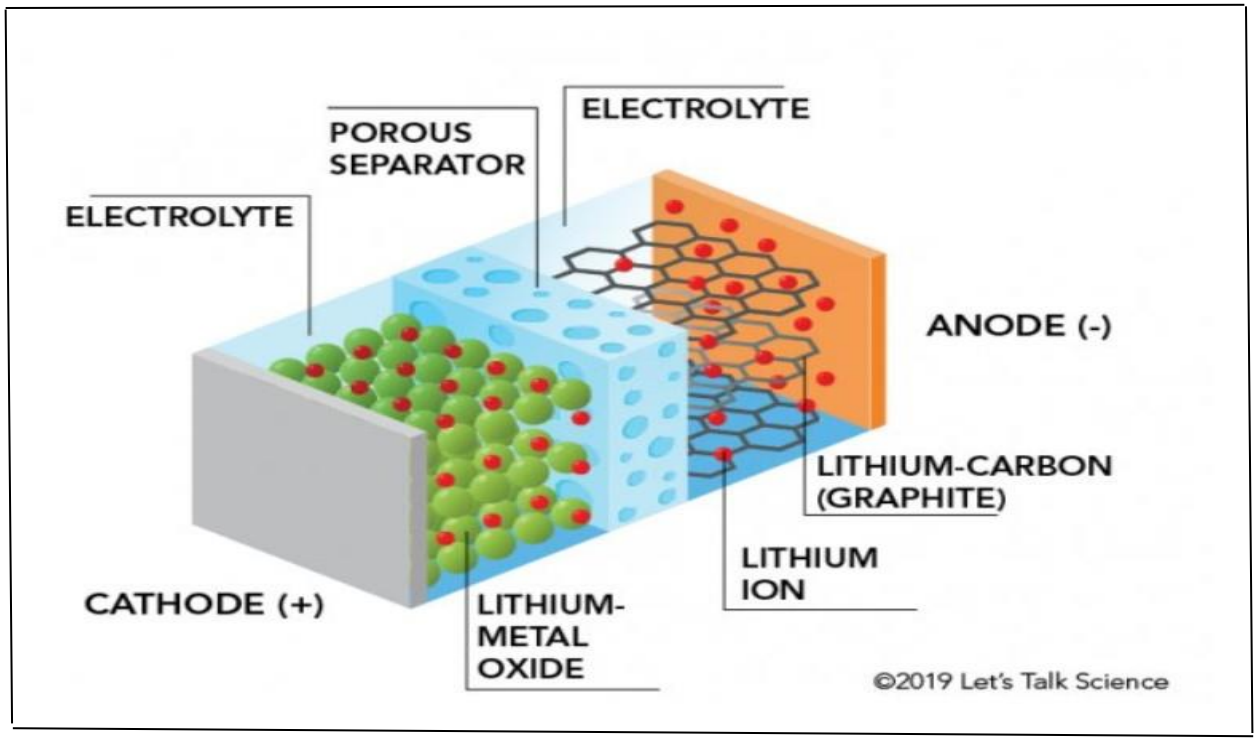


Fig. 1.3 *Parts of a Lithium-Ion Battery [5]*

The rechargeable lithium-ion battery is made of one or more power-generating compartments called cells. Each cell has essentially three components. - positive electrode, negative electrode and electrolyte. A positive electrode connects to the battery's positive or + terminal. A negative electrode connects to the negative or − terminal. and a chemical called an electrolyte in between them. In LIB, negative and positive electrodes are the reactants for electrochemical reactions and electrolyte only provides a conductive medium for transferring lithium ions from one electrode to another electrode during charge-discharge process. The electrical energy flows in to or out from the LIB due to flow of electron through an external circuit during charge or discharge processes respectively. Both electrodes can allow the movement of lithium ion (Li^+) and the process of movement of Li^+ in and out of their structures termed intercalation (insertion) and de-intercalation (extraction) respectively. During charging process of battery, Li^+ ions de-intercalate from the positive electrode (usually lithium compound) and ions diffuse through the Li^+ ion conducting electrolyte and intercalated or deposited back to the

negative electrode and in this situation electrons flow through the external circuit in the same direction. Reverse process occurs with the lithium ions and electrons which are moving back into positive electrode when the battery is discharging.

The electrolyte carries positively charged lithium ions from the anode to the cathode. The movement of the lithium ions creates free electrons in the anode which creates a charge at the positive current collector. The electrical current then flows from the current collector through a device being powered to the negative current collector. The separator blocks the flow of electrons inside the battery.

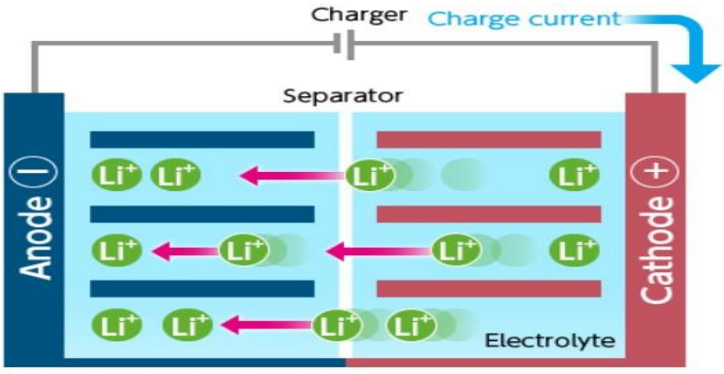


Fig. 1.4 *Lithium-Ion battery during charging*

While the battery is discharging and providing an electric current, the anode releases lithium ions to the cathode, generating a flow of electrons from one side to the other. When plugging in the device, the opposite reaction happens, the cathode releases lithium ions and anode receives them.

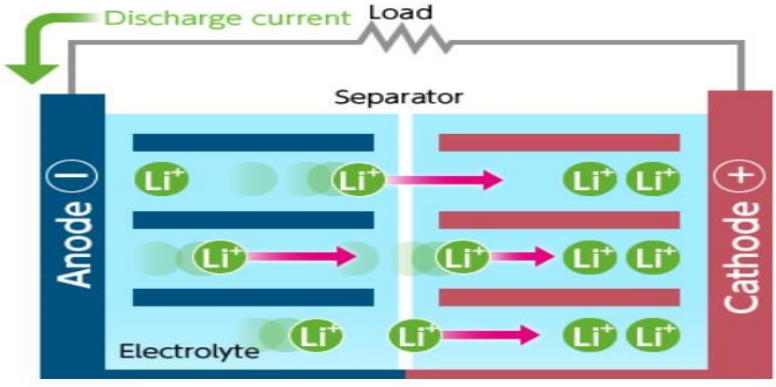


Fig. 1.5 *Lithium-Ion battery during discharging*

The following chemical reactions occur in cathode and anode. The positive electrode (cathode) half reaction in the lithium doped cobalt oxide is

$$LiCoO_2 \leftrightarrow Li_{(1-x)}CoO_2 + xLi^+ + xe^-$$

The negative electrode (anode) half reaction for graphite is

$$xLi^+ + xe^- + C_6 \leftrightarrow Li_xC_6$$

The full reaction is

$$LiCoO_2 + C_6 \leftrightarrow Li_{(1-x)}CoO_2 + Li_xC_6$$

In most commercialized lithium-ion batteries, a mixture of organic solvents based liquid electrolyte is used as a medium to promote ionic conductivity. However, liquid electrolytes create some problems such as leakage, pressure, flammability, electrode corrosion, high specific gravity, a limited temperature range of operation. Normally, a porous separator is placed in between the anode and cathode to separate both electrodes in order to prevent short-circuit. Recently, Li^+ ion conducting polymer electrolytes have received great attention of researchers over the use of its liquid counterpart which plays a critical role of both electrolyte as well as separator in rechargeable lithium-ion batteries. Some critical properties when choosing a proper polymer electrolyte in rechargeable LIB are following:

- **High ionic conductivity:** The ionic conductivity of the electrolyte at room temperature must be higher for application point of view.
- **Electrochemical stability window (ESW):** The polymer electrolyte should have a wide potential window defined by the electrode reactions.
- **Thermal stability:** The electrolyte must have good thermal stability over a wide temperature range because charge/discharge may release heat that may result in degradation.
- **Excellent mechanical stability:** Polymer electrolytes are flexible. They should be capable to compress elastically when stress is applied on them during charge/discharge and ion transport process.

- **Appreciable compatibility:** The polymer electrolyte must be chemically and electrochemically compatible with the electrode materials.
- **Good Li^+ ion transference number:** Ion transference number in polymer electrolyte should be close to unity. A high value of transference number ensures reduced polarization effect during charge-discharge process.
- **Availability:** The polymer electrolytes must be from inexpensive and readily available materials.

1.3.2 Supercapacitors

A supercapacitor (SC), also called an ultracapacitor, is a high-capacity capacitor, with a capacitance value much higher than solid-state capacitors but with lower voltage limits. It bridges the gap between electrolytic capacitors and rechargeable batteries. Supercapacitors, are emerging as an important class of energy storage devices with very high energy density and a low internal resistance, that are able to store and deliver energy at relatively high speed compared to batteries due to the energy storage mechanism which involves a simple charge separation process at the electrode-electrolyte interface.

Supercapacitors are classified into main three different classes depending on their working mechanism: (i) Electrochemical double-layer capacitors (EDLCs), (ii) Pseudo -capacitors, and

(iii) Hybrid capacitors which are shown in Fig. 1.4. All supercapacitors can be characterized by a unique working principle for charge storage which is electrostatic interaction, reversible faradic redox and a combination of the two. The EDLCs store charge through electrostatic interaction between electrode material and charge carriers of electrolyte in which the charge carriers are kept

separately at the electrode-electrolyte interface by physical process. Different carbon-based materials and their derivatives such as activated carbon, carbon nano-tubes, carbon aerogels, graphene, etc. are used as electrode materials for EDLCs [12-13].

Among different carbon materials, porous activated carbons (ACs) have received great attention due to its high specific surface area, good adsorption properties and low cost. For

pseudo capacitors, the energy is stored charge by reversible Faradic redox reactions at the surface of the active material which consists of oxidation-reduction reactions. Transition metal oxides such

RuO_2, MnO_2, V_2O_5, Fe_3O_4, heteroatoms containing covalent organic frameworks and conducting polymers have been used as pseudo capacitor electrode materials to store charge due to their high electrical conductivity and large surface area [13-14]. The third one is hybrid capacitor; the charge storage mechanism is a combination of electrostatic interaction and Faradic. The carbon and metal oxide based composite material is used as an electrode material. The electrode materials of all classes of supercapacitor are summarized in Fig. 1.4.

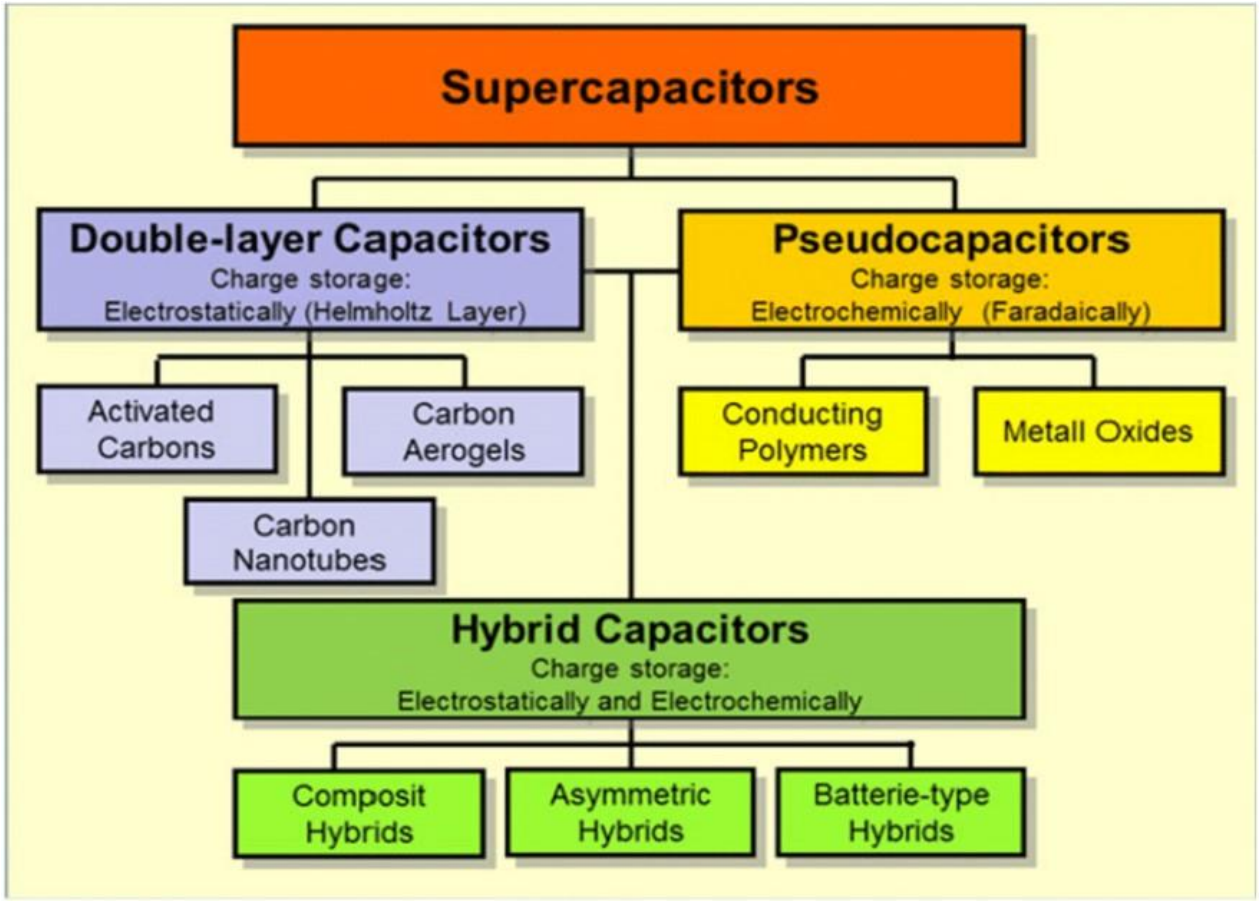


Fig. 1.6 *Hierarchical classification of supercapacitors. (Source: Wikimedia)*

Electrostatic Double Layer Capacitors: These types of capacitors include two electrodes, a separator, and an electrolyte. The electrolyte is the mixture that constitutes positive and negative ions dissolved in water. The two electrodes are separated by a separator. These

supercapacitors use carbon electrodes or derivatives with much higher electrostatic double-layer capacitance. The separation of charge in electrostatic double-layer capacitors is less than in a conventional capacitor; it ranges from 0.3–0.8 nm.

Pseudo Capacitors These are also referred to as electrochemical pseudo-capacitors. These capacitors make use of metal oxide or conducting polymer electrodes with a high amount of electrochemical pseudo capacitance. These types of components store electrical energy by electron charge transfer between electrode and electrolyte. This can be done by a reduction-oxidation reaction commonly known as a redox reaction.

Hybrid Capacitors: These are developed by using the techniques of double-layer capacitors and pseudo-capacitors. In these components, electrodes with different characteristics are used. One electrode with the capacity to display electrostatic capacitance, and the other electrode with electrochemical capacitance. Examples of hybrid capacitors: the lithium-ion capacitor.

1.4 Polymer Electrolytes

Polymer electrolytes (PEs) comprising the polar polymer complexed with ionic salts are important because of their use in different electrochemical devices such as solid-state batteries, fuel cells, supercapacitors, electrochromic devices, smart windows, and sensors. PEs are generally preferred due to some of their special properties such as good electrode–electrolyte contact, ease of preparation, high conductivity, good mechanical stability, wide range of composition, and hence wider control of properties. The conductivity of PEs is quite small, which restricts their use in potential applications. The conductivity of the PEs is increased by incorporating suitable plasticizers in them, but the mechanical properties are relatively poor. The plasticizers have high dielectric constant, low viscosity, low freezing point, and high boiling point. The mechanical properties of PEs are improved by adding simultaneous plasticizer as well as inert insulating matrix and the electrolytes obtained are known as nanocomposite PEs. Nanocomposite PEs show high ionic conductivity (10^{-1}–10^{-4} S/cm), low activation energy, and good mechanical and thermal stability. In this chapter, the synthesis and characterization of proton-conducting nanocomposite PEs are discussed. High ionic conductivity and good mechanical and thermal stability of

nanocomposite PEs suggest that these electrolytes are desirable for their use in electrochemical devices. The emphasis is to be given on lithium ion conducting polymer electrolytes based on the diverse and significant field of application in electrochemical devices such as rechargeable lithium-ion batteries, supercapacitors, etc. as discussed in earlier section and this material also plays cardinal role as a building block of the devices.

However, it is also important to mention that liquid electrolytes are highly conductive and also good interface between electrolyte and electrode material but the main disadvantages are leakage due to flow of the liquids, low energy and power density. The crystalline super ionic conductors and glass electrolytes are hard and fragile but it is difficult to maintain good solid electrolyte interface with intercalating electrodes during cycling as volume of the electrode changes.

Based on the structure and constituent components, polymer electrolytes can be divided into following categories:

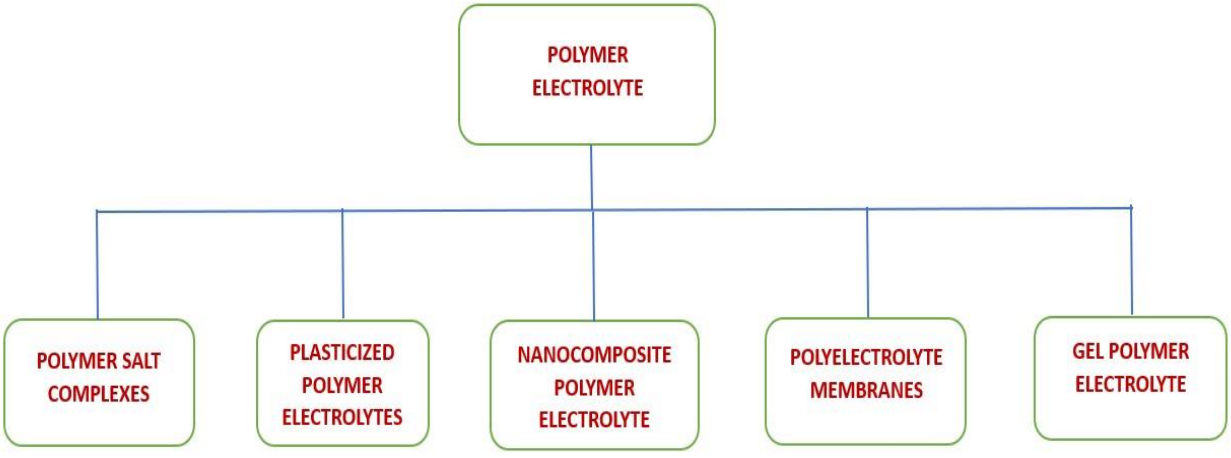


Fig. 1.7 *Classification of Polymer Electrolyte based on structure and components*

Polymer salt complexes: These types of polymer electrolytes are prepared dissolving salts of alkali metals having low dissociation energy into a high molecular weight host polymer matrix. The room temperature ionic conductivity of polymer salt complex (PSC) is generally low.

Plasticized polymer electrolytes: Organic carbonate such as ethylene carbonate, propylene carbonate, etc. or glycol-based liquid having low molecular weight or ionic liquids (ILs) are added to conventional polymer salt complex to prepare this type of polymer electrolyte. Ionic liquids are salt in liquid state. In polymer electrolytes, ionic liquids play the critical role of a plasticizer as well as a supplier of extra source of free charge carriers for electric conduction.

Nano-composite polymer electrolytes: Nano-particles having high surface area are added to conventional polymer salt complexes to prepare this type of polymer electrolyte. This type of polymer electrolyte shows excellent mechanical stability, high ionic conductivity.

Polyelectrolyte membranes: Polymers are in general neutral and in solution they do not undergo dissociation, but there exist some polymers which have own charged functional groups covalently bound to the polymer backbone. The polyelectrolyte is polymeric single ion conductor where the polymer backbone is charged. They released negative or positive ions when dissolved in a proper solvent and the polymer backbone also negatively or positively charged. From application point of view, the negative backbone-based electrolytes are favoured.

Gel polymer electrolytes: These are liquid electrolytes trapped in a physical structure of a neutral polymer matrix. Gel polymer electrolytes show solid like properties when characterized macroscopically and liquid like properties when characterized microscopically.

Gel polymer electrolytes (GPEs) are one of the important classes of ionic materials for application point of view. In general, GPEs are obtained by trapping of liquid electrolytes into host polymer matrix which provides liquid electrolyte like ionic conductivity and solid like dimensional stability. Thus, this makes the GPEs advantageous over liquid and solid electrolytes. Low ionic conductivity for solid polymer electrolytes and evaporation and leakage problem for liquid electrolytes are main drawbacks for realistic application. However, GPEs overcome these problems. Basically, gel polymer electrolytes consist of host polymer matrix, solvents (plasticizers) and salts. The host polymer matrices should have essential properties like polar in nature, low glass transition, highly amorphous, etc.

The essential characteristics of the salts are soluble in chosen plasticizers, presence of large anion group, low dissociation energy, etc. The solvents (plasticizers) should have the following essential properties:

- high dielectric constant enhances the level of salt dissociation,
- low viscosity which leads to high ionic mobility,
- high boiling point which is essential to avoid the solvent evaporation from the polymer electrolyte within the set temperature range.
- low freezing point which prevents the fast turn down of conductivity at low temperature
- presence of chemically active dipoles such as carbonyl group –C=O which induces high polarity.

Apart from these above essential properties, other essential properties of the plasticizers are thermal and electrochemical stability, good chemical compatibility towards both electrodes and good plasticizing effect of the plasticizers (solvents). These gel polymer electrolytes possess ionic conductivity greater than 10-3 S/cm and fast charge transfer occurs at electrode interface. A number of thermoplastic polymer matrices such as poly (methyl methacrylate) (PMMA), poly(acrylonitrile) (PAN), poly (vinylidene fluoride) (PVdF), poly (vinylidene fluoride-co-hexafluoropropylene (PVdF-HFP) etc. are projected as a framework for GPEs. Several salts such as NH_4BF_4, NH_4PF_6, NH_4SCN, $LiPF_6$, $LiBF_4$, $LiCF_3SO_3$, $LiN(CF_3SO_2)_2$ and acid like salts such as H_3PO_4, HCF_3SO_3, aromatic/ aliphatic carboxylic acid etc. are used for ion conduction in gel polymer electrolytes. Several solvents (plasticizers) are used such as EC, PC, DMC, PEG, etc. Recently, plastic crystalline succinonitrile (SN) is used as solid solvent or plasticizer in gel polymer electrolytes to increase the ionic mobility. The SN plasticizer exhibits high dielectric constant of about ~ 55 at room temperature due to its polar character which dissociate salts easily However, recently ionic liquids have received a great attention for the preparation of gel polymer electrolytes due to their unique properties The copolymer P(VdF-HFP) and large amount of different ionic liquids-based gel polymer electrolytes are used in several electrochemical devices such as rechargeable batteries, dye-sensitized solar cells, electric double layer supercapacitors.

From the above-mentioned different types of polymer electrolytes, gel polymer electrolytes and plasticized polymer electrolytes show excellent room temperature ionic conductivity

with reduced mechanical stability. On the other hand, polymer salt complex, nano-composite electrolytes and polyelectrolyte membranes show good mechanical stability with moderate ionic conductivity.

1.5 Polymer Matrix

Polymer matrix is a macromolecule composed of many repeated identical subunits linked by covalent bonds. The subunit forming the rhythmic pattern is called a "monomer". 1-D polymers structure shows different properties from those that have either a 2-D or 3-D structure, and these differences come from how the atoms and chains are linked together in space. Properties of polymer matrices also depend on chemical composition, molecular weight and morphology.

Polymers are studied in the fields of polymer science (which includes polymer chemistry and polymer physics), biophysics and materials science and engineering. Historically, products arising from the linkage of repeating units by covalent chemical bonds have been the primary focus of polymer science. An emerging important area now focuses on supramolecular polymers formed by non-covalent links. Polymers, both natural and synthetic, are created via polymerization of many small molecules, known as monomers. Their consequently large molecular mass, relative to small molecule compounds, produces unique physical properties including toughness, high elasticity, viscoelasticity, and a tendency to form amorphous and semicrystalline structures rather than crystals. A host polymer matrix should have following features to obtain an efficient polymer electrolyte:

- Atoms or groups of atoms present in the host polymer matrix must have

  sufficient electron donor power to form coordinate bonds with cations.
- Polymer matrix should have high molecular weight and low crystalline phase.
- Low barriers to bond relation so that segmental motion of the polymer chain can occur
- A suitable distance between the coordinating centres.

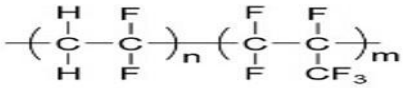
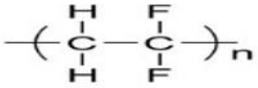
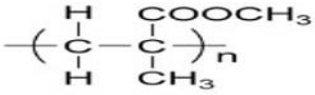
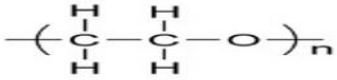
Molecular Formula	Polymer Matrix
	**P(VdF-HFP)** Poly (vinylidene-fluoride- hexafluoropropylene)
	**PVdF** Poly(vinylidene-fluoride)
	**PMMA** Poly (methyl methacrylate)
	**PEO** Poly (ethylene oxide)

Fig. 1.8 *Commonly used Polymer Matrix and their molecular formula*

Poly(vinylidene-fluoride-hexafluoropropylene), P(VdF-HFP):

P(VdF-HFP) is a semi-crystalline copolymer which recently gained attention for polymer electrolytes. It consists of crystalline part poly (vinylidene fluoride) P(VDF) and amorphous part poly(hexafluoropropylene) P(HFP) units. The mechanical stability of this copolymer is mainly attributed to the P(VDF) part, while P(HFP) part provides the amorphous phase which traps the liquid electrolytes and promotes the ionic conduction process [24]. This polymer matrix is suitable as a host material for gel polymer electrolytes because it has enough liquid uptake power with good mechanical stability. Moreover, P(VdF-HFP) can be the right host to solvate more salts due to its high dielectric constant.

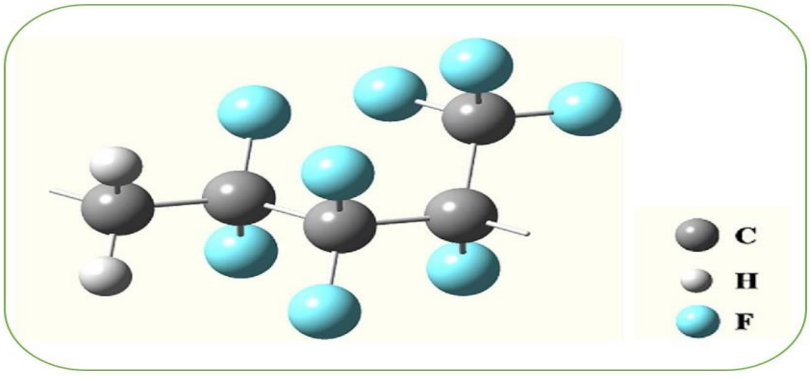


Fig. 1.9 *3D structure of P(VdF-HFP)*

Poly (methyl methacrylate), PMMA:

Poly (methyl methacrylate), more often known as acrylic or acrylic glass, is a commonly used low-cost thermoplastic polymer with boundless applications to everyday life. According to Lewis concept, PMMA is recognized to be a basic polymer, or an electron donor. The presence of ester functional groups, with the carbonyl oxygen atom (C=O) being a basic site, is the reason why PMMA exhibits electron donor ability. PMMA is colourless, transparent, has an excellent life period, and good chemical stability. PMMA itself is amorphous by nature i.e. random arrangement of the asymmetrical carbon atom.

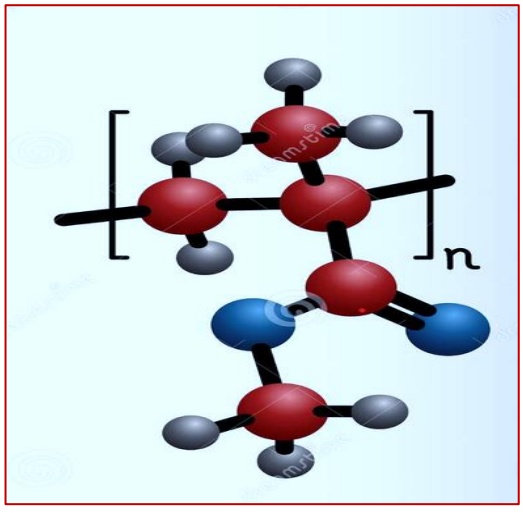


***Fig. 1.10** 3D structure of PMMA*

Poly (ethylene oxide), PEO:

PEO is a linear polymer chain. The monomer of ethylene oxide is an epoxide ring. The monomer forms a chain having the repeat unit of $-CH_2-CH_2-O-$. Fig. 1.8 shows a representation of segment of PEO polymer matrix which shows that crystalline PEO has an extended helical structure with a 1.93 nm repeat unit consisting of seven $-CH_2-CH_2-O-$ units in two turns of the helix i.e. forms 7/2 helix structure. PEO is a semi-crystalline material at ambient condition. PEO has very good solvating properties for a wide variety of salts, due to the interaction of its ether oxygen with cations. Though, PEO can dissolve a broad range of salts, the attention has focused mainly on a small size of lithium and sodium salts specially the lithium salts that form polymer electrolytes of potential application in lithium polymer batteries.

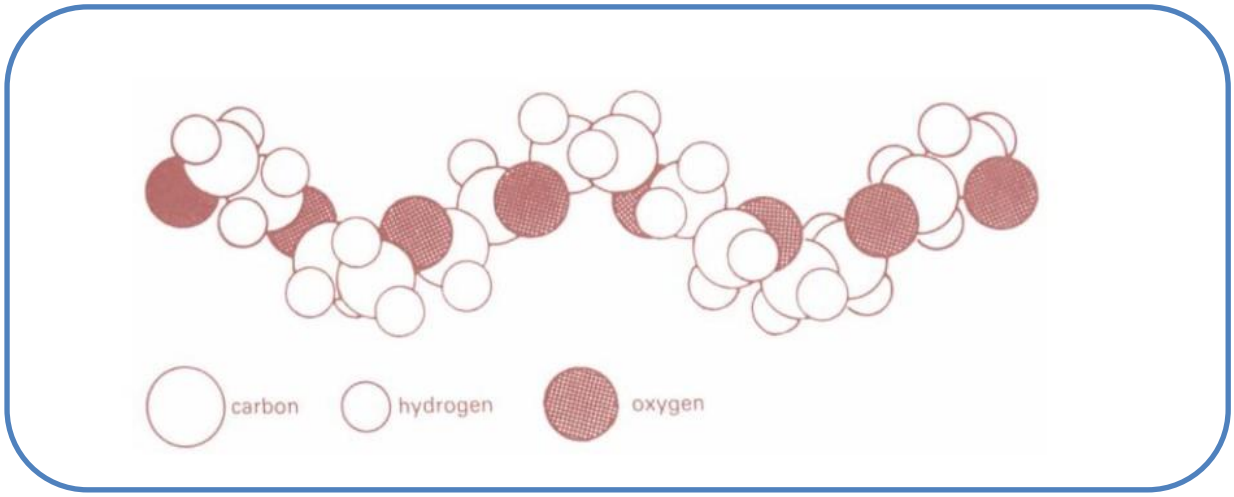


Fig. 1.11 *Unit Cell of a semi-crystalline PEO (Source- MTI Corporation)*

1.6 Solvent

A solvent is a liquid which dissolves both polymer matrix as well as salt, resulting in a solution. The solvent should be miscible with the plasticizers and ionic liquids. Commonly used solvents are organic solvents such as acetonitrile (ACN), tetrahydrofuran (THF), acetone, chloroform, toluene, N, N-Dimethyl methanamide (DMF), N-Methyl-2 pyrrolidone (NMP), etc. Solvents depend on the host polymer matrix. The acido-basic character of solvent seems to have an influence and can be an interesting parameter for the choice of a solvent system, in addition to and the solubility parameters. An acidic solvent can interact with basic sites.

These interactions allow a greater mobility of the macromolecular segments, explaining the important plasticizing effect. For example, toluene is a basic solvent and weakly interacts with PMMA chains. The plasticizing effect is low. The residual solvent molecules are trapped inside the cast films due to the nature of the solvent which can have some undesirable ageing properties on the practical properties of the films. Though solvent have a low boiling point and evaporate easily but vacuum dry is needed to remove the residual solvent.

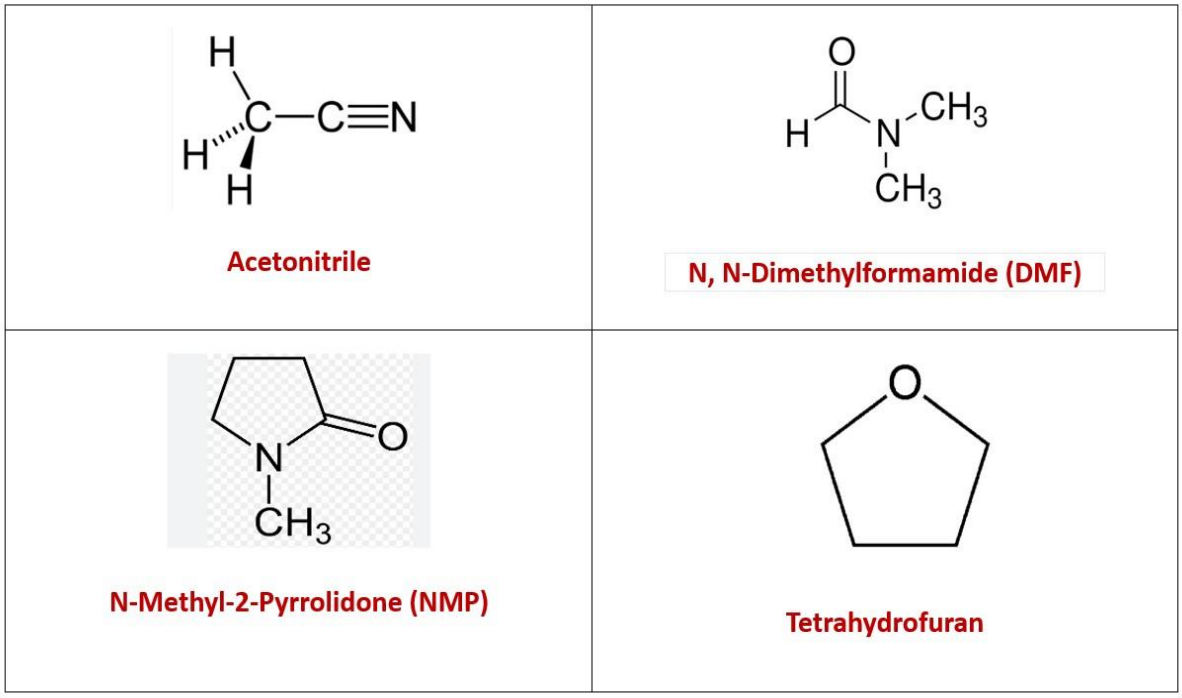


Fig. 1.12 *Structure of some commonly used solvents.*

1.7 Ionic Liquids

Ionic liquids (ILs) are organic salts that are generally liquid below 100 °C. ILs have very low vapor pressure and are non-flammable, making these liquids an environmentally friendly alternative to organic solvents. The physicochemical properties of ILs can be tuned extensively through modification of the cation and anion comprising the liquid. This tunability has led to the utilization of ILs in a variety of task-specific applications. Understanding the underlying molecular interactions responsible for the fascinating properties of ILs is essential for advancing the design of these liquids. Nuclear magnetic resonance (NMR) has been used as an efficient characterization tool of organic compounds for several decades and it is the most powerful technique to help researchers understand the structure and dynamics of ILs. There are a variety of NMR techniques available, including multinuclear, multidimensional, nuclear Overhauser effects (NOEs), relaxation times, and self-diffusion measurements, to thoroughly investigate ILs.

Most recently, ionic liquids (ILs) have received an exponential interest from most of the researchers as novel electrolyte materials or electrolyte components for better electrochemical performance. At room temperature, ILs are molten salts typically consisting of bulky, asymmetric organic cations and inorganic anions. But there are some differences between ionic liquid and inorganic salt. Actually, inorganic salts which require solvation by a solvent to dissociate into an ion pair. ILs do not require salvation and exit as completely dissociated ion pairs in the liquid state at room temperature. Introduction of ionic liquid in the polymer matrix is most promising technique to enhance the physicochemical and electrochemical properties of the polymer electrolytes. Generally, ILs have several excellent properties which make them potential candidates for good electrochemical performances in electrochemical devices including bioscience, biomechanics, electrodeposition the physicochemical properties of ILs can be highly tunable due to their large variety of combination of cations and anions and thus, ILs are regarded as "designer solvents" [107]. But there are some main drawbacks of most ILs, such as high viscosity, low ionic conductivity and high cost which can limit their practical application in electrochemical devices.

Based on their composition, ILs can be basically classified as aprotic, protic and zwitterionic types. ILs used for electrolytes represents only a very tiny part of the bulky family of ILs**.**

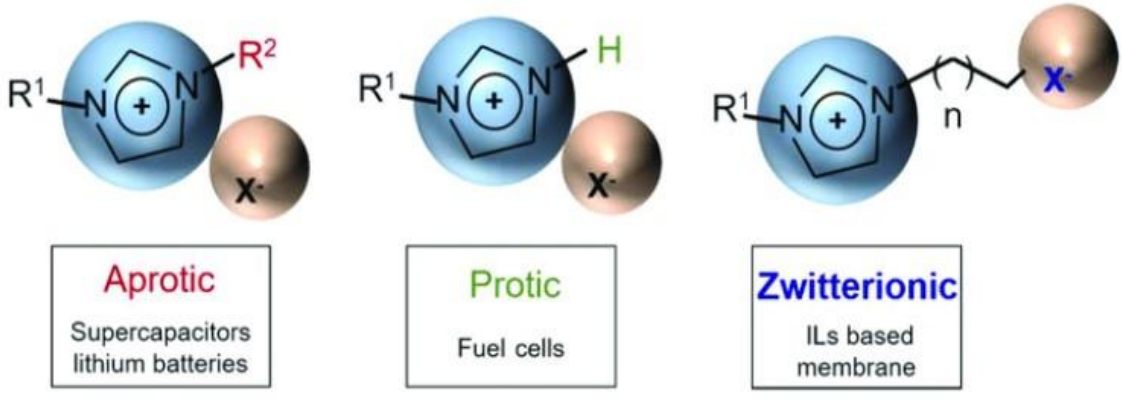


Fig. 1.13 *Categories of Ionic Liquids and their Applications. [7]*

ILs are usually based on several cations such as imidazolium, pyrrolidinium, ammonium, sulfonium, phosphonium cations. ILs also contain several characteristic anions such as tetrafluoroborate (BF^{4-}), hexafluorophosphate (PF^{6-}), bis(fluorosulfonyl)imide (FSI^-), bis(trifluoromethanesulfonic)imide ($TFSI^-$)

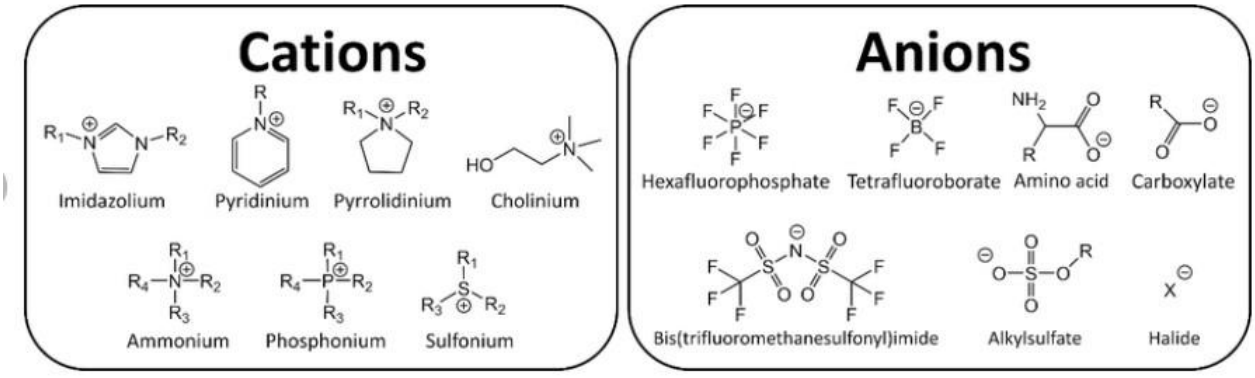


Fig. 1.14 *Cations and Anions in Ionic Liquids*

It has been observed that the imidazolium-based ILs can offer higher ionic conductivity while the pyrrolidinium based ILs have wide electrochemical stability window (ESW). ILs based on cations such as imidazolium, pyrrolidinium, piperidinium and quaternary ammonium have been given importance for battery/supercapacitor applications. The electrochemical performance of supercapacitors is also thought to be related to viscosity and ion size of ILs [98-99]. In most cases, it has been observed that the solubility of Li-salt in the ILs having the same anion is much higher than those systems with different anions [15]. The introduction of ILs into polymer matrix decreases glass transition temperature and melting temperature of host polymer matrix. The supplementary anions provided by ILs may act as coordinating bridges for Li^+ cations between the polymer backbone chains. Their electrostatic interactions with Li^+ cations, even as solvent-separated ion-pairs, may also hinder the formation of crystalline polymer-salt phase. The addition of ILs in the polymer matrix plays a critical role of both plasticizers as well as additional source of free ions for conduction. But the anions provided by ILs also assist Li^+ ions to be freed partially or fully by interacting with the coordination between Li^+ ions and group of host polymer matrix and thus a larger number of charge carriers are produced with improved charge transportation.

Some of merits associated with the use of ILs for fabricating EES devices are as follows: (a) the characteristic properties of IL, includes thermal stability, ionic conductivity, and negligible vapor pressure certainly matches with the industrial requirements; (b) the low volatility and better electrochemical stability of ILs makes them ideal choice as electrolytes for LIBs and SCs; (c) improved energy density and capacity maintenance, hence making it is the key material for large-scale energy storage systems; and (d) the excellent unique feature of ILs, observed from most of the literature, is its capability to operate at elevated temperatures, which makes them the promising candidates for applications in portable electronic devices and hybrid electric vehicles. Along with the polymer host, ILs can be used to formulate solid and gel electrolytes; hence, it would be a capable material for many applications, like flexible electronics, batteries, wearable, fuel cells, bendable SCs etc.

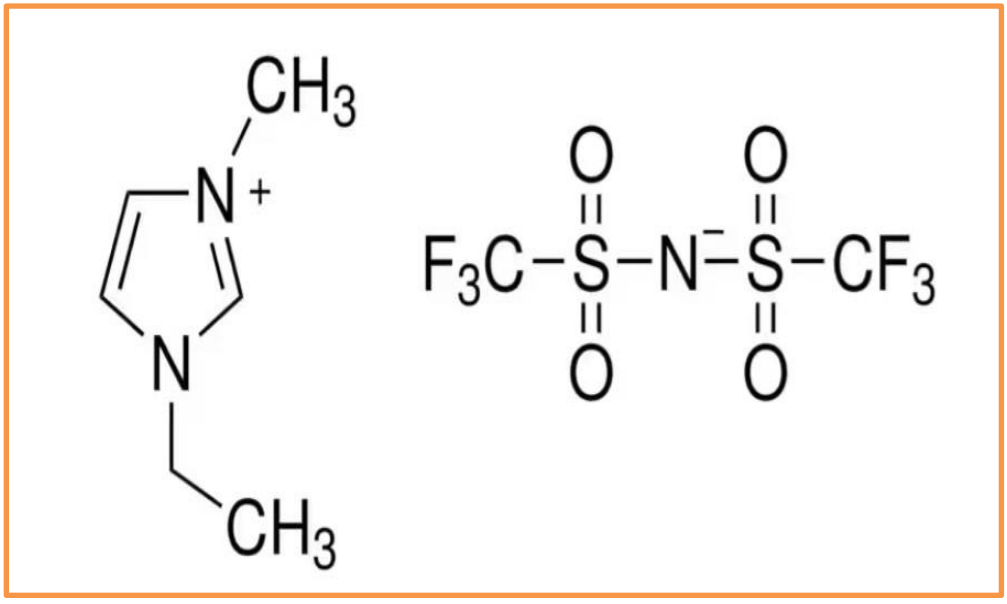


Fig. 1.15 *Structure of EMIMTFSI Ionic Liquid (Source- Sigma Aldrich)*

Table 1.16 *Physiochemical properties of ionic liquids*

Ionic Liquids	T_g (°C)	T_m (°C)	ρ (g/cm^3)	η (cP)	σ_{dc} (mS/cm)	ESW (V)
BMIMTFSI	-87	-3	1.43	40	4.6	4.1
$BMIMBF_4$	-83	…	1.20	75	4.5	6.1
$EMIMBF_4$	-94	15	1.29	42	15.4	4.3
BMIMTf	-82	17	1.29	64	3.6	…
$BMIMPF_6$	-77	10	1.37	182	1.9	3.7
$BDMIMBF_4$	-68	37	1.19	243	1.2	4.6
BMPTFSI	-83	15	1.39	60	3.4	5.7
PMIMTFSI	…	…	…	40	7.4	…
EMIMTFSI	-87	16	1.28	…	…	4.3

1.8 Covalent Organic Frameworks (COFs)

Covalent organic frameworks (COFs) are a class of porous polymers that form two- or three-dimensional structures through reactions between organic precursors resulting in strong, covalent bonds to afford porous, stable, and crystalline materials. COFs emerged as a field from the overarching domain of organic materials as researchers optimized both synthetic control and precursor selection.[1] These improvements to coordination chemistry enabled non-porous and amorphous organic materials such as organic polymers to advance into the construction of porous, crystalline materials with rigid structures that granted exceptional material stability in a wide range of solvents and conditions.[1][2] Through the development of reticular chemistry, precise synthetic control was achieved and resulted in ordered, nano-porous structures with highly preferential structural orientation and properties which could be synergistically enhanced and amplified.[3] With judicious selection of COF secondary building units (SBUs), or precursors, the final structure could be predetermined, and modified with exceptional control enabling fine-tuning of emergent properties.[4] This level of control facilitates the COF material

Covalent organic frameworks (COFs) are a class of crystalline porous organic polymers with permanent porosity and highly ordered structures. Unlike other polymers, a significant feature of COFs is that they are structurally predesignable, synthetically controlled and functionally manageable. In principle the topological design diagram offers geometric guidance for the structural tiling of extended porous polygons and the polycondensation reactions provide synthetic ways to construct the predesigned primary and high order structures. Progress over the past decade in the chemistry of these two aspects undoubtedly established the base of the COF field. By virtue of the availability of organic units and the diversity of topologies and linkages COFs have emerged as a new field of organic materials that offer a powerful molecular platform for complex structural design and tailor made functional development.

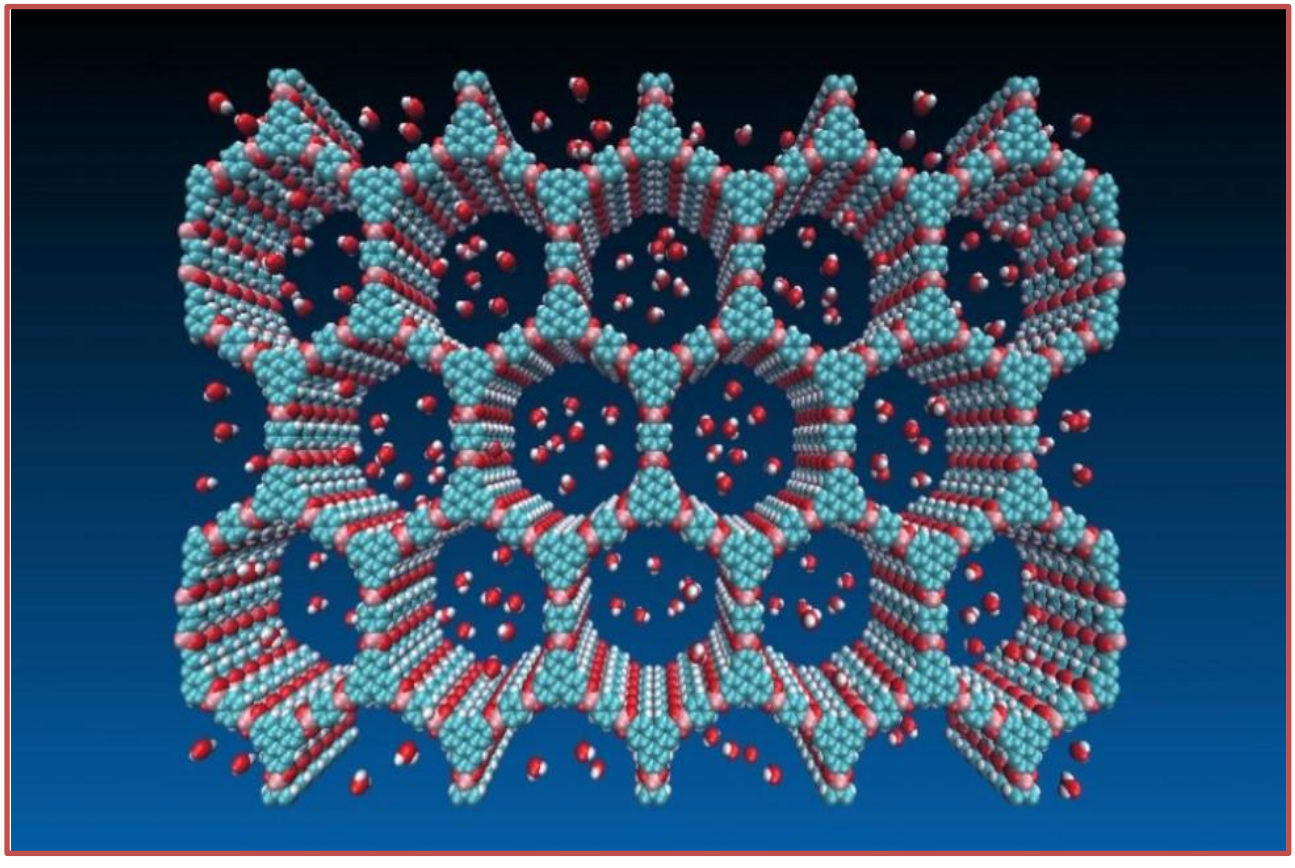


Fig. 1.17 *Covalent Organic Frameworks (COFs) (Source – Royal Society of Chemistry)*

Porous crystalline solids consist of secondary building units (SBUs) which assemble to form a periodic and porous framework. An almost infinite number of frameworks can be formed through various SBU combinations leading to unique material properties for applications in separations, storage, and heterogeneous catalysis.[7]

Types of porous crystalline solids include zeolites, metal-organic frameworks (MOFs), and covalent organic frameworks (COFs). Zeolites are microporous, aluminosilicate minerals commonly used as commercial adsorbents. MOFs are a class of porous polymeric material, consisting of metal ions linked together by organic bridging ligands and are a new development on the interface between molecular coordination chemistry and materials science.[8]

COFs are another class of porous polymeric materials, consisting of porous, crystalline, covalent bonds that usually have rigid structures, exceptional thermal stabilities (to temperatures up to 600 °C), are stable in water and low densities. They exhibit permanent porosity with specific surface areas surpassing those of well-known zeolites and porous silicates.[5]

Reticular synthesis was used by Yaghi and coworkers in 2005 to construct the first two COFs reported in the literature: COF-1, using a dehydration reaction of benzenediboronic acid (BDBA), and COF-5, via a condensation reaction between hexahydroxytriphenylene (HHTP) and BDBA.[18] These framework scaffolds were interconnected through the formation of boroxine and boronate linkages, respectively, using solvothermal synthetic methods.[18]

Boron condensation

The most popular COF synthesis route is a boron condensation reaction which is a molecular dehydration reaction between boronic acids. In case of COF-1, three boronic acid molecules converge to form a planar six-membered B_3O_3 (boroxine) ring with the elimination of three water molecules.[5]

Reversible reactions for COF formation featuring nitrogen to form a variety of linkages (imine, hydrazone, azine, squaraine, phenazine, imide, triazine).

Triazine based trimerization

Formation of CTF-1 COF featuring triazine linkages. Another class of high performance polymer frameworks with regular porosity and high surface area is based on triazine materials which can be achieved by dynamic trimerization reaction of simple,

Another class of high performance polymer frameworks with regular porosity and high surface area is based on triazine materials which can be achieved by dynamic trimerization reaction of simple, cheap, and abundant aromatic nitriles in ionothermal conditions (molten zinc chloride at high temperature (400 °C)). CTF-1 is a good example of this chemistry.[22]

Imine condensation

A structural representation of the TpOMe-DAQ COF Reversible reactions for COF formation featuring a variety of atoms to form different linkages (a double stage connecting boronate ester and imine linkages, alkene, silicate, nitroso).

The imine condensation reaction which eliminates water (exemplified by reacting aniline with benzaldehyde using an acid catalyst) can be used as a synthetic route to reach a new class of COFs. The 3D COF called COF-300[23] and the 2D COF named TpOMe-DAQ[24] are good examples of this chemistry. When 1,3,5-triformylphloroglucinol (TFP) is used as one of the SBUs, two complementary tautomerizations occur (an enol to keto and an imine to enamine) which result in a β-ketoenamine moiety[25] as depicted in the DAAQ-TFP[26] framework. Both DAAQ-TFP and TpOMe-DAQ COFs are stable in acidic aqueous conditions and contain the redox active linker 2,6-diaminoanthroquinone which enables these materials to reversibly store and release electrons within a characteristic potential window.[24][26] Consequently, both of these COFs have been investigated as electrode materials for potential use in supercapacitors.[24][26]

A structural representation of the DAAQ-TFP COF

Solvothermal synthesis

The solvothermal approach is the most common used in the literature but typically requires long reaction times due to the insolubility of the organic SBUs in nonorganic media and the time necessary to reach thermodynamic COF products.[27]

Templated synthesis

Morphological control on the nanoscale is still limited as COFs lack synthetic control in higher dimensions due to the lack of dynamic chemistry during synthesis. To date, researchers have attempted to establish better control through different synthetic methods such as solvothermal synthesis, interface-assisted synthesis, solid templation as well as seeded growth[28][29] First one of the precursors is deposited onto the solid support followed by the introduction of the second precursor in vapor form. This results in the deposition of the COF as a thin film on the solid support.[30]

Some of the properties of COFs are summarized as under:

Porosity

A defining advantage of COFs is the exceptional porosity that results from the substitution of analogous SBUs of varying sizes. Pore sizes range from 7-23 Å and feature a diverse range of shapes and dimensionalities that remain stable during the evacuation of solvent.[14]

Crystallinity

There are several COF single crystals synthesized to date.[32] There are a variety of techniques employed to improve crystallinity of COFs. The use of modulators, monofunctional version of precursors, serve to slow the COF formation to allow for more favourable balance between kinetic and thermodynamic control, hereby enabling crystalline growth.

Conductivity

Integration of SBUs into a covalent framework result in the synergistic emergence of conductivities much greater than the monomeric values. The nature of the SBUs can improve conductivity. Through the use of highly conjugated linkers throughout the COF scaffold, the material can be engineered to be fully conjugated, enabling high charge carrier density as well as through- and in-plane charge transport.

Applications of COFs may be listed as under:

- Energy Storage
- Hydrogen Storage
- Methane Storage
- Gas Separation
- Carbon Capture
- Electrocatalysis
- Pharmaceutical Drug Delivery
- Water Filtration

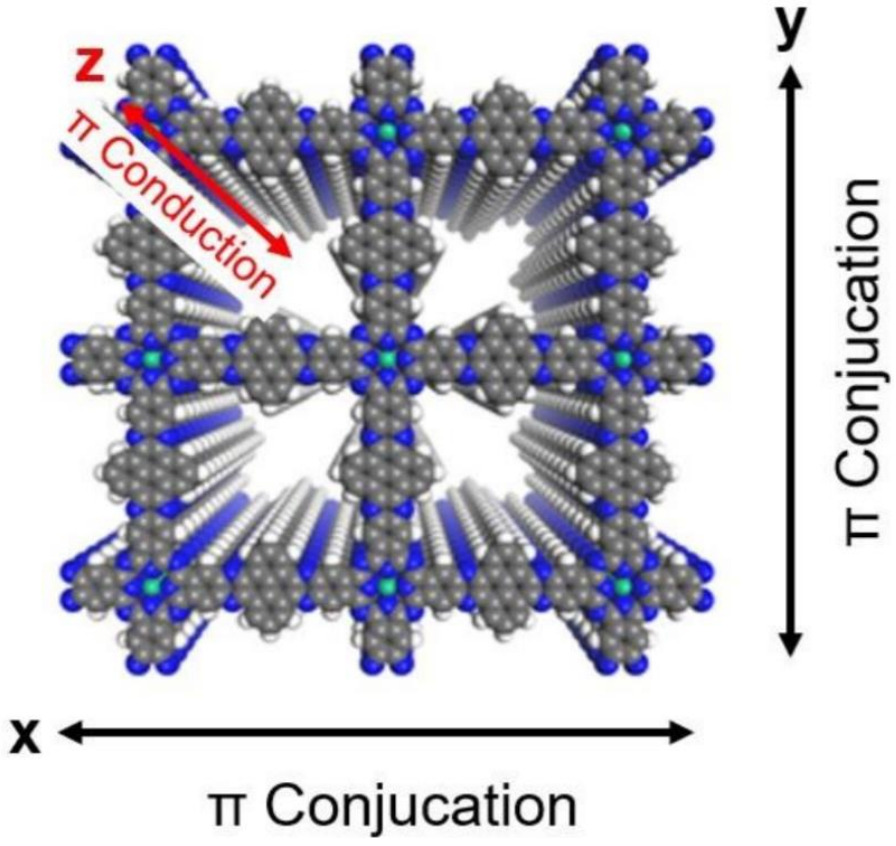


Fig .1.18 *Increased conductivity in 2D COF material [6]*

scanning electron microscope (SEM), and transmission electron microscopy (TEM) can resolve surface structure and morphology, and microstructural information, respectively.[36] Scanning tunnelling microscope (STM) and atomic force microscopy (AFM) have also been used to characterize COF microstructural information as well.[36] Additionally, methods like X-ray photoelectron spectroscopy (XPS), inductively coupled plasma mass spectrometry (ICP-MS), and combustion analysis can be used to identify elemental composition and ratios.[36]

1.9 Objectives

The prime objectives of this thesis are to prepare Energy storage devices which includes Supercapacitors and Lithium-ion battery and also to study various structural, morphological, electrochemical, electrical properties of the material.

Our specific objectives of the thesis are as follows:

1. To Fabricate Gel Polymer Electrolyte based Lithium-ion battery and Supercapacitors.

2. Preparation of Gel Polymer Electrolyte using different redox additives and using P(VDF+HFP) as host polymer matrix.

3. Preparation of Electrode for fabrication process.

4. Characterization of the synthesized samples by different sophisticated techniques like X-ray diffraction (XRD), Field emission scanning electron microscope (FESEM), Fourier transform infrared spectroscopy (FTIR), Thermogravimetric Analysis (TGA), Differential Scanning Calorimetry (DSC), Cyclic Voltammetry (CV),Galvanostatic Charge Discharge Analysis(GCD), Calculating Specific Capacitance, Calculating Li ion transport number and also to make a comparative study of performance of different samples made for fabricating the energy storage devices.

5. The final objective of this thesis is to fabricate an energy storage device having enhanced electrical properties using different materials which will pave the way for overcoming the present constraints of energy storage devices (Supercapacitors and Li-ion batteries)

References:

[1]. P. Pal and A. Ghosh, “Dynamics and relaxation of charge carriers in poly (methyl methacrylate)-based polymer electrolytes embedded with ionic liquid,” Phys. Rev. E 92 (6), 062603 (2015).

[2]. P. Pal and A. Ghosh, “Dynamics and relaxation of charge carriers in poly (methyl methacrylate)-lithium salt-based polymer electrolytes plasticized with ethylene carbonate,” J. Appl. Phys. 120, 045108 (2016).

[3]. P. Pal and A. Ghosh, “Investigation of ionic Conductivity and relaxation in plasticized PMMA-LiClO4 solid polymer electrolytes,” Solid State Ionics 319, 117-124 (2018).

[4] R. P. Feynman, A lecture in engineering science, In California Institute of Technology. edition. 1960.

[5] Drexler, K. Eric. Engines of creation. Anchor, 1986.

[6] R. G. Gordon, MRS Bull. 25 (2000) 52.

[7] P. Motiarty, Rep. Prog. Phys. 64 (2001) 297.

[8] Kuo-Feng Lin, Hsin-Ming Cheng, Hsu-Cheng Hsu, Li-Jiaun Lin, Wen-Feng Hsieh, Chemical Physics Letters 409 (2005) 208–211

[9] K. Aryal, B. N. Pantha, J. Li, J. Y. Lin, and H. X. Jiang, Applied Physics Letters 96,052110 (2010)

[10] Ryu Abe, Kazuhiro Sayama, and Hideki Sugihara, J. Phys. Chem. B 2005, 109, 16052- 16061

[11] O. Vigil, F. Cruz, A. Morales-Acevedo, G. Contreras-Puente, Materials Chemistry and Physics 68 (2001) 249–252

CHAPTER 2

REVIEW OF PAST WORKS

An electrochemical double layer capacitor, commonly known as a supercapacitor or ultracapacitor, is a type of energy storage device that stores electrical charge through the formation of an electrochemical double layer at the interface between an electrolyte and high surface area electrodes. Unlike conventional capacitors that store energy through dielectric polarization, supercapacitors store energy through the accumulation of ions at the electrode-electrolyte interface, forming an electrochemical double layer. A lithium-ion coin cell is a type of small, coin-shaped lithium-ion battery. These batteries are commonly used in various portable electronic devices, such as watches, calculators, memory backup circuits, and remote controls. They are known for their high energy density, long cycle life, and low self-discharge rate compared to other types of small batteries. For the current study extensive review of published works were studied which gave a direction to carry out the present research in the field of gel polymer electrolyte and subsequent fabrication of gel polymer-based supercapacitors and CR2032 lithium-ion coin cell.

Electrochemical double-layer capacitors (EDLCs) that are flexible and solid-state with a non-liquid electrolyte. Nonetheless, the preparation of gel polymer electrolyte (GPE) remains a formidable problem. Both having good mechanical properties and a high ionic conductivity. This work presents a straightforward and innovative technique to enhance the mechanical characteristics and conductivity of GPE film for use as an electrolyte and separator in EDLC. Ionic liquid (IL) is cross-linked with poly (ethylene oxide) (PEO) and benzophenone (Bp) to create the GPE film, which is then exposed to ultraviolet (UV) light. GPE is then absorbed using a non-woven cellulose separator (FPC). The electrolyte film with n = 10 and the flexible EDLC worked along with inexpensive active carbon by adjusting the mass ratio (n) between IL and PEO.

For lithium-ion batteries, ionic gel electrolyte (IGE) is regarded as a promising next-generation safe electrolyte (LIB). Here, the high ionic liquid loading filler (DAAC-TEP--COF), a stable crystalline porous material that provides a rapid ion channel to boost ionic conductivity for enhanced LMB performance, was applied to the polymeric ionic liquid/ionic liquid (PIL/IL)-based IGE. At 30°C, the composite PIL/IL-based IGE with DAAC-TEP--COF has an ionic conductivity of 0.28 mS cm−1, which is approximately 2.2 times greater than the PIL/IL-based IGE without COF. At 60°C, it reaches 1.26 mS cm−1. The larger IL concentration in the

composite IGE with DAAC-TEP-COF, the disruption of ILs' Coulombic ordering, and the quicker diffusion of IL anions in the composite IGE are all responsible for the increased ionic conductivity.

Supercapacitors' high-power density and extended cycle life make them an increasingly appealing option for usage in electric vehicles and electronics [1-3]. The most popular materials for supercapacitors are carbon-based materials due to their high surface area, superior conductivity, extended cycle life, and affordable price. Double-layer capacitance is the basis of carbon material energy storage mechanisms. Surface functions mostly involving quinone, hydroxyl, and carbonyl groups produce a pseudocapacitive contribution of fast Faradaic reactions, all of which might enhance the capacitive qualities [4–8]. Nevertheless, the application's exposure to the detrimental effects of these functionalities' instability with cycling is restricted [9, 10]. Another alternative method used to promote the energy storage for carbon materials is introducing redox additives or redox active electrolytes. Many inorganic cationic redox couples such as Fe^{3+}/ Fe^{2+} [11], VO^{3+}/ VO^{3+} [12] and Cu2+/Cu0 [13,14].

Poly (vinylidene fluoride-co-hexafluoropropylene) P(VdF–HFP) copolymer matrix, based on which succinonitrile (SN) plastic crystal plasticizer, lithium trifluromethanesulfonate (LiOTf) salt, and 1-butyl-1-methylpyrrolidinium trifluromethanesulfonate ionic liquid, we have synthesized highly conducting and electrochemically stable solid like ionogels with solid like properties. It is found that the ionogels' ionic conductivity is increased when SN is present. The composition with the maximum ionic conductivity (∼12.18 mS cm–1) and Li+-ion transference number (∼31%) is P(VdF–HFP) with a ratio of 40:40:20 (w/w/w) and 0.5 M LiOTf (ionogel-3). In trials involving lithium plating and stripping at various current densities, Ionogel-3 has demonstrated long-term stability performance and enhanced electrochemical compatibility with electrodes at 30 °C. At current densities of C/3, C/5, and 150 mAh g–1, the Li-ion battery made using ionogel-3 has demonstrated exceptional specific discharge capabilities.

High energy density supercapacitors (SCs) employing activated carbon (AC) electrodes and gel polymer electrolytes (GPEs) based on dual redox additives. Poly (vinylidene fluoride-co-hexafluoropropylene) was used as the host polymer in the preparation of the GPEs. Adiponitrile

was utilized as a plasticizer, 1-ethyl-3-methylimidazolium bis(trifluoromethylsulfonyl)imide was used as an ionic liquid (IL), and dual redox additives included diphenylamine (DPA) and copper iodide (CuI). The microstructural analyses demonstrated that the amorphous character of the host polymer matrix was improved by plasticizers, ILs, and redox additives. Up to about 200 °C, the GPEs remained thermally stable. For the dual redox additive-based GPE-IL + DPA + CuI, the electrical conductivity at ambient temperature and the electrochemical potential window are 3.3 × 10–3 S cm–1 and 6.4 V, respectively. How well the dual redox-fabricated SCs performed electrochemically

Ion transport, utilizing broadband dielectric spectroscopy and segmental dynamics in solid polymer electrolytes based on poly (ethylene oxide) (PEO) and sodium tetrafluoroborate salt as a function of PEO polymer matrix molecular weight at a given salt concentration (EO/Na = 18). The PEO polymer matrix was found to have a molecular weight (Mv) ranging from 1 × 105 to 6 × 105 g/mol. The complex impedance plot yielded the ionic conductivity of the PEO-based electrolytes, which was correlated with the ion diffusion coefficient, crystallinity, and glass transition temperature. The universal power law model was utilized to investigate the AC conductivity spectra, with the exception of the low frequency region, where the electrode polarization contribution predominated. There was a correlation between the segmental dynamics of polymer chains and ion transport, as evidenced by the Vogel-Tammann-Fulcher (VTF) connection being followed by the temperature dependence of ionic conductivity and the hopping frequency. The derivative dielectric constant spectra were used to study the segmental dynamics. The Kohlrausch-Williams-Watts and Havriliak-Negami functions provided a good description of the modulus spectra. The conductivity relaxation time's temperature dependency was likewise in line with the VTF connection. Higher molecular weight PEO-based polymer electrolytes were discovered to have more cooperative ion transport than other polymer electrolytes.

Ion transport and segmental dynamics have been investigated in cross-linked poly (ethylene glycol) diacrylate-based solid-like polymer electrolytes containing 1-ethyl-3-methylimidazolium tetrafluoroborate ($EMIMBF_4$) ionic liquid and lithium tetrafluoroborate ($LiBF_4$) lithium salt using broadband dielectric spectroscopy. The conductivity spectra at different temperatures have been analysed using the power law model coupled with the

Poisson–Nernst–Planck model to account for the electrode polarization effect dominating the low frequency region of the spectra. It is observed that the temperature dependence of the ionic conductivity, hopping frequency, and ion diffusivity follows the Vogel–Tammann–Fulcher (VTF) relation. The dielectric relaxation data have been also analysed in terms of electric modulus and derivative dielectric spectra. The temperature dependence of segmental relaxation time and conductivity relaxation time obtained from the derivative dielectric loss spectra and modulus loss spectra, respectively, obeys the VTF relation. A strong coupling between the segmental relaxation of polymer chains and the ionic transport in the cross-linked polymer electrolytes has been observed. The scaling of the conductivity spectra and the modulus loss spectra indicates that the ion transport in these cross-linked polymer systems obeys the time–temperature superposition principle.

Copolymers poly(ionic liquid) (PIL), poly(triphenyl-4-vinylbenzylphosphonium chloride) and a series of its random copolymers with non-ionic hydrophobic poly(methyl methacrylate) (PMMA) are synthesized by conventional free radical polymerization (CFRP) and reversible addition-fragmentation chain-transfer (RAFT) polymerization. The understanding of some fundamental aspects about ion transport and relaxation mechanism in PIL and PIL copolymers are investigated using dielectric spectroscopy via several theoretical models. The influence of copolymer compositions, physical blending of neat PIL and PMMA, size of counter anions (Cl^- and $TFSI^-$) and variation of molecular weights on thermal stability, moisture sensitivity, ionic transport and relaxation properties are also studied. An enhancement of thermal stability and ionic transport property of the PIL copolymer is observed compared to those of the physically mixed blend of two homopolymers with same compositions. The incorporation of hydrophobic PMMA segment definitely decreases the moisture content in PIL copolymers than the PIL itself. In all these PIL- based systems, the temperature dependence of ionic conductivity, relaxation time and ion diffusivity are well described by Vogel-Tammann-Fulcher model. The studies of some fundamental properties of these new PIL copolymers with less moisture sensitivity may help in using them as potential polymer electrolytes in energy storage devices.

Lithium-ion batteries (LIBs) play significant roles in our modern life because of their significant intrinsic merits, such as their high capacity, low density, very low redox potential of the lithium metal, etc.[1–7] Among the different components of LIBs, the electrolytes are more crucial for the development of advanced LIBs with high specific capacity and energy density.[7–10] Generally, organic liquid electrolytes are used in traditional LIBs. These liquid electrolytes create serious problems such as leakage, flammability, explosiveness, etc. Moreover, the growth of lithium dendrites on lithium metal electrodes produces dead lithium and builds an unstable solid electrolyte interface (SEI). In addition, a short circuit may happen, affecting directly the cycle life and safety of the LIBs.[11,12] Recently, solid-state ionogels (IGs) are considered more promising and new alternative candidates than liquid electrolytes to address these issues. IGs are composed of an inorganic host network and an ionic liquid electrolyte (ILE) containing ionic liquids (ILs) and lithium salts.[13–18] In IGs, the major part is ILE, and IGs display the main properties of ILE except outflow.[17,19–21] Basically, ionic liquids are molten salts at ambient conditions and typically consist of an asymmetric organic cation such as imidazolium and an inorganic anion.[22,23] Recently, ILs have been considered promising, novel, and safe electrolytes for LMBs due to their suitable basic properties, such as high ionic conductivity, a wide electrochemical potential stability window, etc.[24,25] Generally, poly(vinylidene fluoride-*co*-hexafluoropropylene) [P(VdF-HFP)], poly(methyl methacrylate) (PMMA), and poly(ethylene oxide) (PEO) are used as common host polymer matrices to prepare IGs.[26] The cross-linked IGs synthesized via UV-photo or thermal polymerization technique have received great attention due to their flexibility, leakage proof, high thermal stability, high ionic conductivity at room temperature, wide potential stability window, high lithium–ion transference number (>0.5), blocking of lithium dendrite formation, etc.[2,27–31] Recently, studies of ion transport mechanisms in ionogels have also received great attention for fundamental research. Generally, ion transport in polymer electrolytes occurs via ionic hopping and segmental motion of polymer chains in the amorphous region of the polymer matrix.[32] Impedance or dielectric spectroscopy has been widely used to study the controlling parameters (ionic conductivity, segmental motion, etc.) for ion transport.[33] in some work have prepared cross-linked ionogels films based on poly(ethylene glycol) diacrylate (PEGDA) and ILE via thermal polymerization for the fabrication of LMBs. The synthesized ionogels showed superior electrolyte parameters such as flexibility, thermal stability, ionic conductivity, a

potential stability window, a lithium–ion transference number, and the stability of the SEI. The temperature dependence of the ionic conductivity obtained from the complex impedance plot followed the VTF relationship. We have also studied the performance of the LMBs, fabricated with this ionogels as an electrolyte at different current rates and rate capabilities.

Since all-solid-state supercapacitors (ASSCs) can prevent some issues such electrolyte leakage that can occur in liquid electrolyte-based supercapacitors, more attention has been paid to their design. But ASSCs have a lower specific energy, which is typically closely related to the used electrolyte's extremely low ionic conductivity. A redox-active ionic liquid-based ionogels electrolyte (IGE) comprising carbon nanotubes (CNTs), poly (vinylidene fluoride-co-hexafluoropropylene) (PVDF-HFP), and 1-butyl-3-methylimidazolium iodide (BMIMI) IL was prepared by solution-casting in order to produce high-specific-energy ASSCs with superior performance. The greatest ionic conductivity of 17.6 mS cm^1 is presented by the PVDF-HFP/BMIMI/CNTs IGE that is obtained by optimizing the mass ratios of BMIMI/PVDF-HFP and CNTs/PVDF-HFP. A PVDF-HFP/BMIMI/CNTs IGE and two identical activated carbon electrodes form a sandwiched ASSC was fabricated later.

Redox additives of VOSO4 and Na2MoO4 were respectively added into two polyvinyl alcohol (PVA)eH2SO4 gels to form two gel polymer electrolytes (GPEs). These two redox-active GPEs were separated by a Nafion 117 membrane and assembled with a pair of activated carbon electrodes to construct quasi-solid-state supercapacitors, in which PVAeH2SO4eVOSO4 and PVAeH2SO4eNa2MoO4 GPEs worked on the sides of the negative and positive electrodes of the supercapacitor, respectively. Cyclic voltammetry, galvanostatic charge discharge and electrochemical impedance spectroscopy techniques were used to evaluate the electrochemical performances of the supercapacitor with optimized PVAeH2SO4 eVOSO4 and PVAeH2SO4eNa2MoO4 GPEs. After the introduction of VOSO4 and Na2MoO4, the specific capacitance and energy density of the supercapacitor with PVAeH2SO4eVOSO4 jPVAeH2SO4eNa2MoO4 GPEs can reach 543.4 F g_1 and 17.9 Wh kg_1, respectively, which are about four times those of the supercapacitor with a PVAeH2SO4 GPE. The enhanced energy storage is attributed to the reversible Faradaic reactions related to VOSO4 and Na2MoO4 in the corresponding gel polymer electrolytes. In addition, the supercapacitor shows good cyclic durability.

Ionic liquid gel polymer electrolytes (GPE) possess advantages of high ionic conductivity, outstanding safety and high compatibility with electrodes. However, the ionic liquid plasticizers in GPE for elevating the ionic conductivity will decrease the mechanical strength of GPE. Polymerized ionic liquids (PIL) combine the properties of polymer and ionic liquids, so the application of them possesses several superiorities beyond ionic liquids. In this research, one PIL poly(1-[2-(2-(2-(Methacryloyloxy)ethoxy)ethoxy)ethyl]-3-methylimidazolium bis(trifluoromethylsulfonyl)imide)-co-poly(poly(ethylene glycol) methyl ether methacrylate) is synthesized and blended with host polymer PVDF, ionic liquid (1-butyl-1-methylimidazolium bis(trifluoromethylsulfonyl)imide, [BMIM]TFSI) and lithium salt LiTFSI to prepare PIL gel electrolyte (PIL-GPE@IL) membrane applying in lithium battery. Besides the moderate mechanical strength, the PIL-GPE@IL combined with ionic liquid display a high ion conductivity of at 30 ◦C and outstanding electrochemical stability with an oxidation potential of 4.26 V vs. Li+/Li. Furthermore, the Li/LiFePO4 cells assembled with the PIL-GPE@IL show excellent rate performance and cycle performance, which exhibit an initial specific discharge capacity of approximate 143 mAh g ¯1 at current density of 0.5C accompanied by an excellent capacity retention of 97% within 120 cycles. This work demonstrates the capability of the as-prepared PIL-GPE@IL using in lithium batteries to boost the performance.

Flexible supercapacitor is an important energy supply source for wearable electronic devices. Here, a novel dual redox-mediated double network (DN) gel polymer electrolyte (GPE) is effectively used to build an integrated supercapacitor with outstanding electrochemical performance. The remarkable mechanical properties and quick self-healing ability of the polyacrylic acid/lauryl methacrylate/sodium carboxymethyl GPE are attributed to the combined action of the DN structure and several physical interactions, including hydrophobic association, hydrogen bonding, and ionic coordination. CuSO4_FeSO4 can act as carrier donors and anti-freezing agents in addition to being ionic cross-linking agents. This gives the GPE exceptional conductivity (0.17 S/cm) and low temperature adaptation. Benefiting from Cu2+/Cu+ redox processes, the GPE-based integrated supercapacitor exhibits an exceptional specific capacitance of 414.96 mF/cm2 and a high energy density of 84.21 μWh/cm2.

References:

[1] Grafting modification of poly (vinylidene fluoride-hexafluoropropylene) *via* Cu(0) mediated controlled radical polymerization By Yingdong Duan , Qizheng Li , Biyun Peng , Shaobo Tan , Zhicheng Zhang.

[2] Self-healable, mechanically durable and cold-resistant integrated supercapacitor enabled by dual metallic redox-mediated multiple cross-linking gel polymer electrolyte By Yongcun Liu, Wenye Zhang, Xiaoxiang Su, Wenjie He, Jia Yang, Gang Qin, Xiang Yu, Qiang Chen.

[3] Highly ion conductive cross-linked ionogels for all-quasi-solid-state lithium-metal batteries. By P.Pal, Ashwini Ghosh

[4] Improving the energy density of quasi-solid-state supercapacitors by assembling two redox-active gel electrolytes. By Le-Qing Fan, Ji Zhong, Can-Yang Zhang, Ji-Huai Wu, Yue-Lin Wei

[5] Improved redox-active ionic liquid-based ionogels electrolyte by introducing carbon nanotubes for application in all-solid-state supercapacitors Le-Qing Fan, Qiu-Mei Tu, Cheng-Long Geng, Yong-Lan Wang, Si-Jia Sun, Yun-Fang Huang, Ji-Huai Wu.

[6] Ion transport and relaxation in phosphonium poly (ionic liquid) homo- and co-polymers Palash Banerjee, Pulak Pal, Aswini Ghosh, Tarun K. Mandal

[7] Preparation of imidazolium based polymerized ionic liquids gel polymer electrolytes for high-performance lithium batteries Huizhe Niu, Minling Ding, Nan Zhang, Xin Li, Xiangyu Su, Xin Han, Nan Zhang, Ping Guan, Xiaoling Hu

[8] Robust Succinonitrile Plastic Crystal-Based Ionogels for All-Solid-State Li-Ion and Dual-Ion Batteries. By Pulak Pal, Aswini Ghosh

CHAPTER 3

INSTRUMENTS AND APPARATUS

3.1 Morphological Analysis

The morphological analysis for the samples prepared for this thesis has been done with FESEM.

3.1.1 Field Emission Scanning Electron Microscope (FESEM)

A FESEM is an electron microscope which uses electron beam liberated by field emission source instead of light. Field emission scanning electron microscopy (FESEM) is an advanced technology used to capture the microstructure image of the materials. FESEM is typically performed in a high vacuum because gas molecules tend to disturb the electron beam and the emitted secondary and backscattered electrons used for imaging.

Image formation in the SEM depends on the signals produced from the electron beam and specimen interactions. These interactions can be classified into two major categories: elastic interactions and inelastic interactions. Elastic scattering results from the deflection of the incident electron by the atomic nucleus or outer shell electrons of the specimen. This kind of interaction is characterized by very small amount of energy loss during the collision and by a wide-angle directional change of the scattered electron. Incident electrons that are elastically scattered through an angle of more than 90° are called backscattered electrons (BSE), and produce a useful signal for imaging the sample. Inelastic scattering occurs through a variety of interactions between the incident electrons and the electrons and atoms of the sample and results in the primary beam electron transferring considerable amount of energy to that atom. The most widely used signal produced by the interaction of the primary electron beam with the specimen is the secondary electron emission signal.

When the primary beam strikes the sample surface causing the ionization of specimen atoms, loosely bound electrons may be emitted and these are referred to as secondary electrons. As they have low energy, typically an average of around 3–5 eV, they can only escape from a region within a few nanometres of the material surface. These can be used to give information about the surface topography, morphology of the sample with good resolution.

In addition to these signals, a number of other signals are produced when an electron beam strikes a sample, including the emission of continuous x-rays, characteristic x-rays, auger electrons and cathodoluminescence.

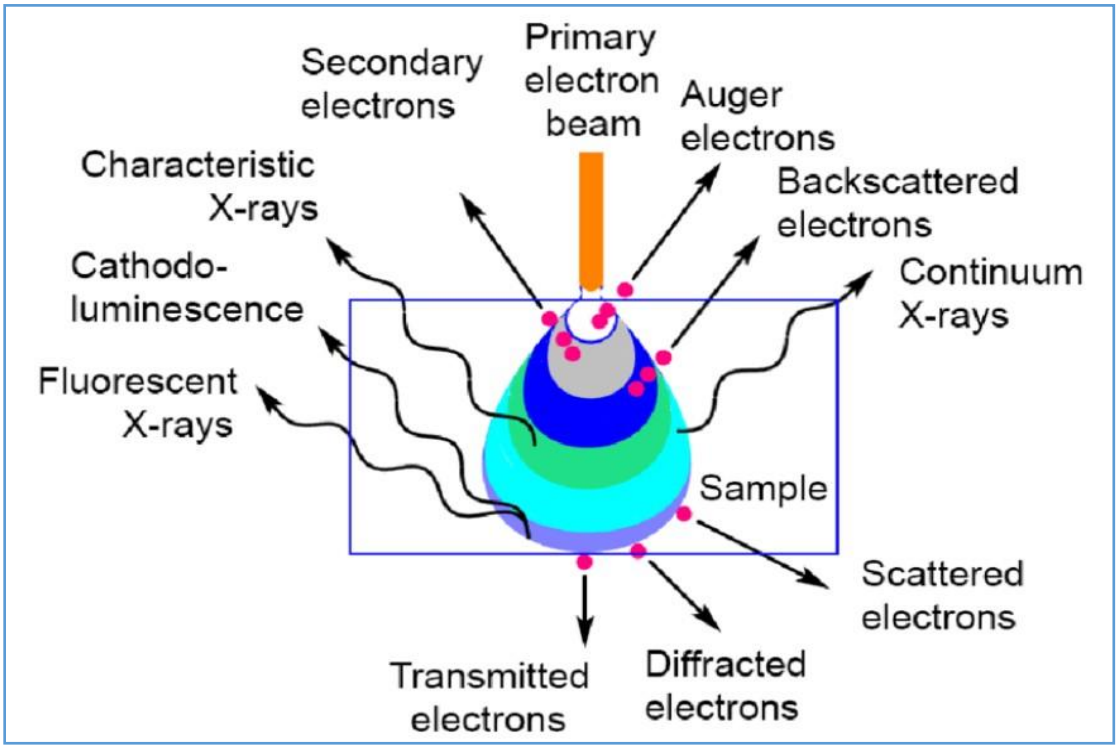


Fig. 3.1 *Schematic drawing of signals generated when a high-energy beam of electrons interacts with a sample.*

Parts of FESEM

FESEM consists of electron gun to generate electron beam, electromagnetic lenses and aperture to focus the electron beam, detector, and vacuum system:

Electron Gun

The electron gun produces a stable electron beam with high current, small spot size, adjustable energy and small energy dispersion. The first-generation SEM system generally used thermionic emission sources like tungsten "hairpin" (=4.5eV) or lanthanum hexaboride (LaB6) (=2.4eV) cathodes, but for the modern FESEMs, the trend is to use field emission sources, which provide enhanced current and lower energy dispersion. Emitter lifetime is another important issue for selection of electron sources. The most widely used electron gun is

composed of three parts: a V shaped hairpin tungsten filament (the cathode), a Wehnelt cylinder and an anode. Thermionic sources require a high temperature to overcome the work function of the metal so that the electrons can escape from the cathode. Though they are inexpensive and the requirement of vacuum is relatively low but there are certain disadvantages, such as short lifetime, low brightness, and large energy spread which restrict their applications. For modern electron microscopes, field emission electron guns (FEG) are a good alternative for thermionic electron guns. In the FEG, a single crystal tungsten wire with very sharp tip is used as the electron source. In this system, a strong electric field forms on the finely oriented tip and the electrons are drawn toward the anodes forms concentrated electron beam.

Electron Lenses:

Electron beam can be focused by electrostatic or magnetic field. But electron beam controlled by magnetic field has smaller aberration, so only magnetic field is employed in SEM system. Coils of wire, known as "electromagnets" are used to produce magnetic field and the trajectories of the electrons can be adjusted by the current applied on these coils.

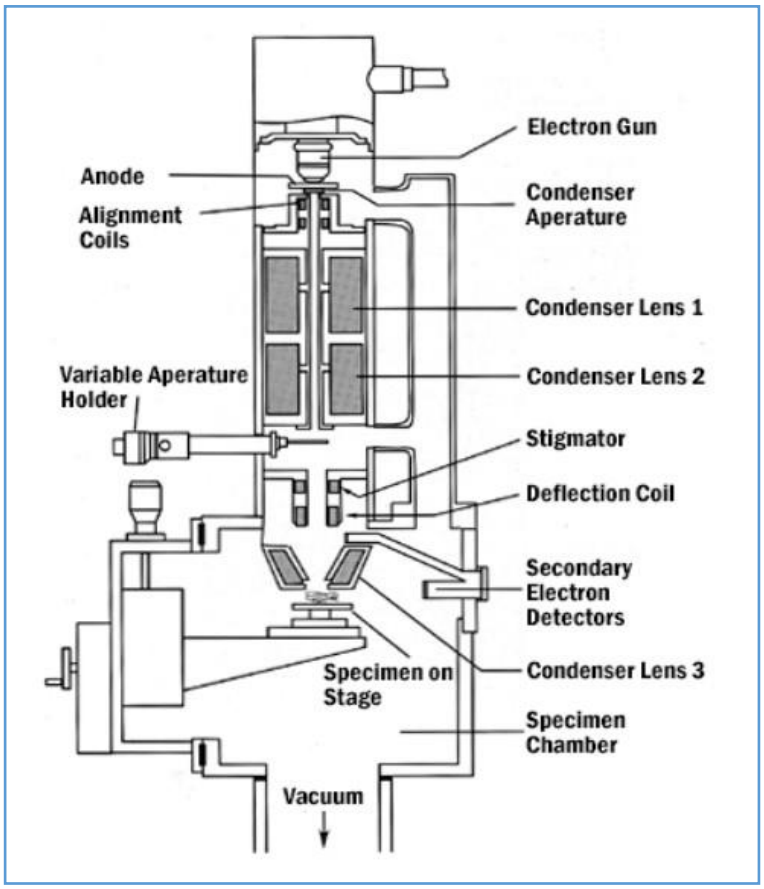


Fig. 3.2 *Schematic diagram of a Scanning Electron Microscope (Source: ResearchGate)*

Condenser lens:

The electron beam will diverge after passing through the anode plate from the emission source. By using the condenser lens, the electron beam is converged and collimated into a relatively parallel stream. A magnetic lens generally consists of two rotationally symmetric iron pole pieces in which there is a copper winding which provides magnetic field. There is a hole in the centre of pole pieces that allows the electron beam to pass through. A lens-gap separates the two pole pieces, at which the magnetic field focuses the electron beam. The position of the focal point can be controlled by adjusting the condenser lens current.



Fig. 3.3 *Experimental set up of FESEM*

Scan Coils:

The scan coils deflect the electron beam over the object according to a zigzag pattern. The formation of the image on the monitor occurs in synchrony with this scan movement. The scan velocity determines the refreshing rate on the screen and the amount of noise in the image. Scan coils often consist of upper and lower coils, which prevent the formation of a circular shadow at low magnification.

Objective lens:

The objective or "probe forming" lens is located at the base of electron column just above sample. The beam is again divergent after passing through the apertures below the condenser lens and must be convergent again. The objective lens focuses the electron beam onto the sample and controls final size and position.

Sample preparation:

FESEM is vacuum based instrument, so sample must be vacuum tolerant. In addition to that, strong radiation by electrons can damage or destroy a sample through heating or other effects. Even in quite good vacuum (10^{-8} mbar), samples can become coated with gold/platinum in the microscope to retain the true surface details. Some samples, those are insulating in nature, are charged up under the electron beam and repel the incoming electron beam. This degrades the resolution and usually requires some prevention technique such as coating the sample with a conducting layer.

Energy dispersive X-ray analysis (EDAX)

This technique gives an overall mapping of the sample by analysing near-surface elements and estimates the elemental proportion in percentages at different positioned is used in conjugation with SEM. An electron beam with energy of 10–20 keV strikes the conducting sample's surface, causing X-rays to emit from the material, and the energy of the emitted X-rays depend on the material under examination does not fit under a technique for surface science, as the X-rays are generated in a region of about 2 microns in depth. By moving the electron beam across the material, an image of each element in the sample can be obtained. It generally takes long hours to acquire the images, as the intensity of the X-ray is low. The composition or amount of nanoparticles near and at the surface can be estimated using the EDX, provided they contain some heavy metal ions. For instance, nanoparticles like silver, gold, and on the surface can be easily identified using EDX.

3.2 Crystal Structure Analysis

Crystal structure analysis helps to understand the structure of crystalline material. It can be used to determine either the lattice parameters, arrangement of individual atoms in a single crystal, or the phase analysis in case of polycrystalline materials. XRD is often used for crystal structure analysis.

3.2.1 X-Ray Diffractometer

X-Ray diffraction analysis (XRD) is a non-destructive technique that provides detailed information about the crystallographic structure, chemical composition, and physical properties of a material [24]. X-ray diffraction (XRD) is a useful technique to ensure the structure of the prepared polymer electrolytes, lithium salts and nano-particles. It is based on the constructive interference of monochromatic X-rays and a crystalline sample. X-rays are shorter wavelength electromagnetic radiation that are generated when electrically charged particles with sufficient energy are decelerated. In XRD, the generated X-rays are collimated and directed to a nanomaterial sample, where the interaction of the incident rays with the sample produces a diffracted ray, which is then detected, processed, and counted. The intensity of the diffracted rays scattered at different angles of material are plotted to display a diffraction pattern.

Each phase of the material produces a unique diffraction pattern due to the material's specific chemistry and atomic arrangement. The diffraction pattern is a simple sum of diffraction patterns of each phase. Imperfection in the sample material would affect the pattern of the diffracted signal. In this case, the factors that contribute to the imperfection of the sample would heterogenity, crystal structure [4].

Working Principle

In XRD, a collimator beam of X-rays is incident on a specimen and is diffracted by the crystalline phases in the specimen. Using Bragg equation for first order diffraction, lattice.

spacing may be found from the diffraction angles. ***Bragg's law*** is the basic law which governs the X-ray diffraction technique of structural analysis. In ***Bragg's law,*** the interaction between x-rays and the electrons of the atoms is described as a process of reflection of x-rays by the atomic planes.

These rays will reinforce each other, only when this path difference is equal to an integral multiple of the wavelength.

The ***Bragg's law*** can be written as:

$$\mathbf{2d\sin\theta = n\lambda}$$

Where **n** is an integer and **λ** is the wavelength of the x-rays used, **θ** is Bragg's angle and **d** is the interplanar spacing.

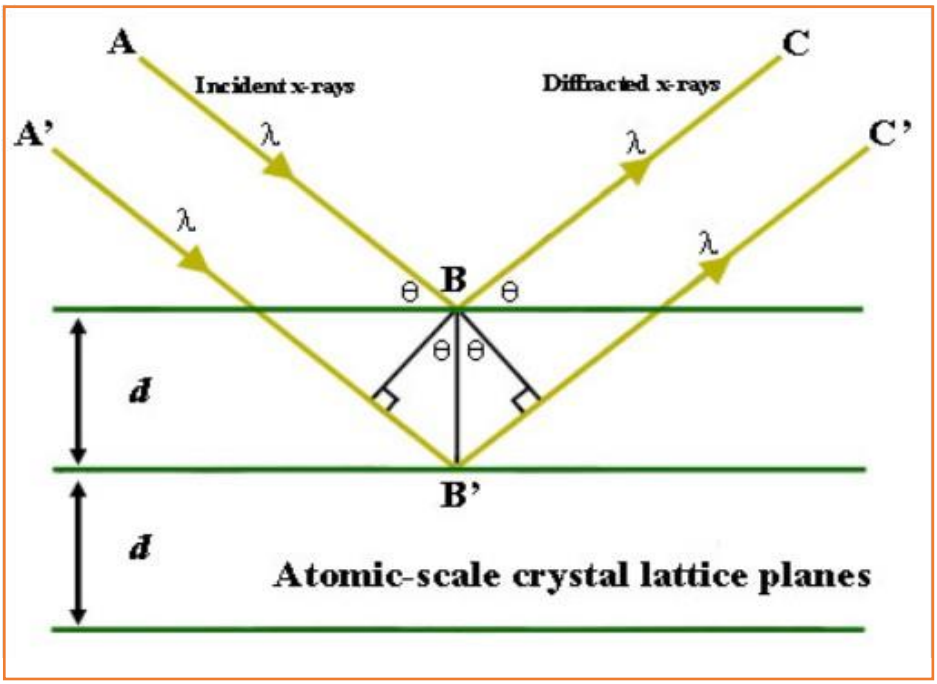


Fig. 3.4 *Bragg equation deduction*

The basic measurement geometry used in most of the x-ray diffraction instrument is depicted under. angle of both the incoming and the exiting beam is θ with respect to the specimen surface. The diffraction pattern is collected by varying the incidence angle of the inward x-ray beam by θ and the scattering angle by 2θ while measuring scattered intensity I(2θ) as a function of the latter. Therefore, two angles have to be varied during a θ/2θ scan. In one case the x-ray source remains fixed while the sample is rotated around θ and the detector moves by 2θ. In another case, the sample is fixed while both the source of x-ray and the detector rotate by θ simultaneously, but clockwise and anticlockwise, respectively. The central part of a

diffractometer or goniometer performed the rotations. Typically, the experimental sample is mounted on the rotational axis, while the detector and/or x-ray source moves along the periphery, but both axes of rotation coincide.

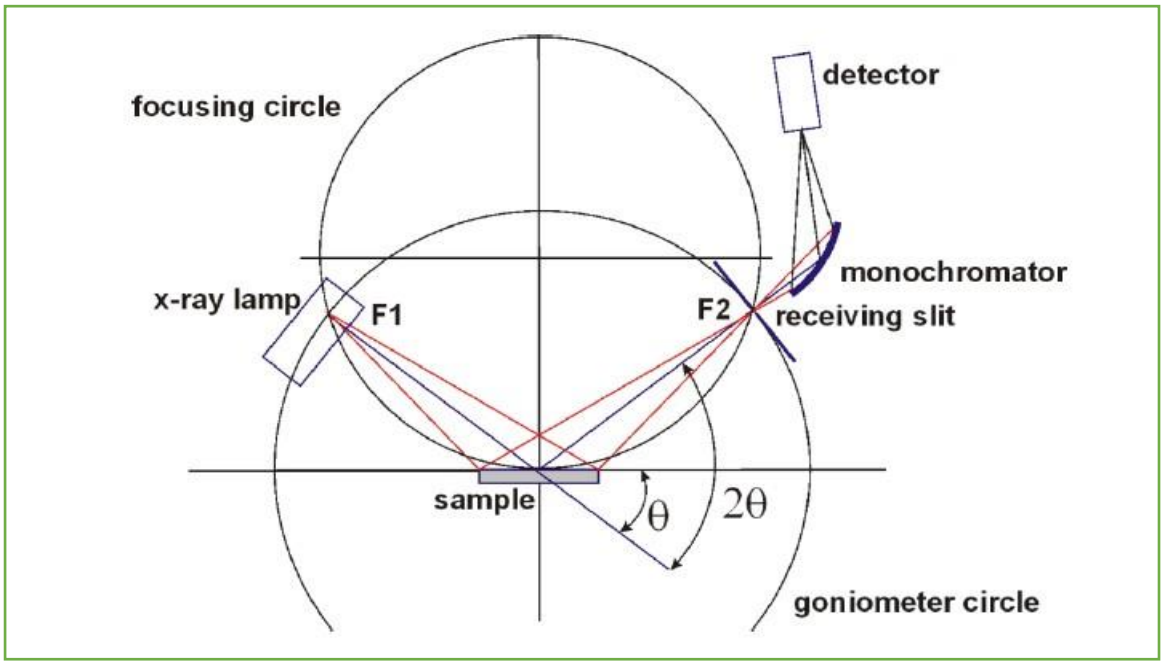


Fig. 3.5 *Schematic of Bragg-Brentano geometry. (Source - ResearchGate)*

Most of powder diffractometers use Bragg-Brentano parafocusing geometry, offering high-resolution and high beam-intensity analysis at the cost of very precise alignment requirements and carefully prepared samples.

The incident angle ω between X-ray source and the sample is always 1/2 of the detector angle 2θ: 1) **ω:2θ** or **θ:2θ scan**: with the X-ray tube fixed, the sample rotates at θ/min and the detector always at 2θ/min; and 2) **θ: θ scan**: the sample is fixed and the tube rotates at the same rate as the detector at θ/mi. Sample surface is kept on the tangent plane of the focusing circle defined by three spots at sample, X-ray source and receiving slit. The incident- and diffracted-beam slits move on a circle that is centred on the sample. Divergent X rays from the source hit the sample at different points on its surface. During the diffraction process the X rays are refocused at the detector slit.

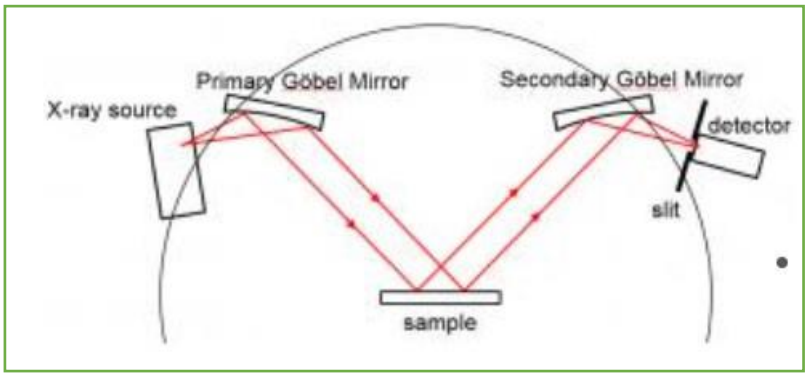


Fig. 3.6 *Schematic of Parallel Beam geometry*

The Parallel Beam optics provides accurate measurement of diffracted X-ray positions unaffected by sample shape. It is generally used to analyze powder sample profiles, the degree of preferred orientation and thin films.

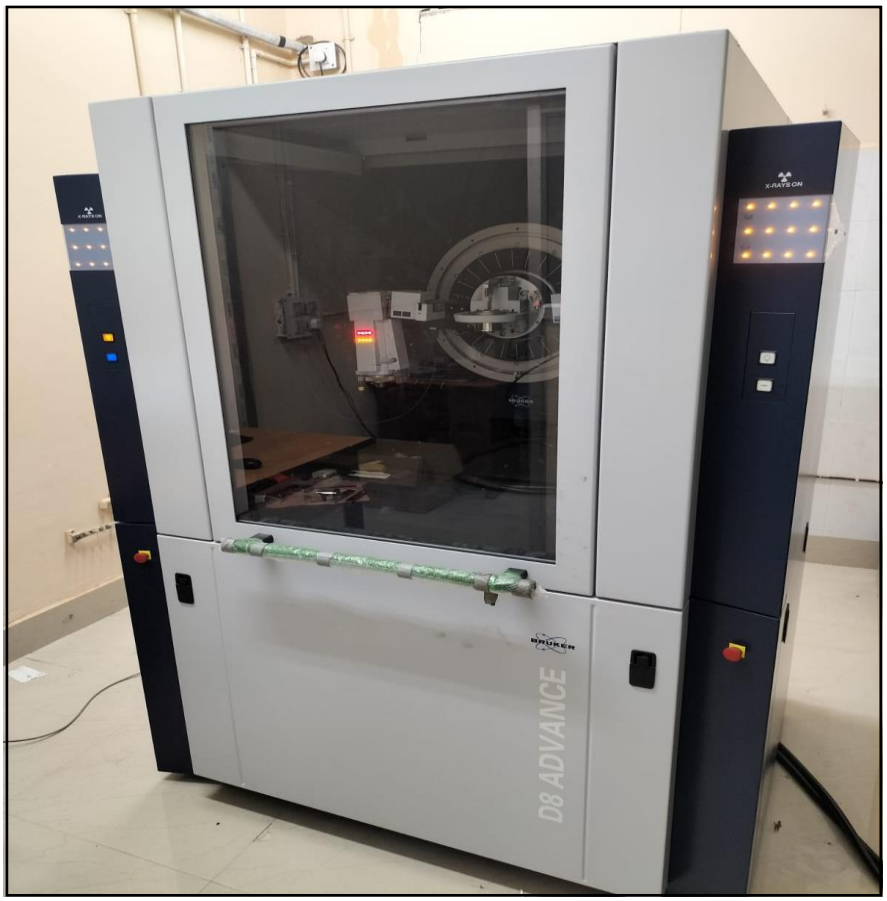


Fig 3.7 *Experimental set up of X-Ray Diffractometer (Bruker D8 Series)*

3.3 Absorbance Spectra Analysis

Absorbance is a measure of how much infrared radiation is absorbed by a sample at a particular wavelength. Absorbance values typically range from 0 (no absorption) to higher values, and the higher the absorbance, the more radiation is absorbed by the sample. Transmittance on the other hand is the fraction of incident infrared radiation that passes through a sample without being absorbed. Transmittance values range from 0% (no transmission) to 100% (complete transmission), and a higher transmittance indicates less absorption by the sample. As absorbance increases, transmittance decreases, and vice versa. This relationship is logarithmic. In FTIR spectroscopy, both absorbance and transmittance are essential for interpreting the spectrum. The spectrum provides information about the functional groups and chemical composition of the sample based on the absorption or transmission of specific wavelengths of infrared light.

3.3.1 Fourier Transform Infrared Spectroscopy (FTIR)

FTIR Spectroscopy, Fourier-transform infrared spectroscopy, is concerned with the vibration of molecules. Each functional group has its own discrete vibrational energy which can be used to identify a molecule through the combination of all of the functional groups. This makes FTIR microscopy ideal for sample ID, multilayer film characterization, and particle analysis. FTIR spectroscopy takes advantage of how IR light changes the dipole moments in molecules that correspond to a specific vibrational energy. Vibrational energy corresponds to two variables: reduced mass (μ) and bond spring constant (k). For k constant, we can look at C-C, C=C, and C≡C showing an increase of 800 cm^{-1} across the series. Substituting atoms in a C- C bond with nitrogen and oxygen causes a shift of 100 cm^{-1}. By looking at the two series, it can be seen that bond strength alters the wavenumbers more than mass. Since every functional group is composed of different atoms and bond strengths, vibrations are unique to functional groups, and classes of functional groups (e.g. O-H and C-H stretches appear around 3200 cm^{-1} and 2900 cm^{-1}, respectively). A correlation chart with various functional group vibrations can be seen. Since the collection of vibrational energy bands for all of the functional groups a molecule is unique to every molecule, these peaks can be used for identification using library searches of comprehensive sample databases.

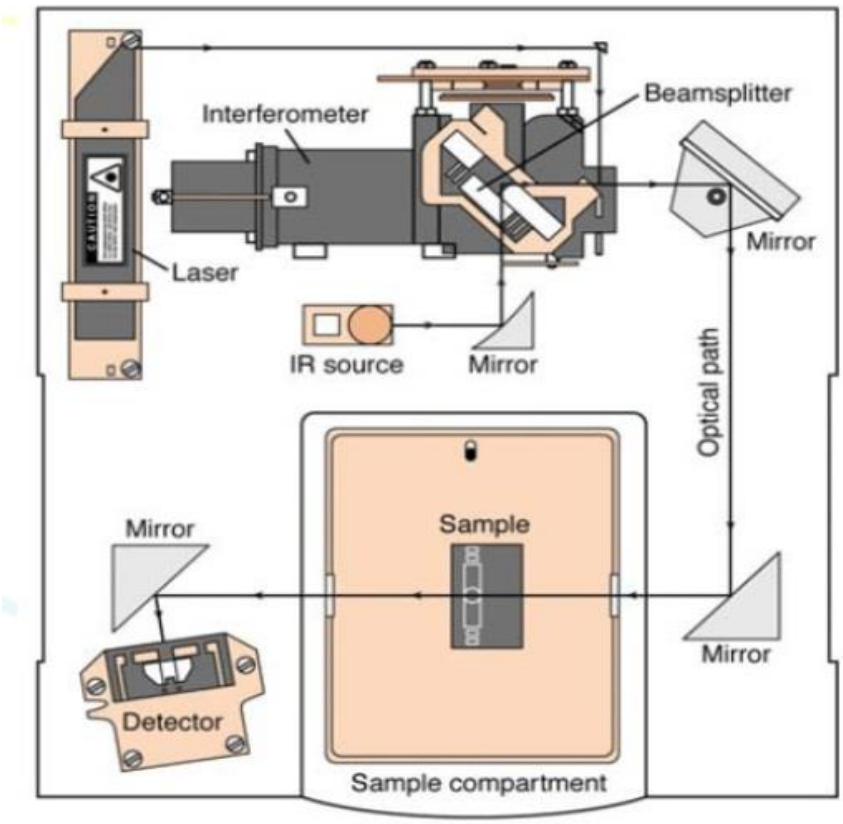


Fig 3.8 *Different parts of Fourier Transform Infrared Spectrometer (FTIR)*

Working principle:

The three major parts of an FTIR are the source, interferometer, and detector The source is typically a broadband emitter such as a mid-IR ceramic source (50-7,800 cm^{-1}), a near-IR halogen lamp (2,200 – 25,000 cm^{-1}), or a far-IR mercury lamp (10-700 cm^{-1}). The interferometer is the heart of FTIR and consists of a beam-splitter, a stationary mirror, a moving mirror, and a timing laser (box in figure 4). The beam-splitter splits the light from a source into two paths with half the light going to a stationary mirror and the other half going to a moving mirror. In many FTIR systems, the beam-splitter is placed at 45 degrees to the incident beam, but for high throughput applications, a low angle interferometer is preferred as the P and S polarizations converge close to the Brewster's Angle. Common beam-splitter materials are KBr (375 – 12,000 cm^{-1}) for mid-IR, Quartz (4,000 – 25,000 cm^{-1}) for near-IR, and Mylar (30 – 680 cm^{-1}) for far-IR. The beams from the moving and stationary mirrors are recombined back at the beam-splitter and steered toward the sample. The difference in the path of the mirrors causes

constructive and destructive interference over the course of time it takes for the moving mirror to make a pass. The signal versus mirror position (and, thus, time) is called an interferogram. A laser is used to determine the position of the moving mirror using the precisely known wavelength of the laser (Figure 5). He-Ne lasers are the industry norm due to their excellent wavelength stability compared to solid-state or diode lasers. This laser stability allows for spectral additions, library searches, and other functions that need high wavenumber accuracy.

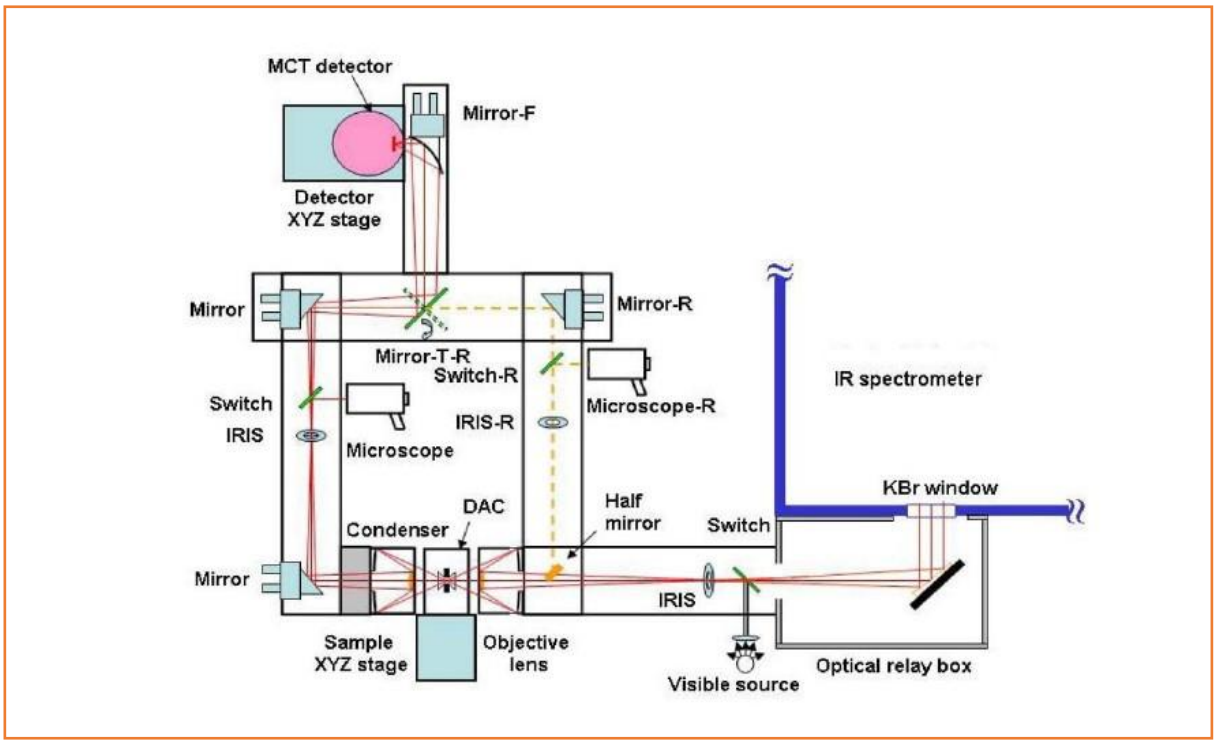


Fig 3.9 *Schematic diagram of FTIR spectrometer [3]*

Near infrared

The Near-IR portion of the electromagnetic spectrum falls between 4,000 to 12,800 cm. This region consists of overtones (two of the same vibrational modes occurring simultaneously) and combinations (two different vibrational modes occurring simultaneously). Since these modes are not strictly quantum mechanically allowed, the intensity of the modes is often quite low. These spectra are often complex, and chemometric techniques, such as multivariate analysis, are used. In spite of the drawbacks, there are clear advantages to Near-IR spectroscopy. Firstly, the path length of the light is such that bulk samples can be analysed with little to no sample preparation. Secondly, water does not affect signal as it does in mid-IR.

Far infrared

The Far Infrared region lies between 10 cm-1 and 700 cm-1. The bonds that show in this region are 3+ atom functional groups, such as -C-C-C- bending, and lattice vibrations in crystalline materials. Since these are highly dependent on conformation or crystal structure, materials with the same chemical structure, but different crystal structures may be distinguished using Far-IR.

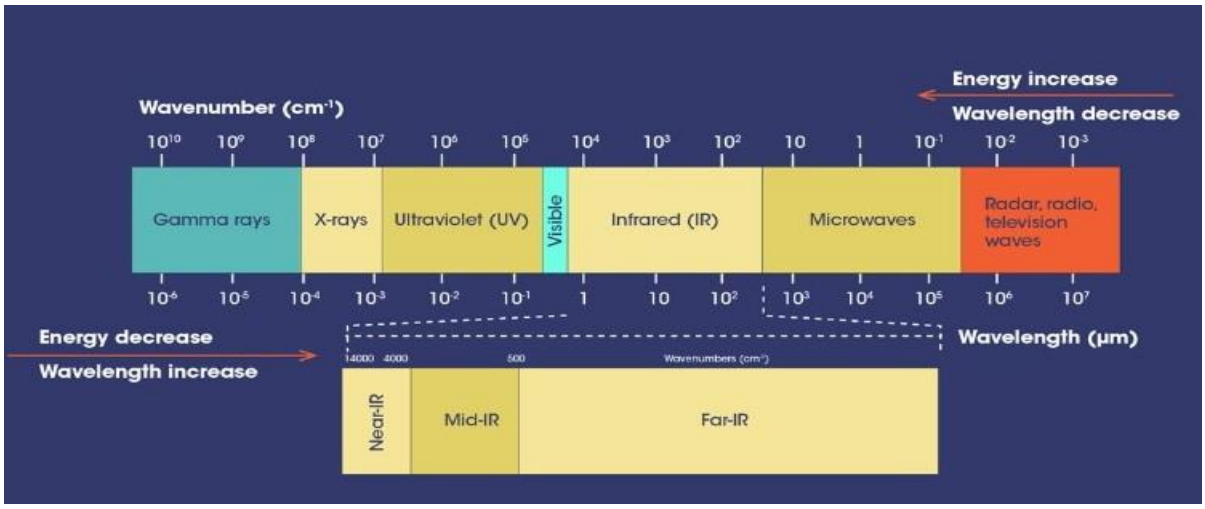


Fig 3.10 *Electromagnetic spectrum, for infrared spectroscopy types [2]*

The output of interferometer against different types of light in FTIR Spectroscopy is shown in Fig 2.11. Depending upon the nature of light the output signal of the interferometer varies.

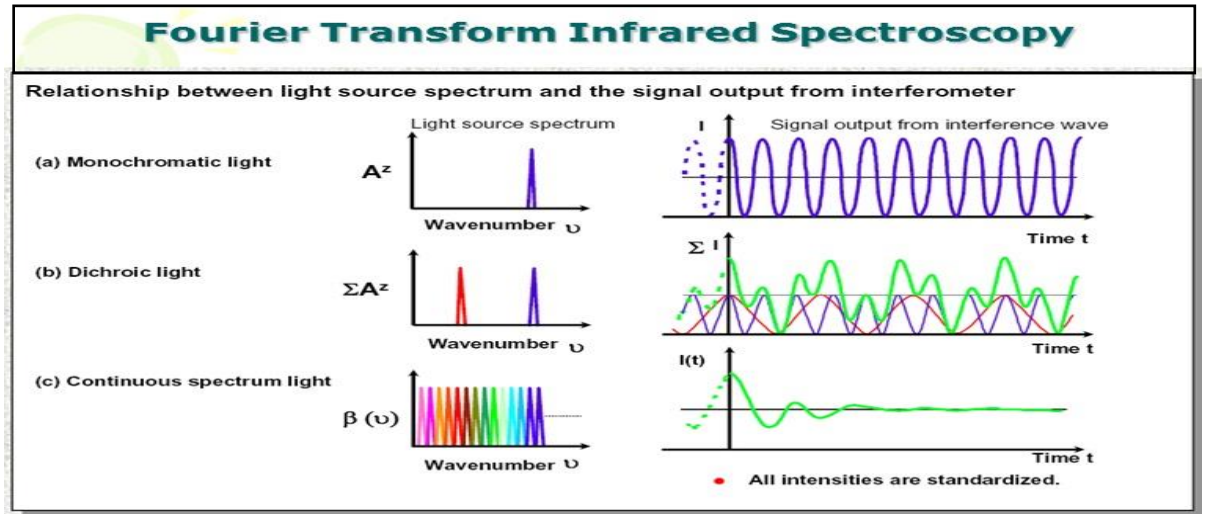


Fig 3.11 *Schematic diagram representing light source and output of interferometer.[2]*

The basis of all quantitative analysis in FTIR is Beer's law, which relates concentration to absorbance, given by the following relation

$$A = \mu c €$$

where A is the absorbance, μ is the absorptivity, € is the path length and c is the concentration.

When an interferogram is measured with a sample in the infrared beam and Fourier transformed a single beam spectrum is produced. The transmittance is defined as

$$T = \frac{I}{I_0}$$

where I and I0 are the intensity of beam with and without sample respectively i.e. I0 is background spectrum and I is the sample spectrum.

Absorption, A can be obtained from Transmittance, T as

$$A = -\log_{10} T$$

For qualitative study the IR spectra can be plotted in either transmittance mode or absorption mode. But, for quantitative analysis, the plot must be in absorption mode because absorption is proportional to concentration but not transmittance.

Deconvolution of FTIR spectra

Deconvolution is a technique used to determine the position and intensity of several peaks that overlap to give broad spectral features. The deconvoluted FTIR spectra of all the samples which done using a Gaussian function for the identification of the bands, which appeared in these spectra, and their assignments. By determining the number of all independent components of the vibrational bands out a quantitative analysis was carried out to find the concentration distribution of these components. The peak frequency, half-width at half-height and area was

allowed to float during the iterations and proportion of a particular vibrational band was determined from the area of that fitted Gaussian band divided by the total area of all the bands. The band deconvolution analyses were accomplished using graphical analysis software (Origin lab v 8.5). A typical deconvolution of a FTIR spectrum is shown as under.

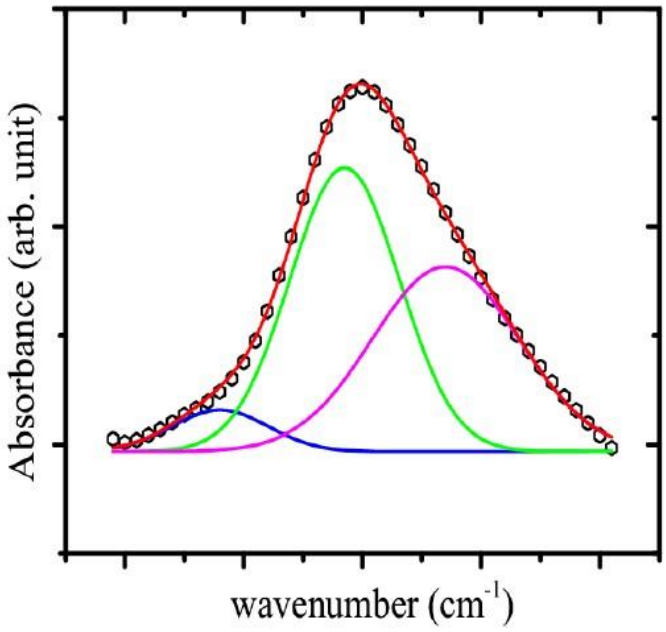


Fig 3.12 *Band deconvolution of a FTIR spectrum (Source – Wiki media)*

FTIR spectroscopy thus offers and reliable sample analysis both qualitatively and quantitatively. For our thesis FTIR Spectroscopy has been used characterization of the gel polymer electrolytes for supercapacitors and Li-ion Batteries.



Fig 3.13 *Experimental Setup of FTIR Spectrometer.*

3.4 Thermal Analysis

Thermal analysis refers to a variety of techniques in which a property of a sample is continuously measured as the sample is programmed through a predetermined temperature profile. Among the most common techniques are thermo gravimetric analysis (TGA) and differential scanning calorimetry (DSC).

3.4.1 Thermogravimetric Analysis (TGA)

Thermogravimetric analysis or TGA measures weight changes in an experimental material as a function of temperature under a controlled N2 atmosphere. In TGA the mass loss versus increasing temperature of the sample is recorded. The basic instrumental requirements are simple: a precision balance, a programmable furnace, and a recorder (Figure 1). Modern instruments, however, tend to be automated and include software for data reduction. In addition, provisions are made for surrounding the sample with an air, nitrogen, or an oxygen atmosphere. *Fig. 2.14* shows that gradually raising the temperature of an experimental sample in a furnace as its weight is measured in an analytical balance that remains outside of the furnace. The mass loss is observed in TGA if a thermal event involves loss of a volatile component. The different chemical reactions, such as combustion in which weight losses are involved, whereas different physical changes, such as melting, does not involve weight losses. The weight of the experimental sample is plotted against temperature to demonstrate thermal transitions in the material such as loss of solvent and plasticizers in polymer electrolytes, water of hydration in inorganic materials, and finally, decomposition of the material. Application sectors are mainly determination of carbon black content, decomposition temperature, moisture content of organic and inorganic materials, oxidation stability, performance of stabilizers, plasticizer content of polymers, low molecular weight monomers in polymers, etc. A TGA instrument was used to find the range of stabilization of the samples in the present cases. At first the sample (approximately 7-10 mg), was placed in an empty alumina pan and Al2O3 was placed in another pan as a reference. The temperature of the furnace was increased at a rate of 10 K/min in N2 atmosphere. The change in weight and heat difference was noted for valuable information regarding thermal property.

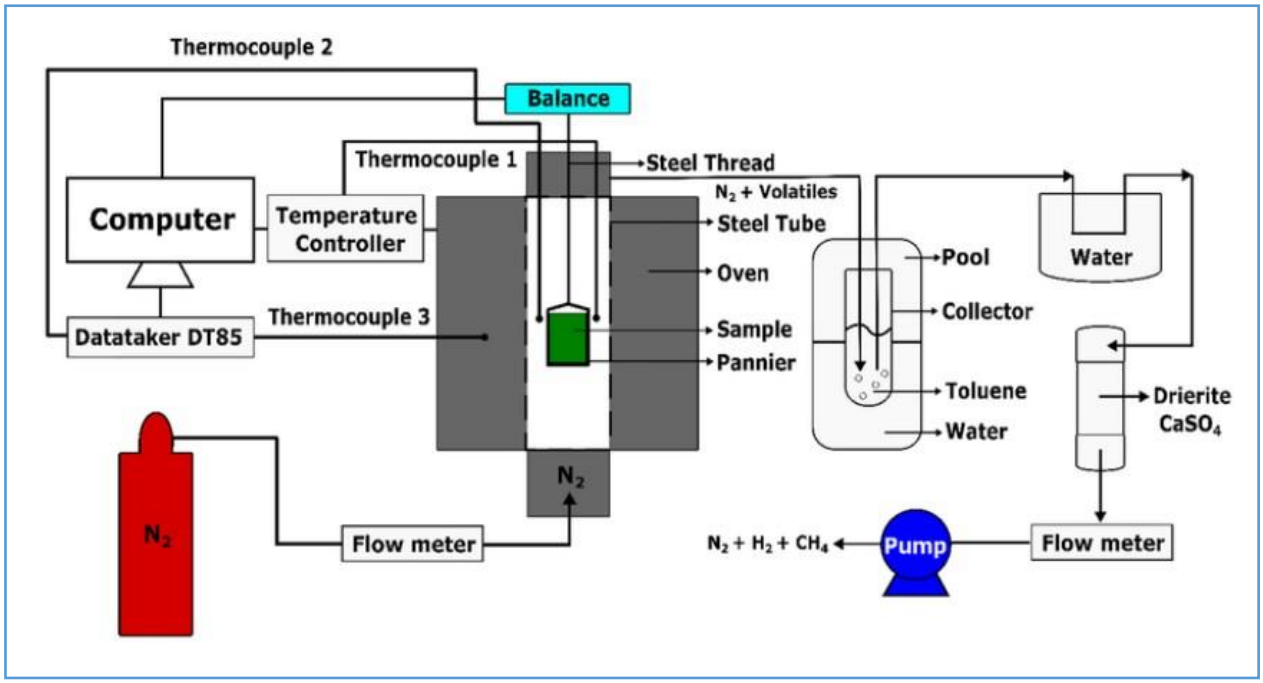


Fig 3.14 *Schematic representation of Thermogravimetric Analysis (TGA) set-up. (Ref: ResearchGate)*

.

Types of TGA

There are three types of thermogravimetry:

- Isothermal or static thermogravimetry: In this technique, the sample weight is recorded as a function of time at a constant temperature.
- Quasistatic thermogravimetry: In this technique, the sample temperature is raised in sequential steps separated by isothermal intervals, during which the sample mass reaches stability before the start of the next temperature ramp.
- Dynamic thermogravimetry: In this technique, the sample is heated in an environment whose temperature is changed in a linear manner.

TGA can be used to evaluate the thermal stability of a material. In a desired temperature range, if a species is thermally stable, there will be no observed mass change. Negligible mass loss corresponds to little or no slope in the TGA trace. TGA also gives the upper use temperature of a material. Beyond this temperature the material will begin to degrade.

TGA is used in the analysis of polymers. Polymers usually melt before they decompose, thus TGA is mainly used to investigate the thermal stability of polymers. Most polymers melt or degrade before 200 °C. However, there is a class of thermally stable polymers that are able to withstand temperatures of at least 300 °C in air and 500 °C in inert gases without structural changes or strength loss, which can be analysed by TGA.[2] [3] [4]

3.4.2 Differential Scanning Calorimetry (DSC)

Differential scanning calorimetry (DSC) is a thermoanalytical technique in which the difference in the amount of heat required to increase the temperature of a sample and reference is measured as a function of temperature.[1] Both the sample and reference are maintained at nearly the same temperature throughout the experiment. Generally, the temperature program for a DSC analysis is designed such that the sample holder temperature increases linearly as a function of time. The reference sample should have a well-defined heat capacity over the range of temperatures to be scanned. Additionally, the reference sample must be stable, of high purity, and must not experience much change across the temperature scan. Typically, reference standards have been metals such as indium, tin, bismuth, and lead,[2] but other standards such as polyethylene and fatty acids have been proposed to study polymers and organic compounds, respectively.

From thermodynamics it is well known that knowledge about heat capacity from zero Kelvin up to the temperature of interest enables description of important material properties. With a completely known heat capacity (and known heat of transitions) the thermodynamic properties of a material are known [4], U and H are total thermal motion and energy, S is disorder, and G and F are measures of stability. Calorimetry is generally based on the following relationship

$$dQ = C \cdot \Delta T = c \cdot m \cdot \Delta T$$

In differential form, assuming time independent sample mass and specific heat capacity

$$\frac{dQ}{dt} = \Phi = C \cdot \frac{dT}{dt} = c \cdot m \cdot \beta$$

where dQ is the heat exchanged, ΔT is the temperature change caused by the exchanged heat, Φ is the heat flow rate, C is the heat capacity, c = C/m is the specific heat capacity, m is the sample mass, and β is the scan rate (heating or cooling).

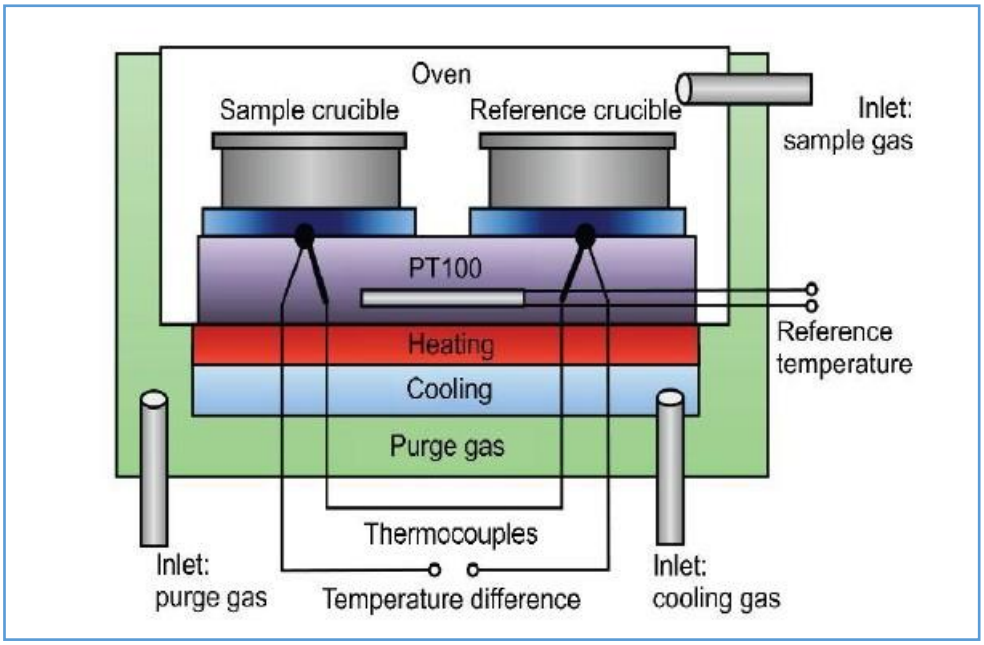


Fig 3.15 *Schematic diagram of DSC measurement technique. (Source-Wikimedia)*

To determine the thermodynamic properties such as glass transition temperature (Tg), crystallization temperature (Tc), differential Scanning Calorimetry (DSC) of the powdered samples can be performed in a Differential Scanning Calorimeter in the temperature range from –80 °C to 500 °C in nitrogen atmosphere.

A typical DSC curve shown in *Fig. 2.16* shows the glass transition temperature (T_g), which is an endothermic baseline shift. The peak crystallization temperature (T_p) denotes where crystallization rate being maximum. The melting temperature (T_m) indicates the melting of the sample. The percentage crystallinity of a polymer can be found from the crystallization peak of the DSC curve since the melting enthalpy can be calculated from the area under a melting peak. In case of semi-crystalline polymer matrix such as PEO, P(VdF-HFP) etc. based polymer electrolytes the percentage of crystalline phase of P(VdF-HFP) (X_c) can be calculated using the equation

$$X_c = \Delta H_m / \Delta H_{PEO}$$

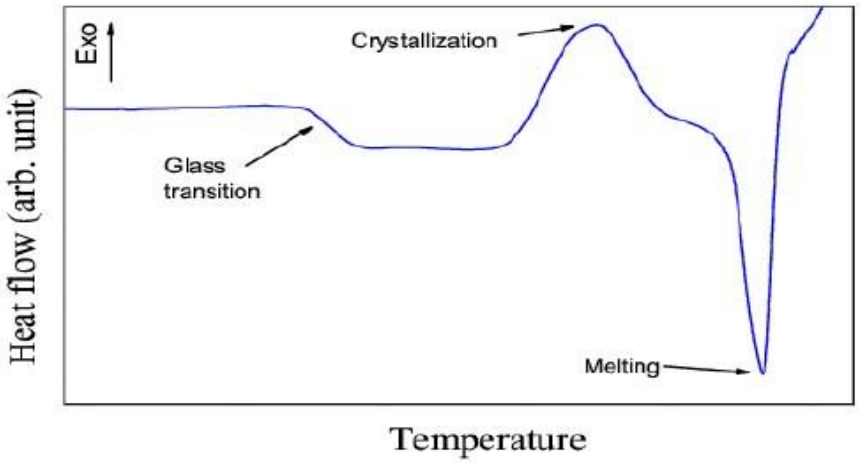


Fig 3.16 *DSC curve for a polymer electrolyte sample at different temperature [2]*

where ΔHm is the melting enthalpy of the sample and ΔHPEO is the melting enthalpy of completely crystalline samples [5]. DSC traces of the prepared samples for determining the characteristic transitions such as glass transition and melting temperature were carried out using a differential scanning calorimeter (model- Universal TA Q2000). Appropriate amount of the as-prepared polymer electrolyte films samples was encapsulated in an aluminium pan and was placed inside sample chamber along with a reference pan under constant flow of ultra-high pure N2 (50 ml/min) at a heating scan rate of 10 ^{0}C/min and the data were then recorded.

Types of DSC

There are two main types of DSC:

- Heat-flux DSC - It measures the difference in heat flux between the sample and a reference
- Power differential DSC - It measures the difference in power supplied to the sample and a reference.

Differential scanning calorimetry can be used to measure a number of characteristic properties of a sample. Using this technique it is possible to observe fusion and crystallization events as well as glass transition temperatures T_g. DSC can also be used to study oxidation, as well as other chemical reactions.[13][14][16] .DSC is used widely for examining polymeric materials to determine their thermal transitions. Important thermal transitions include the glass transition temperature (T_g), crystallization temperature (T_c), and melting temperature (T_m).

3.5 Electrical and Electrochemical Analysis

Electrical and electrochemical analysis of the samples were done using a Potentiostat (Gamry 1000). A potentiostat is an electronic instrument that controls the voltage difference between a Working Electrode and a Reference Electrode. Both electrodes are contained in an electrochemical cell. The potentiostat implements this control by injecting current into the cell through an Auxiliary, or Counter, electrode. In almost all applications, the potentiostat measures the current flow between the Working and Counter electrodes. The controlled variable in a potentiostat is the cell potential and the measured variable is the cell current.

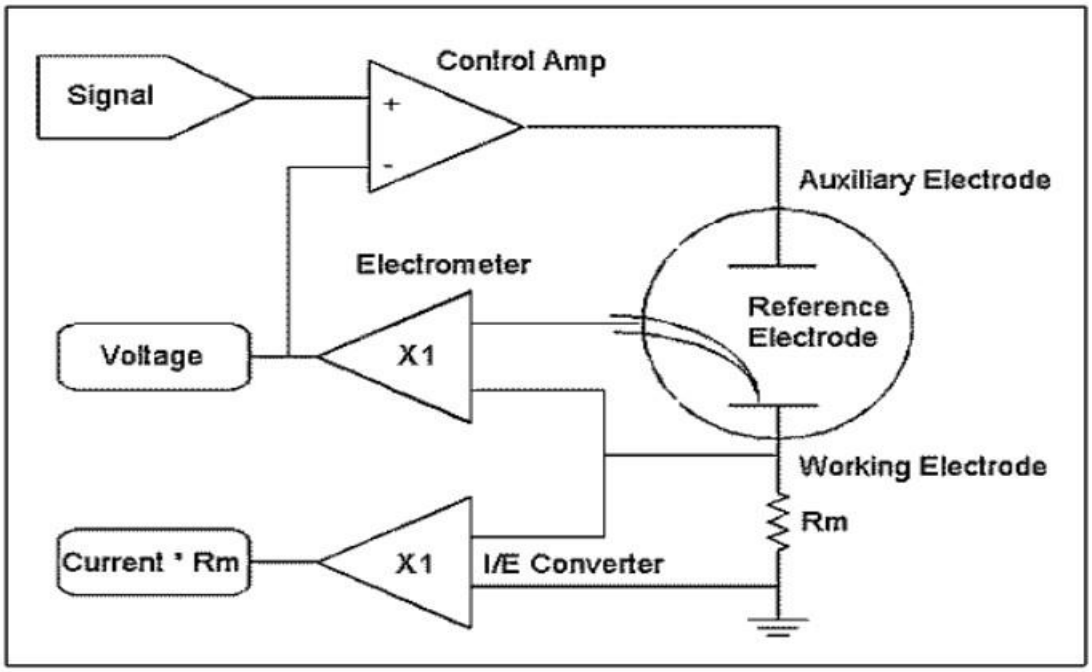


Fig 3.17 Simple schematic of a potentiostat. (Source-Wikimedia)

The electrometer circuit measures the voltage difference between the reference and working electrodes. Its output has two major functions: it is the feedback signal in the potentiostat circuit, and it is the signal that is measured whenever the cell voltage is needed.

The control amplifier is a servo amplifier. It compares the measured cell voltage with the desired voltage and drives current into the cell to force the voltages to be the same.

Using a potentiostat, data was collected for Supercapacitors and DC Conductivity, Electrochemical impedance spectroscopy (EIS), cyclic voltammetry (CV) and galvanostatic charge-discharge (GCD) characteristics have been evaluated.

3.5.1 DC Conductivity

Complex impedance measurements and frequency-dependent conductivity spectra are common techniques used to determine the electrical properties of polymer electrolyte films. Here's how they work:

Complex impedance Measurement

- Complex impedance plots are generated by applying an AC (alternating current) signal to the polymer electrolyte film and measuring the resulting voltage across the material.
- The impedance consists of a real part (resistance) and an imaginary part (reactance). The real part represents the resistance to the flow of current, while the imaginary part represents the reactance due to the capacitive or inductive behaviour of the material.
- From these impedance plots, parameters such as the bulk resistance and capacitance of the material can be determined.
- The DC conductivity can be calculated from the real part of the impedance at zero frequency (Z' or resistance at $\omega = 0$).

Frequency dependent Conductivity Spectra

- Frequency-dependent conductivity spectra are obtained by measuring the conductivity of the polymer electrolyte film over a range of frequencies.
- Typically, AC measurements are performed over a range of frequencies, and the conductivity (σ) is calculated using the relationship between the applied electric field and the resulting current
- By plotting conductivity as a function of frequency, different mechanisms contributing to the conductivity, such as ionic motion and electrode polarization, can be distinguished.

The DC conductivity can be determined from the low-frequency limit of the conductivity spectrum (σ (0)), which corresponds to the conductivity at zero frequency

3.5.2 Electrochemical Impedance Spectroscopy (EIS):

Electrochemical Impedance Spectroscopy (EIS) is indeed a powerful tool for investigating the electrochemical performance of various systems, including electrical double layer (EDL) capacitors, also known as supercapacitors or ultracapacitors. EIS measures the impedance of a system as a function of frequency. This allows for the identification of different electrochemical processes occurring within the EDL capacitor over a wide frequency range. EIS can separate the contributions of different processes, such as ionic conductivity, charge transfer resistance, and double layer capacitance, to the overall impedance of the system. This makes it possible to analyze and optimize each component independently. EIS is a non-destructive technique, meaning that it can provide valuable insights into the electrochemical behaviour of EDL capacitors without altering or damaging the device. Changes in impedance spectra can indicate aging, degradation, or the presence of impurities in the electrolyte. EIS is a versatile and powerful technique for characterizing the electrochemical behaviour of EDL capacitors, providing valuable insights for their design, optimization, and performance evaluation.

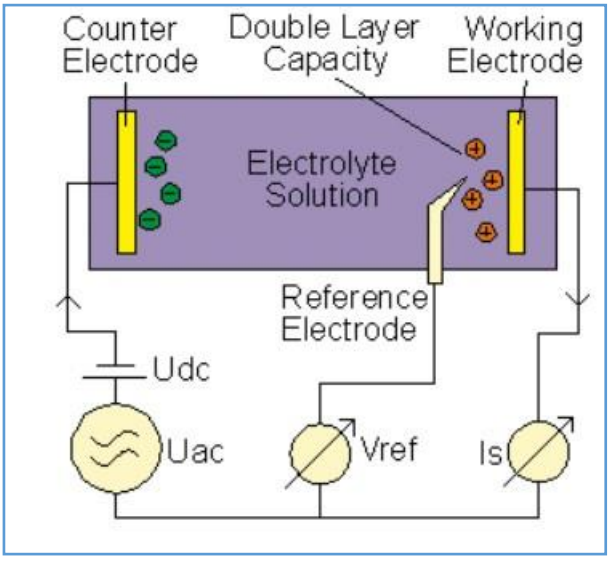


Fig 3.18 *Set-up of three electrode electrochemical cell. (Ref: Novocontrol Technologies)*

In addition to the two parallel plate electrodes (denoted as Counter and Working electrode), a third voltage reference electrode is placed close to the polarization layer and measures the voltage difference of the polarization double layer capacity to the working electrode. In contrast to dielectric, conductivity and impedance material spectroscopy where all electrodes are made

of inert metal as e.g. gold, stainless steel or platinum, this applies for the electrochemical cell only for the counter electrode feeding current into the electrolyte. The working electrode consists of the metal to be characterized in combination with the electrolyte. The reference electrode is usually an open tipped glass capillary filled with a standard electrolyte coupled to a standard metal in order to create a defined electrochemical potential to the electrolyte. The total potential drop across the cell is summed up by all contributions of the chemical process like mass transport, chemical and adsorption steps, electron transfer, etc. By measuring the impedance spectrum $V_{Ref}^{*}(\omega)/I_S^{*}(\omega)$ and fitting it with an equivalent circuit model, the several process contributions can be separated from each other. The typical evaluation includes determination of Warburg impedance related to mass transport, electron transfer resistance, electrolyte resistance and double layer capacity.

3.5.3 Cyclic Voltammetry (CV)

Cyclic voltammetry (CV) is another essential electrochemical technique used to characterize the behaviour of electrochemical systems, including EDL capacitors. Cyclic voltammetry involves applying a linearly changing potential (voltage) to an electrochemical cell while measuring the resulting current response. The potential is swept back and forth between two limits at a constant rate. In a typical setup, the electrochemical cell consists of working, reference, and counter electrodes immersed in an electrolyte solution. The working electrode is usually the material being studied (e.g., an electrode material in an EDL capacitor), the reference electrode maintains a stable potential, and the counter electrode completes the electrical circuit. During a cyclic voltammetry experiment, the applied potential is swept linearly with time between two defined limits, often referred to as the forward and reverse scan directions. The potential sweep rate can be adjusted depending on the system being studied.

The current response is measured as a function of the applied potential. As the potential is swept, electrochemical reactions occur at the electrode-electrolyte interface, resulting in changes in current flow. These reactions can involve processes such as ion insertion/extraction, redox reactions, or double-layer charging/discharging, depending on the system. The resulting voltammogram (plot of current vs. potential) provides valuable information about the electrochemical behaviour of the system. Peaks and features in the voltammogram correspond to specific electrochemical processes, such as oxidation or reduction of species, capacitive charging/discharging, or diffusion-limited processes.

Cyclic voltammetry is widely used in various fields, including electrochemistry, materials science, battery research, corrosion studies, and sensor development. In the context of EDL capacitors, CV can provide insights into the capacitive behaviour, charge storage mechanisms, and electrochemical stability of electrode materials and electrolytes. Overall, cyclic voltammetry is a versatile and powerful technique for studying the electrochemical properties of materials and devices, providing valuable insights into their behaviour under different operating conditions.

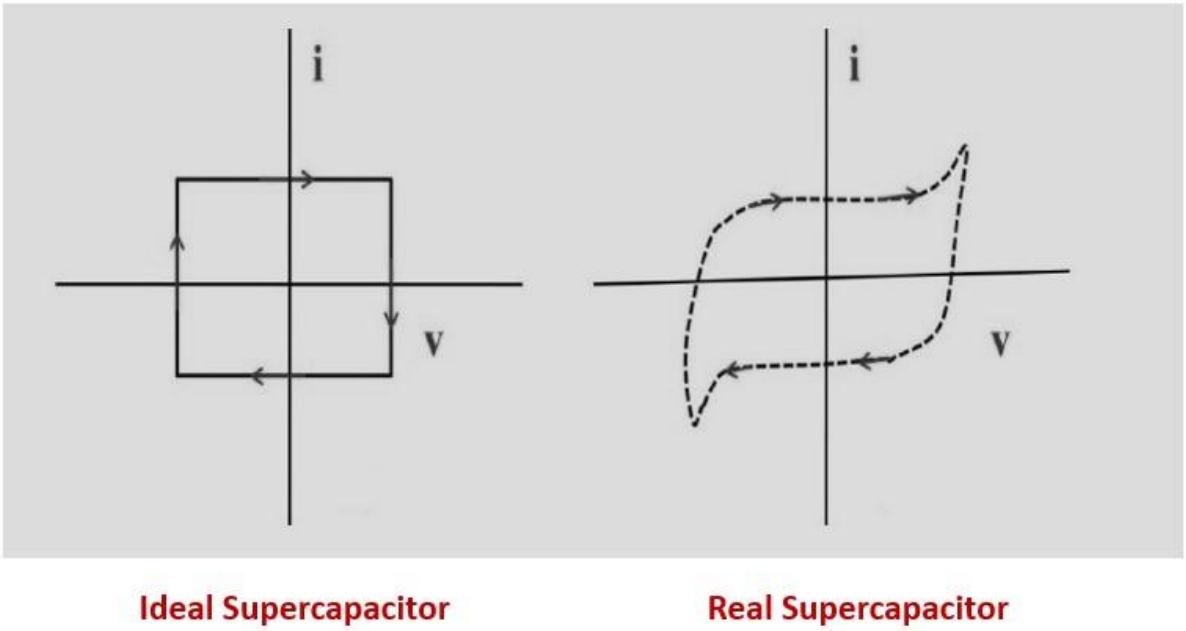


Fig 3.19 Cyclic voltammetry of an ideal supercapacitor and a real supercapacitor.

The value of specific capacitance can be evaluated from the expression:

$$C_{sp}^{cv} = \frac{\int idV}{2 \times m \times S \times \Delta V}$$

, where the numerator is the integrated area of the CV curve, m is the single electrode mass of active material (activated carbon) in g, S is the scan rate and ΔV is cell voltage range.

Cyclic voltammetry (CV) has become an important and widely used electroanalytical technique in many areas of chemistry. It is often used to study a variety of redox processes, to determine the stability of reaction products, the presence of intermediates in redox reactions,[10] electron

transfer kinetics,[11] and the reversibility of a reaction.[12] It can be used for electrochemical deposition of thin films or for determining suitable reduction potential range of the ions present in electrolyte for electrochemical deposition.[13] CV can also be used to determine the electron stoichiometry of a system, the diffusion coefficient of an analyte, and the formal reduction potential of an analyte, which can be used as an identification tool.

3.5.4 Charge Discharge Studies (CD)

Charge-discharge testing is a fundamental technique for characterizing the performance of supercapacitors, also known EDL capacitors. Charge-discharge testing involves applying a known voltage or current to the supercapacitor to either charge or discharge it. During charging, electrical energy is stored in the supercapacitor by accumulating ions at the electrode-electrolyte interface. During discharge, this stored energy is released as the ions return to the electrolyte. The supercapacitor is connected to a power supply or a potentiostat/galvanostat, which controls the voltage or current applied to the device. The voltage or current is monitored over time to track the charging or discharging process. The experiment can be performed under various conditions, such as different voltage or current profiles, temperatures, and electrolytes. During charging, the voltage or current is applied to the supercapacitor, causing ions from the electrolyte to accumulate at the electrode surfaces, forming an electric double layer. This process is typically rapid and can be completed within seconds or milliseconds, depending on the specific supercapacitor design and operating conditions. During discharge, the stored energy in the supercapacitor is released as the ions return to the electrolyte. This process can also occur rapidly, allowing supercapacitors to deliver high-power bursts of electrical energy when needed. The voltage or current output during discharge is monitored to assess the energy storage and delivery capabilities of the supercapacitor. Charge-discharge testing allows for the determination of key performance metrics of supercapacitors, including specific capacitance, energy density, power density, cycle life. Charge-discharge testing is essential for evaluating the suitability of supercapacitors for various applications, including energy storage in hybrid and electric vehicles, renewable energy systems, portable electronics, and power backup systems. Charge-discharge testing is a crucial technique for characterizing the performance and behavior of supercapacitors, providing valuable insights into their energy storage capabilities, power handling capabilities, and durability.

The perturbation can be either by potential step (potentiostatic method) or by current step (galvanostatic method).

Potentiostatic (Voltage Step) Method:

The potentiostatic (voltage step) method is an electrochemical technique used to study the kinetics and mechanisms of electrode processes. It involves applying a constant potential (voltage) step to a working electrode and monitoring the resulting current response as a function of time. This method is particularly useful for studying electrochemical reactions at the electrode-electrolyte interface, such as electron transfer processes, adsorption, and desorption phenomena.

In the potentiostatic method, the following steps are typically involved:

1. Electrode setup: A three-electrode system is commonly used, consisting of a working electrode (where the electrochemical reaction of interest occurs), a reference electrode (to provide a stable reference potential), and a counter electrode (to provide the necessary current to the working electrode).
2. Potential step: Initially, the working electrode is held at a potential where no electrochemical reaction occurs (open circuit potential or a preset potential). Then, a potential step is applied, changing the working electrode potential to a value where the desired electrochemical reaction can take place.
3. Current measurement: After the potential step, the current response is measured as a function of time. The current-time transient provides information about the kinetics of the electrochemical process occurring at the working electrode.
4. Data analysis: The current-time transient can be analysed using various models and equations to extract kinetic parameters, such as the heterogeneous electron transfer rate constant, diffusion coefficients, and reaction mechanisms. Depending on the nature of the electrochemical process, different models and analysis techniques may be applied.

It is important to note that the potentiostatic method assumes that the applied potential step is instantaneous and that the system is initially at equilibrium. In practice, however, there may be non-ideal behavior, such as ohmic drop (iR drop) or capacitive effects, which need to be accounted for during data analysis.

The behaviour of the current 'i' with respect to time on application of the potential step V_0 can be expressed as:

$$i = \frac{V_0}{R} \exp(-\frac{t}{\tau})$$

The capacitor cells start discharging when the operation is reversed and the pattern of discharge curve is similar to the charging curve but with the reverse polarity of the current. The charge-discharge curves can be integrated numerically to obtain the total charge stored or released from the cell. The capacitance C can be evaluated by dividing the total charge by the applied voltage V0, i.e.

$$C = \frac{\int i dt}{V_0}$$

The potentiostatic method is widely used in various fields, including electrochemistry, battery research, corrosion studies, and electrocatalysis. It allows researchers to investigate the kinetics of electron transfer reactions, and the effects of different experimental conditions (e.g., potential, electrolyte composition, electrode material) on the electrochemical behavior of the system.

Galvanostatic Method:

The galvanostatic method is another key technique used for characterizing supercapacitors and other electrochemical energy storage devices. Here's an overview of how it works:

1. Principle: The galvanostatic method involves applying a constant current to the supercapacitor and monitoring the resulting voltage response over time. Unlike the charge-discharge method where the voltage is allowed to vary, in galvanostatic testing, the current remains constant throughout the experiment.
2. Experimental Setup: Similar to charge-discharge testing, the supercapacitor is connected to a power supply or potentiostat/galvanostat. In this case, the galvanostat mode is selected,

allowing a constant current to be applied to the device. The voltage across the supercapacitor is continuously measured during the experiment.

3. Current Application: A constant current is applied to the supercapacitor, causing ions from the electrolyte to accumulate at the electrode surfaces during charging or release during discharging. The current remains constant throughout the experiment, allowing for precise control and measurement of the electrochemical processes.

4. Voltage Response: As the supercapacitor charges or discharges under the constant current, the voltage across the device changes accordingly. This voltage response is monitored over time to track the progress of the charging or discharging process. The voltage may initially rise during charging and fall during discharging until it reaches a steady-state value.

5. Performance Analysis: Galvanostatic testing provides valuable information about the electrochemical behavior and performance of supercapacitors. By analysing the voltage response over time, key parameters such as charge/discharge kinetics, internal resistance, and capacitance can be determined. This data can be used to assess the energy storage efficiency, power handling capabilities, and overall performance of the supercapacitor.

When a supercapacitor cell is charged by a constant current i, the total voltage V developed across the cell can be expressed as:

$$V = iR_i + \frac{\int idt}{C}$$

As the current is constant, the expression can be written as:

$$V = i(R_i + \frac{t}{C_e})$$

Thus, for a current step, the voltage across an ideal supercapacitor cell, whose capacitance value Ce is expected to be constant, increases linearly with time. A schematic voltage-time (V-t) curve showing the linear variation is shown. After the full charging of the supercapacitor at the maximum permissible or desired voltage level, it can be discharged galvanostatically. The

decrease in voltage across the cell is also linear with respect to time. In the real EDL supercapacitors, an initial sharp drop in voltage while charging-discharging of the capacitor is observed due to an ohmic loss due to internal resistance of the cell. An ohmic internal resistance (IR) is referred to equivalent.

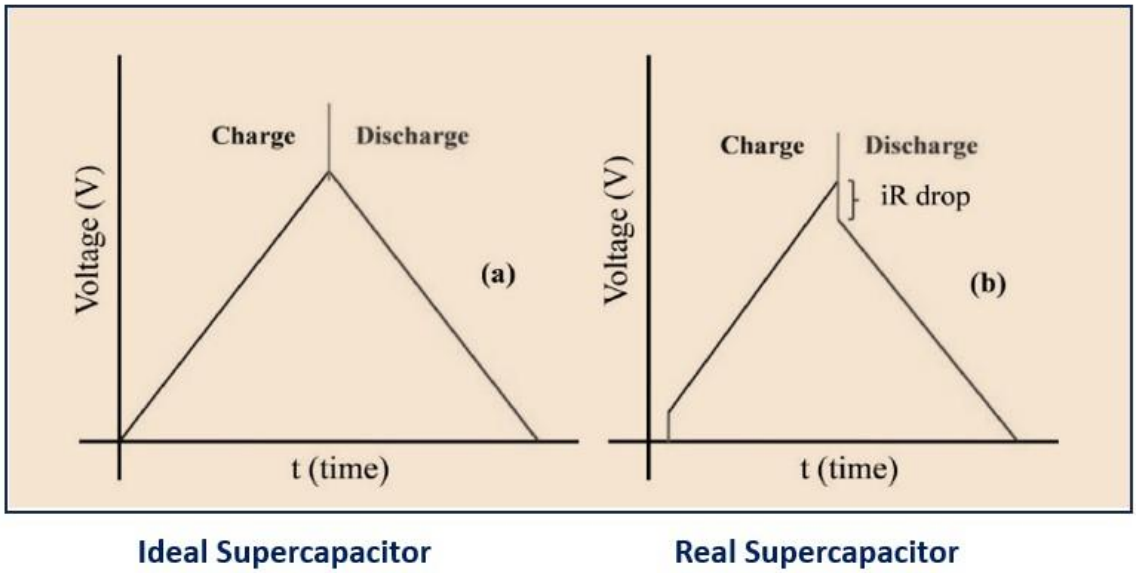


Fig 3.20 Charge-discharge behaviour of an ideal supercapacitor and a real supercapacitor

series resistance (ESR) of the supercapacitor cell. The value of ESR was calculated from following relation

$$ESR = \frac{\Delta V_{IR}}{2 \times i},$$

where the numerator is internal ohmic voltage drop and i is the applied discharge current. The overall capacitance of the supercapacitor cells has calculated from linear portion of the discharge curves using following relation:

$$C_{cell}^{dis} = \frac{i}{m_{tam} \times \left(\frac{\Delta V}{\Delta t}\right)},$$

where i (A) is the discharge current, m_{tam} is the total active mass (mass of activated carbon in both electrodes) in supercapacitor in g and V/t is slope of the discharge characteristic after IR drop.

The charge-discharge experiment can be carried out for several cycles (from 4000 to 8000 cycles) to test the stability cyclic efficiency of the cell. The ratio of discharge time to charging time referred to Coulombic Efficiency (CE), is calculated using following relation

$$\eta\% = \frac{\Delta t_d}{\Delta t_c} \times 100\%,$$

The energy density(E) and power density(P) are calculated from charge-discharge characteristics at different current rates using following relations

$$E = \frac{C_{cell}^{dis} \times (\Delta V)^2}{2} \times \frac{1000}{3600}$$

$$P = \frac{E \times 3600}{\Delta t}$$

Galvanostatic method is a powerful tool for characterizing the electrochemical behavior and performance of supercapacitors, providing valuable insights for their design, optimization, and application. The shape and features of the potential-capacity curves can provide insights into the kinetics of the electrochemical reactions, phase transitions, and thermodynamic properties of the electrode materials. The galvanostatic method is widely used in the characterization of battery materials, including lithium-ion batteries, sodium-ion batteries, and other energy storage systems. It helps researchers understand the electrochemical behavior, identify potential limitations, and optimize the performance of these systems.

3.5.5 Lithium- Ion Transference Number Measurement

The lithium-ion transference number, often denoted as t_Li^+ or t+, is a critical parameter that quantifies the fraction of the total ionic conductivity in an electrolyte that is contributed by lithium ions. It is an important property in the context of lithium-ion batteries and other electrochemical devices involving lithium-ion transport.

The lithium-ion transference number is defined as the ratio of the lithium-ion conductivity to the total ionic conductivity of the electrolyte:

$$t_+ = \frac{\sum I_+}{\sum (I_+ + I_-)}$$

$$t_- = \frac{\sum I_-}{\sum (I_+ + I_-)}$$

The value of the lithium-ion transference number ranges from 0 to 1. A transference number of 1 indicates that all the ionic conductivity in the electrolyte is due to the migration of lithium ions, while a value of 0 means that lithium ions do not contribute to the ionic conductivity at all. The lithium-ion transference number has significant implications for the performance and efficiency of lithium-ion batteries. A higher transference number is generally desirable because it means that a larger fraction of the current is carried by lithium ions during charging and discharging processes, leading to improved energy efficiency and reduced concentration polarization within the electrolyte. However, in practice, most liquid and polymer electrolytes used in lithium-ion batteries have relatively low lithium-ion transference numbers, typically in the range of 0.2 to 0.5. This is because other ions, such as anions from the lithium salts or impurities, also contribute to the overall ionic conductivity. Therefore, Li+ ion transference number in lithium polymer electrolytes is a crucial issue due to their application in solid-state lithium-ion battery (LIB) as both the electrolyte and the separator. There are various experimental techniques to measure the transference number such as **(a)** Tubandt‟s method, **(b)** Wagner‟s polarization technique, **(c)** Electrochemical potential measurement technique,

(d) AC impedance technique, **(e)** DC conductivity method and **(f)** Combined DC/AC technique.

In the present work, the Li^+ ion transference number was measured using combined DC/AC technique. According to this technique AC impedance of the cell was recorded having a symmetric cell configuration of M (Li metal) || MX (lithium polymer electrolytes) || M (Li metal) and charge transfer resistance was determined. Thereafter, the symmetric cell is polarized by applying a small DC polarization voltage (10 mV). The Li^+ ion transference number was calculated by the following relation:

$$t_{Li^+} = \frac{[I_{ss}(\Delta V - R_0 I_0)]}{[I_0(\Delta V - R_{ss} I_{ss})]},$$

To improve the lithium-ion transference number and enhance battery performance, researchers have explored various strategies, including the use of ceramic solid electrolytes, single-ion conductors, or the incorporation of additives or fillers that can selectively enhance lithium-ion transport while suppressing the mobility of other ions. Lithium-ion transference number measurement is an essential tool for evaluating the transport properties of lithium ions within electrolytes and gaining insights into the electrochemical behavior of lithium-ion batteries. It helps in the development of advanced electrolyte formulations and battery designs for improved performance and durability.

References:

[1] G. Höhne, W. Hemminger and H. J. Flammersheim, Differential scanning calorimetry, 2nd edition (Springer) (2003).

[2] R. Reichelt, Editor, Scanning Electron Microscopy, Springer, New York, USA (2007).

[3] R. F. Egerton, Physical Principles of Electron Microscopy Springer, New York, USA (2005).

[4] B. Wunderlich, Thermal analysis, Academic Press, New York (1990).

[5] P. J. Haines, Thermal methods of analysis: principles, applications and problems, Blackie Academic& Professionals, London (1995).

[6] G. Schaumburg, Dielectric Newletter 1 ((March 1994)).

[7] T. a. A. EC-Lab® Software, V10.1x, Biologic-Science Instruments, copyright Feb. 2011, EC-Lab Software, Technique and Application, V10.1x, Biologic- Science Instruments, copyright Feb. 2011.

[8] K. Karuppasamy, P. A. Reddy, G. Srinivas, A. Tewari, R. Sharma, X. S. Shajan and D. Gupta, J. Member. Sci. 514 (2016).

[9] S. Ferrari, E. Quartarone, P. Mustarelli, A. Magistris, M. Fagnoni, S. Protti, C. Gerbaldi and A. Spinella, Journal of Power Sources 195 (2010).

[10] J. Evans, C. A. Vincent and P. G. Bruce, Polymer 28 (1987).

CHAPTER 4

SAMPLE PREPARATION AND FABRICATION

4.1 Introduction

For the current study polymer electrolytes embedded with ionic liquids, plasticizers and covalent organic frameworks (COFs) were synthesized. For this GPE -1, GPE-2, GPE-3 polymer electrolytes were synthesized having different composition. Electrodes were prepared using activated carbon (AC), carbon black (CB) and PVdF in definite ratio by weight. Finally with the prepared samples supercapacitors are fabricated and comparative study of the samples were done which will be discussed in detail in Chapter 5 of this study. Finally, the electrolyte with the best characterization results is used to fabricate a lithium-ion coin cell and the performance of the coin cell was evaluated. The characterization results and performance analysis of the lithium-ion coin cell will be discussed in Chapter 5 of this study. For the current study different characterization techniques were used which includes XRD, FESEM. FTIR for structural analysis, DSC and TGA for thermal analysis of polymer electrolytes. Electrical characterization was carried out on the prepared samples in a wide frequency range of 0.01 Hz - 3 GHz and in a wide temperature range. For the current study electrochemical measurements was done on the fabricated lithium-ion batteries and supercapacitors using polymer electrolytes as an electrolyte/separator using a multichannel electrochemical analyzer, the details of which will be discussed in subsequent chapters.

4.2 Sample preparation

For the current study three different samples were prepared with polymer to form the electrolytes of the supercapacitors the preparation technique of which is discussed here. The details of electrode preparation are discussed here.

4.2.1 Preparation of P(VdF-HFP) – Ionic Liquid EMIMTFSI based Gel Polymer Electrolytes

For the current study Poly (vinylidene fluoride-hexafluoropropylene) (P(VdF-HFP), having average molecular weight approximately 455,000 g/mol was used as a host polymer. Lithium bis(trifluoromethanesulfonyl)imide (LiTFSI, ≥ 99.0%) was used as salt. The ionic liquid used

1-Ethyl-3-methylimidazolium bis(trifluoromethylsulfonyl)imide (EMIMTFSI) for our study. All chemicals were procured from Sigma Aldrich and stored inside the argon gas filled glove box with <0.5 ppm H_2O and < 0.5 ppm O_2.



Fig. 4.1 *Host Polymer used for the study*

No additional purification was performed before using these chemicals. Acetone (Merck purity ≥ 99.5 %) was used for the preparation of the polymer electrolyte. The ionic liquid-based P(VdF-HFP) gel polymer electrolyte films of following compositions were prepared using "standard solution cast" technique:

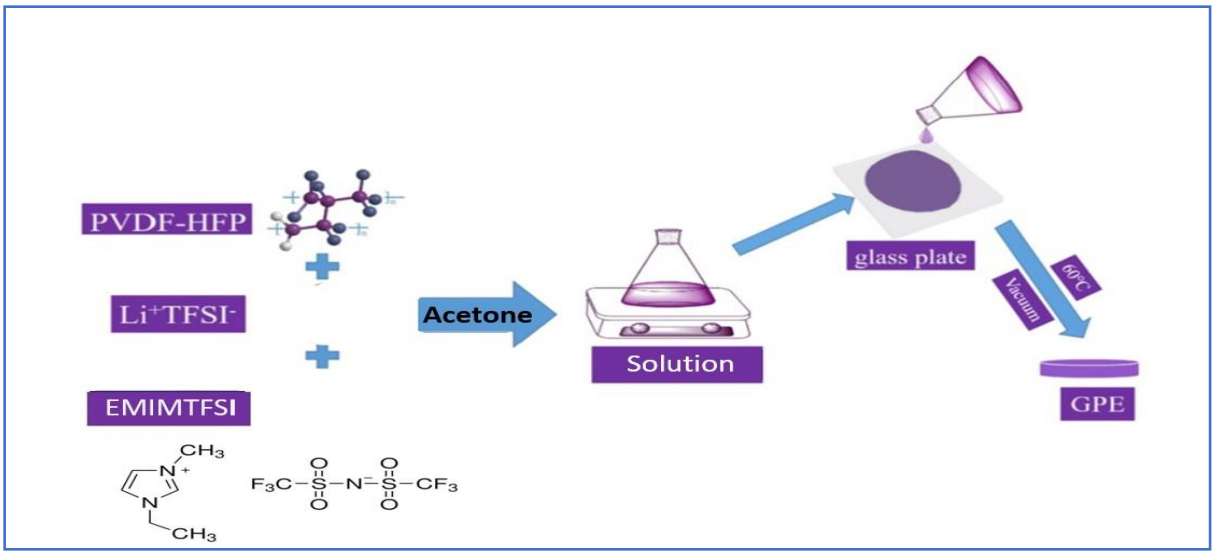


Fig. 4.2 *Schematic of Solution Cast Technique for preparing gel polymer electrolyte using PVdF-HFP as host polymer, LITFSI salt and EMIMTFSI as ionic liquid*

Gel Polymer Electrolyte Preparation (GPE-1)

The host polymer matrix P(VdF-HFP) embedded and incorporated with EMIMTFSI ionic liquid-based gel polymer electrolytes were prepared using solution cast technique The chemicals used for this preparation are P(VdF-HFP) as host polymer and EMIMTFSI as ionic liquid. P(VdF-HFP) and EMIMTFSI was taken in the ratio 20:80 weight %. Density of EMIMTFSI is 1.52 gm/ml. The host polymer P(VdF-HFP) is dissolved in acetone taken in a glass beaker and was placed on a magnetic stirrer having a hot top and it was heated at 70^0 C till the polymer pellets gets dissolved. After that EMIMTFSI was added to the solution and was stirred further under heat till a viscous and homogeneous solution is formed due to evaporation of solvent at ambient temperature. Finally, the solutions were cast onto polytetrafluoroethylene containers to get homogeneous and free-standing films by slow evaporation of the solvent at ambient condition. The thickness of the prepared free-standing polymer films was in the range from 0.35 mm to 0.5 mm.

GPE -1: EMIMTFSI/P(VdF-HFP) with ratio 80:20 (w/w)

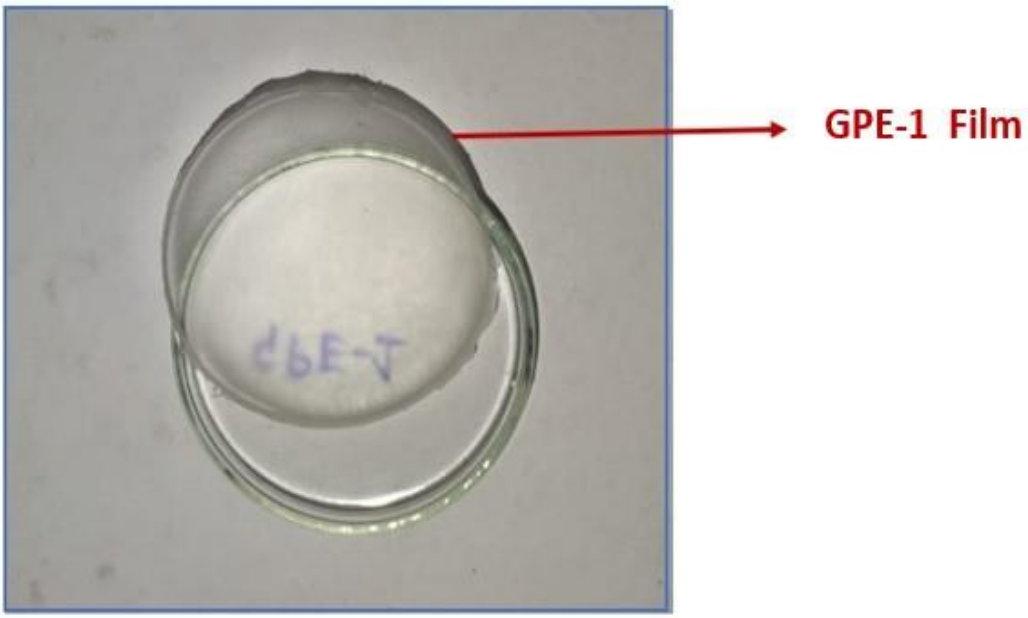


Fig. 4.3 *GPE -1 polymer film after casting*

Gel Polymer Electrolyte Preparation (GPE-2)

The chemicals used for this preparation are P(VdF-HFP) as host polymer and EMIMTFSI as ionic liquid and LITFSI as the salt. P(VdF-HFP) and EMIMTFSI was taken in the ratio 1:4 by weight. Density of EMIMTFSI is 1.52 gm/ml. The host polymer P(VdF-HFP) is dissolved in acetone taken in a glass beaker and was placed on a magnetic stirrer having a hot top and it was heated at 70^0 C till the polymer pellets gets dissolved. After that EMIMTFSI was added to the solution and was stirred further under heat. After stirring for an hour over the magnetic stirrer LITFSI salt (30 % by weight) was added and the stirring process was continued under heat till the LITFSI salt gets completely dissolved in the solution and a viscous and homogeneous solution is formed due to evaporation of solvent at ambient temperature. Finally, the solutions were cast onto polytetrafluoroethylene containers to get homogeneous and free-standing films by slow evaporation of the solvent at ambient condition. The thickness of the prepared free-standing polymer films was in the range from 0.35 mm to 0.5 mm.

GPE -2: EMIMTFSI/P(VdF-HFP) with ratio 80:20 (w/w)
LITFSI salt (30 % by weight)

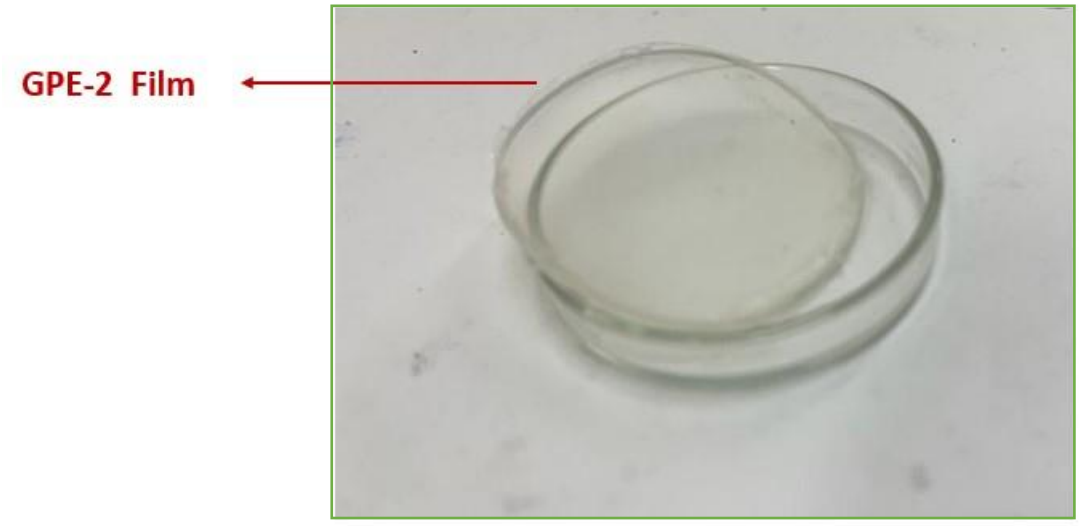


Fig. 4.4 *GPE -2 polymer film after casting*

Preparation of Covalent Organic Frameworks (DAAQ-TEP-COF)

DAAQ-TEP -COF was prepared by a condensation reaction of DAAQ and TEP. DAAQ and TEP are two monomers which were used to synthesize DAAQ-TEP-COF. TEP (70 mg) and 60 mg of DAAQ were added to a 1,4-dioxane/mesitylene (v:v = 1:1) mixture solution in a pressure bottle reactor [31] The mixture was stirred at room temperature until the solid was dissolved completely. Then, 0.4 mL (6 M) of aqueous acetic acid solution was added to the reactor under a nitrogen atmosphere before the solution was heated at 100 °C for 72 h. The precipitate was collected via centrifugation, washed six times using 1,4-dioxane, tetrahydrofuran, and acetone in sequence, and dried at 100 °C under vacuum to produce DAAQ-TEP-COF as a red powder in 90% yield. One of the most remarkable features of COFs is their exceptionally high surface area and permanent porosity. This high porosity makes them attractive for applications such as energy storage.

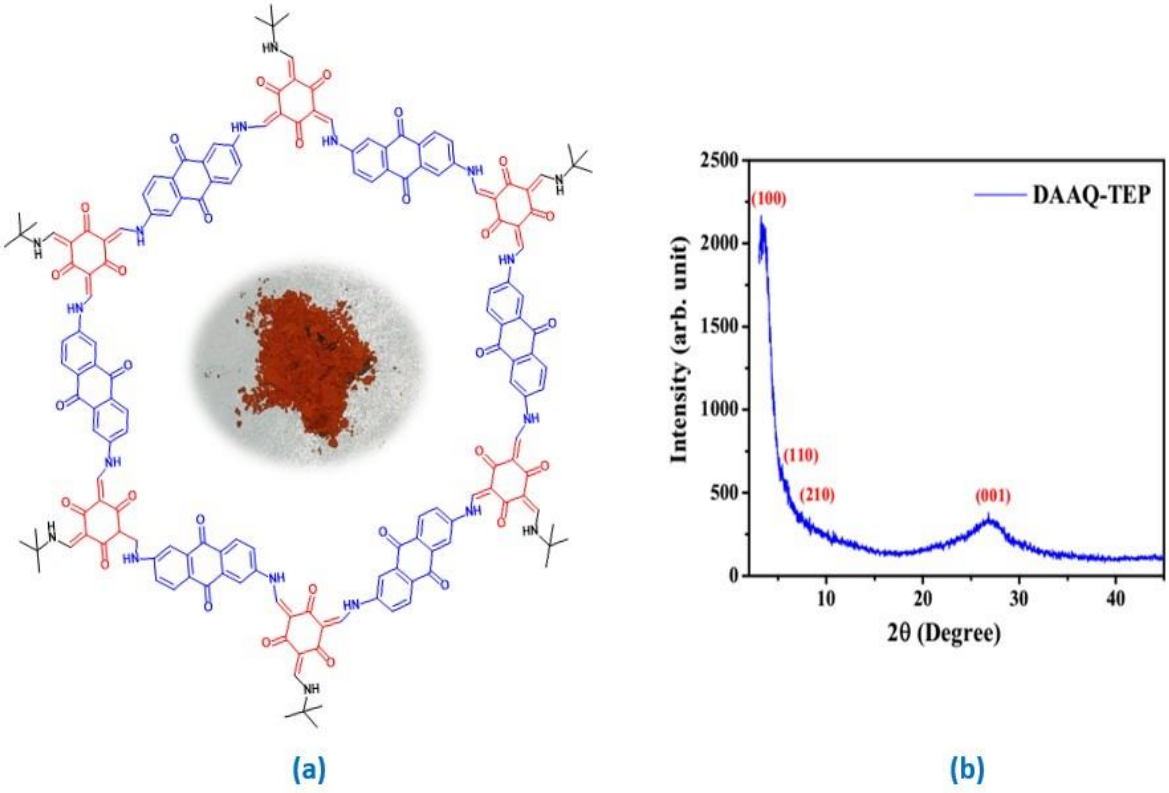


Fig. 4.5 *(a) Structure of DAAQ-TEP COF (b) XRD of DAAQ-TEP COF*

Monomers are the building blocks of polymers. For this study we have used DAAQ monomer and TEP monomer to form DAAQ-TEP COF.

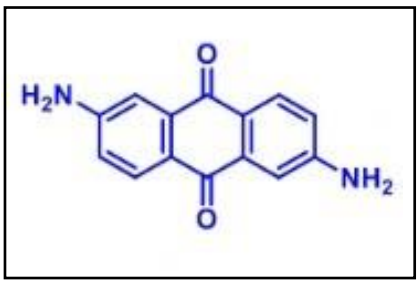


Fig. 4.6 *Structure of DAAQ monomer*

The conductivity of COFs can be tuned and optimized for various applications, such as energy storage (e.g., supercapacitors, batteries). 2-dimensional COFs (2DCOFs) with a regular 1D channel usually provide short and fast ion conduction path, which makes themselves the potential candidates as the ideal ionic conductors by absorbing ILs in ionic liquid -based gel polymer electrolyte. Furthermore, the structure and transport properties of the ILs encapsulated into COF ionic conductors usually play an essential important role in the ion transport of electrolytes. Once encapsulated into the nanosized pore of COFs ionic conductors, the ILs present significantly different structure and dynamics behaviours from the bulk phase.[32,33] DAAQ-TEP COF has been used along with EMIMTFSI ionic liquid to enhance ionic conductivity and obtain high performance of the ionic liquid based for a lithium-ion battery.

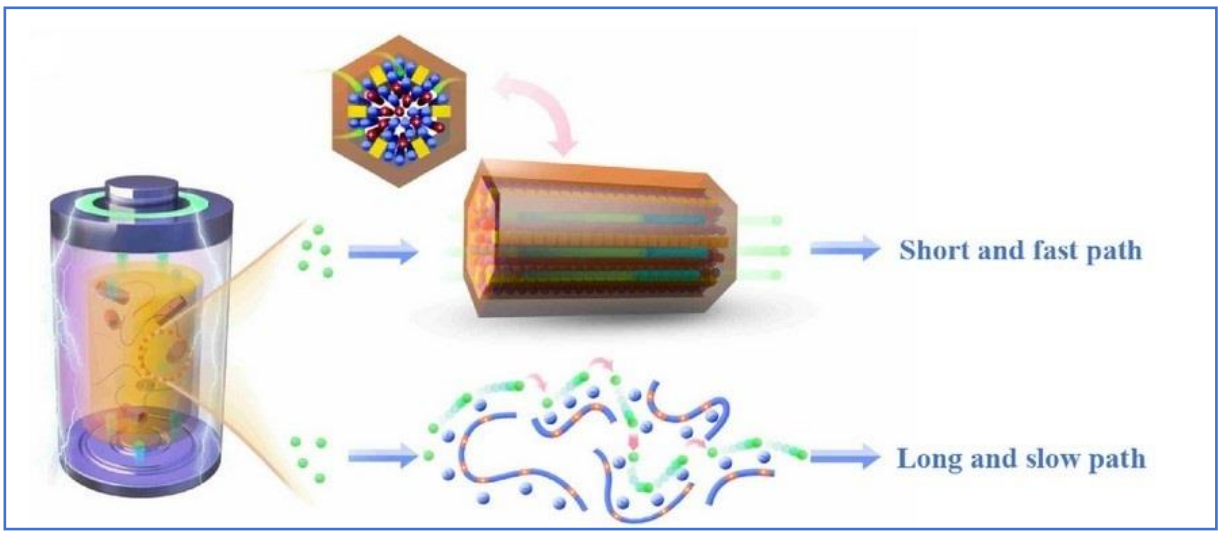


Fig. 4.7 *Schematic showing conduction mechanism of ions in presence of COF. [4]*

Gel Polymer Electrolyte Preparation (GPE-3)

For this preparation the chemicals used are P(VdF-HFP) as host polymer, EMIMTFSI as ionic liquid, LITFSI as salt and DAAQ-TEP COFs (covalent organic frameworks) as additives. For this electrolyte preparation Covalent Organic Frameworks (COFs) (1% by weight) was initially taken in a beaker. Around 2 ml of dimethyl formamide (DMF) was added to it and the mixture is sonicated till the COF mixes uniformly in the solution. After COF has thoroughly mixed in the solution, P(VdF-HFP) pellets were added to the solution. P(VdF-HFP) and EMIMTFSI was taken in the ratio 1:4 by weight. The solution was placed on a magnetic stirrer having a hot top and it was heated at 70^0 C till the polymer pellets gets dissolved in this solution. After that EMIMTFSI ionic liquid was added to the solution and was stirred further under heat. After stirring for an hour over the magnetic stirrer LITFSI salt (30 % by weight) was added and the stirring process was continued under heat till the LITFSI salt gets completely dissolved in the solution and a viscous and homogeneous solution is formed. Finally, the solutions were cast onto polytetrafluoroethylene containers and the containers were kept overnight in a heat chamber at 70^0 C to get homogeneous and free-standing films. The thickness of the prepared free-standing polymer films was in the range from 0.35 mm to 0.5 mm.

GPE -3: EMIMTFSI/P(VdF-HFP) with ratio 80:20 (w/w)
LITFSI salt (30 % by weight) and DAAQ-TEP COF (1 % by weight)

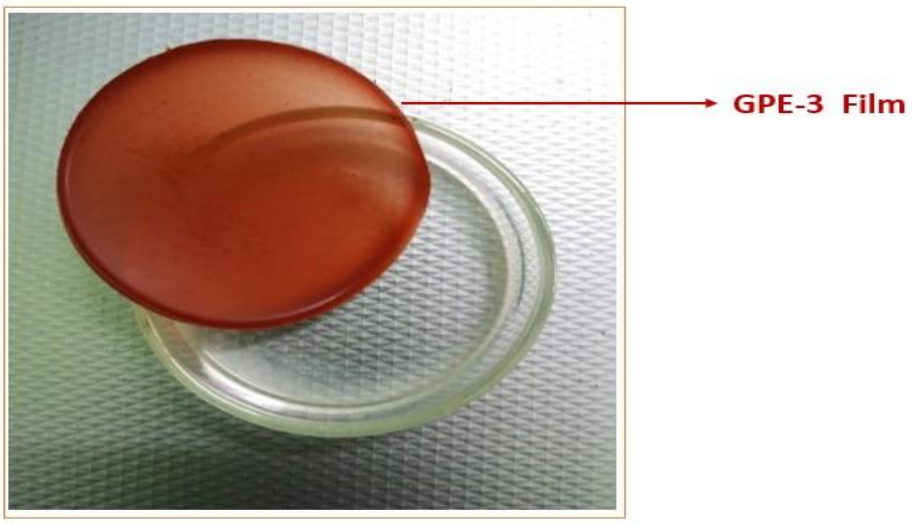


Fig. 4.8 *GPE -3 polymer film after casting*

This gel polymer electrolyte was used to fabricate a lithium-ion coin cell due to its superior properties obtained after characterization of the sample. The characterization results of all the samples GPE-1, GPE-2 GPE-3 will be discussed in detail in Chapter 5 of this study. The performance of the lithium-ion coin cell fabricated with this gel polymer was also evaluated the details of which will be discussed in detail in Chapter 5 of this study.

4.2.2 Preparation of Electrode for Energy Storage Devices

For the current study electrode was prepared for Lithium-ion battery and Electrochemical double layer capacitors.

Electrode for Lithium Ion Battery

For full cell lithium-ion battery fabrication, LiCoO2 (MTI Corp.)/LiFePO4 (Sigma Aldrich) was used as an active material for cathode. LiCoO2/LiFePO4 cathode was prepared by coating a N-methyl-2 pyrrolidone (NMP) (Sigma Aldrich) based slurry containing LiCoO2/LiFePO4 powder, acetylene carbon black (MTI Corp.) and PVdF (MTI Corp.) in the ratio of 80:10:10 (wt.%) onto aluminium (Al) foil (MTI Crop.). After coating on the aluminium (Al) foil, the electrodes were dried at 90 ^{0} C under vacuum for one day. Similarly, negative electrode was prepared by coating a N-methyl-2 pyrrolidone (NMP) based slurry of graphite powder (MTI Corp.), acetylene carbon black and PVdF in the ratio of 75:15:10 (wt %) onto copper (Cu) foil (MTI Crop.).

Electrode for Electrochemical Double Layer Capacitor

For this the Activated Charcoal, Carbon Black and PVdF were taken in a centrifuge tube. They were taken by the weight ratio of 75:10:15. 400 µl of DMF was added into it to form a slurry. Now flexible graphite sheet is taken and cut into strips of width 1 cm. The tip of 1x1 $cm^2$was coated with the slurry thus we get activated carbon electrodes. Wt. of Activated Charcoal: 40 mg (75%), Wt. of Carbon Black: 5.33 mg (10%), Wt. of PVdF: 8 mg (15%) (M/wt. 534,000 g/mol) activated carbon (AC, TCI Chemicals, Japan) and acetylene carbon black (CB, MTI Crop.) powders were kept in vacuum overnight at approximately 90 ^{0} C before use. The electrodes for supercapacitor were prepared by coating a N-methyl-2 pyrrolidone (NMP, sigma Aldrich) based homogeneous

slurry containing AC powder, acetylene carbon black and PVdF (MTI Crop.) in the ratio of 70:10:20 (w/w) on a flexible graphite sheet in a desktop coating machine (Ranga Techno Impex, India). After coating on the flexible graphite sheets with 0.5 mm thickness (NICKUNJ Eximp Entp P LTD), the electrodes were dried at 90 ^{0} C under vacuum for 1 day. After drying at 90 ^{0} C, the electrodes were cut into 1 cm x 1 cm square shape (average area ≈1 cm^2). The average thickness of electrodes was about 150 - 160 µm for activated carbon mass loading of about 1.3 - 1.5 mg/cm^2.

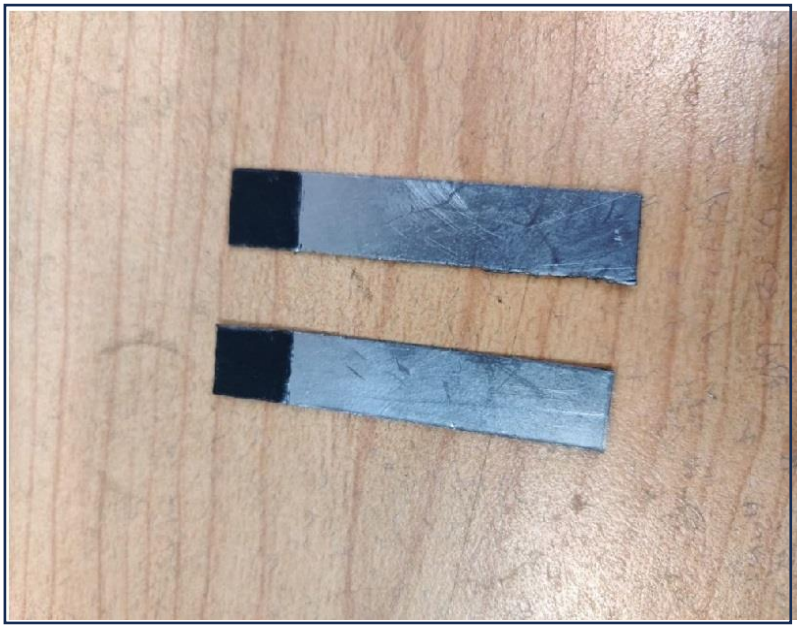


Fig. 4.9 *Electrodes for EDL Capacitor*

4.3. Fabrication of Energy Storage Devices

The fabrication of energy storage devices, such as batteries and supercapacitors, involves various processes and materials The electrodes and electrolytes which were prepared for this study was used to fabricate electrochemical double layer capacitor and GPE-3 was further used to fabricate a lithium -ion coin cell (CR 2032). It involves the electrode preparation, electrolyte preparation, cell assembly. These processes are already discussed in previous stages. Common fabrication techniques include slurry coating and drying (e.g., doctor blade, slot-die coating), calendering (compressing and smoothing electrode layers),roll-to-roll processing for continuous manufacturing ,vacuum or inert atmosphere processing for sensitive materials, thermal treatment (e.g., annealing, sintering) for material activation or structure enhancement

4.3.1 Electrochemical Double Layer Capacitor

An electrochemical double layer capacitor, also known as a supercapacitor or ultracapacitor, is a type of energy storage device that stores electrical energy electrostatically by forming a double layer of electrolyte ions at the electrode-electrolyte interface. The electrochemical double layer capacitor (EDLC) is fabricated from two symmetrical activated carbon coated flexible graphite electrodes with a gel polymer electrolyte separating them. The EDL capacitors are fabricated and characterized inside the argon gas filled glove box (mBRAUN, LAB star ECO) with H2O < 0.5 ppm O2 < 0.5 ppm.

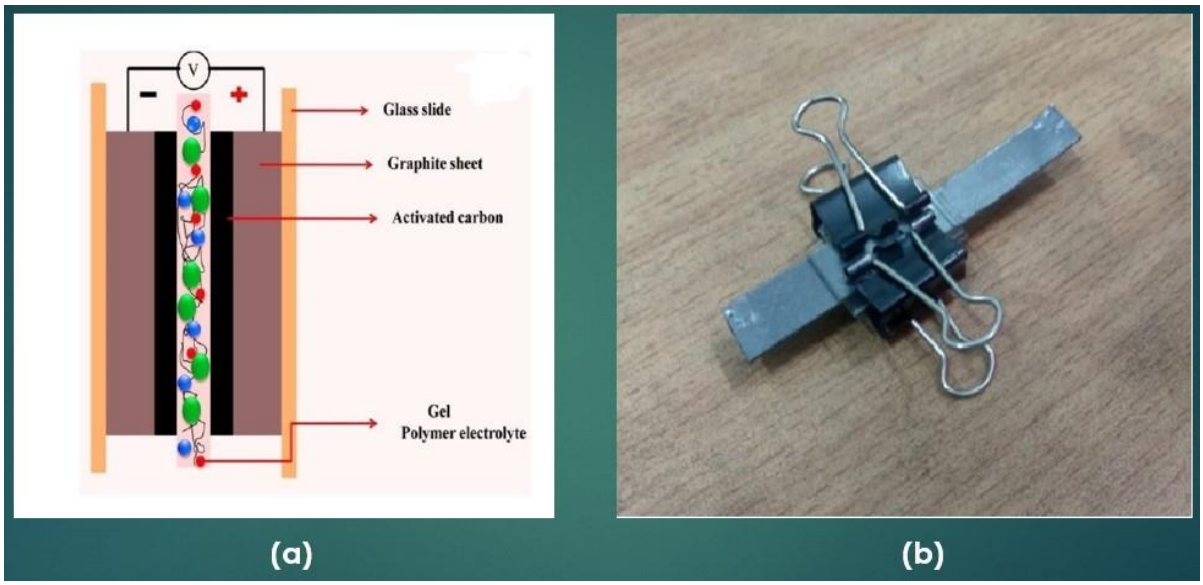


Fig. 4.10 *(a) Schematic diagram of the EDL capacitor containing gel polymer electrolytes, (b) Practically fabricated EDL capacitor in lab.*

In order to characterize the electrochemical performance of supercapacitors (EDLCs), the different physical techniques were adopted mainly, (i) electrochemical impedance spectroscopy (EIS), (ii) cyclic voltammetry (CV) and (iii) galvanostatic charge-discharge (GCD) methods. Electrochemical performance of the cells assembled as above were studied using VMP3 (Biologic) multi-channel potentiostat/ Galvanostat and analysed using EC Lab® software. The characterization details of fabricated supercapacitor for the current study will be discussed in detail in Chapter 5

4.3.2 Full Cell Lithium-Ion Batteries (LIBs)

A full cell lithium-ion battery refers to a complete lithium-ion battery cell, which consists of several key components which includes cathode, anode, electrolyte separator, current collector, casing. For our work polymer electrolyte was used. Here, CR2032 coin cell type LIBs has been used. The sizes of the different kinds of coin cells restrict the diameter of the electrode material that can be used, for example, CR2032 is 20 mm in diameter; the electrodes are usually 13 mm. $LiFePO_4$ have been used as an active material of cathode while graphite has been used as an active material of anode.

Configuration: $LiFePO_4$ || GPE-3 || Li

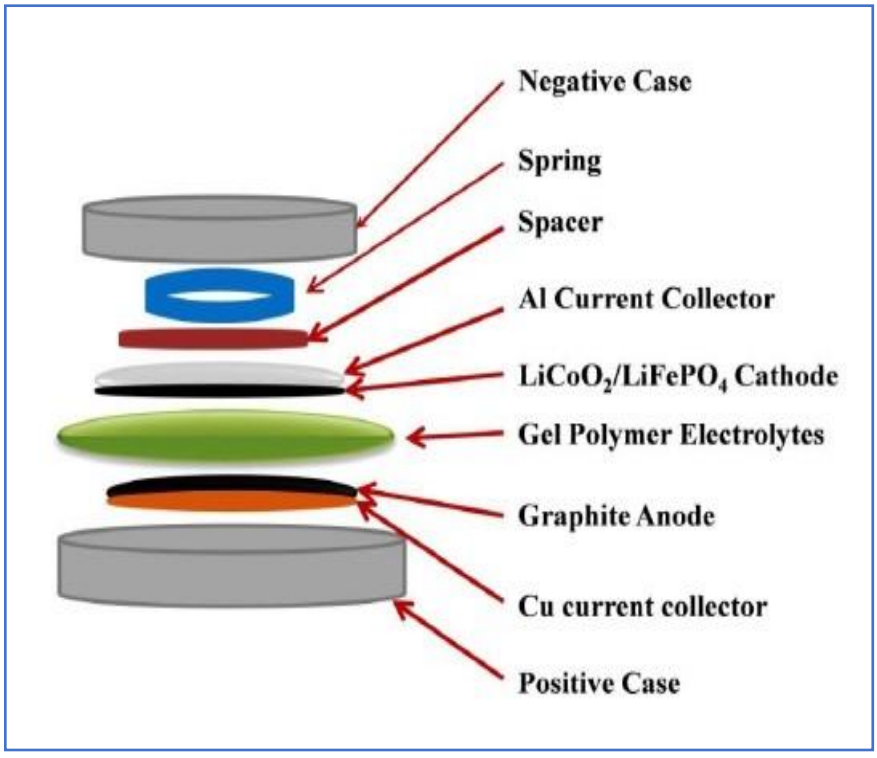


Fig. 4.11 *Schematic diagram of coin cell type full cell lithium-ion battery[5]*

The electrochemical redox reaction takes place at the electrode-polymer electrolyte interface when the current passes through the cell. The galvanostatic charge-discharge experiment is used for measuring the specific capacity and rate capability of the material. The charge and discharge rate are selected depending upon the theoretical specific capacity of the cathode material under study. The current used for charging-discharging of the electrochemical cell

under study is indicated by C rate. The theoretical capacity of the electrode (cathode) and expressed as $C_{ED} = W_{AM} \times C$. Here, W_{AM} is weight of the active material and C is the theoretical specific capacity of active material. The theoretical capacity of LiCoO2 and LiFePO4 active cathode materials are 160 and 170 mAh/g respectively. The C-rate, which is the current rate at which charge discharge cycling is performed, can be deducted as follows

$$C_{rate} = \frac{W_{AM} \times C}{n}$$

where, C_{rate} is the rated capacity i.e. total capacity of the battery could deliver in "n" hours.

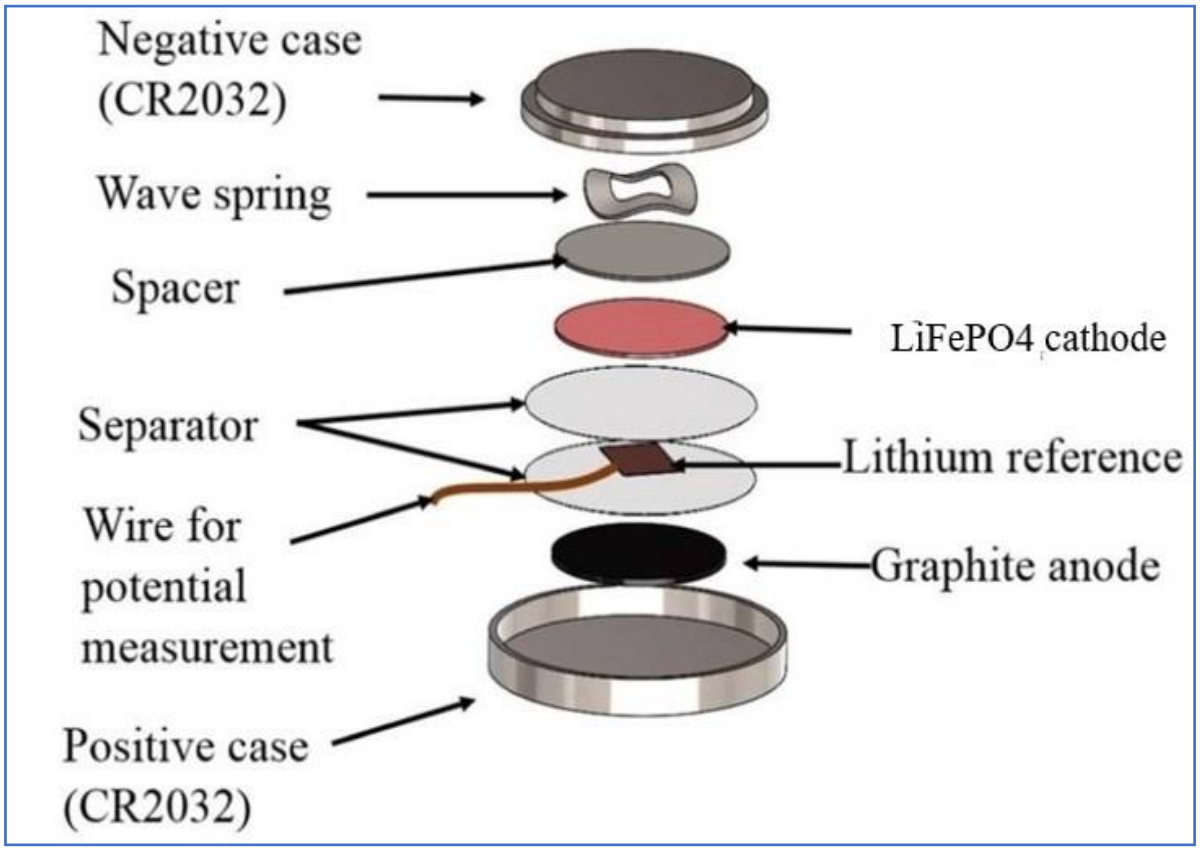


Fig. 4.12 *Different components of CR2032 coin cell. (Ref- ResearchGate)*

The coin cell CR2032 type lithium-ion full cell is fabricated inside the argon gas filled glove box (mBRAUN, LAB star ECO) with H2O < 0.5 ppm O2 < 0.5 ppm. The electrochemical performances of the cells assembled as above are studied using VMP3 (Biologic) multi-channel potentiostat/ Galvanostat and analysed using EC Lab® software at room temperature.



Fig. 4.13 *Glove box for fabrication.*

References:

[1] R. Reichelt, Editor, Scanning Electron Microscopy, Springer, New York, USA (2007).

[2] R. F. Egerton, Physical Principles of Electron Microscopy Springer, New York, USA (2005).

[3] G. Höhne, W. Hemminger and H. J. Flammersheim, *Differential scanning calorimetry, 2nd edition (Springer)* (2003).

[4] B. Wunderlich, Thermal analysis, Academic Press, New York (1990).

[5] P. J. Haines, Thermal methods of analysis: principles, applications and problems, Blackie Academic& Professionals, London (1995).

[6] G. Schaumburg, *Dielectric Newletter* **1** ((March 1994)), p. 4.

[7] T. a. A. EC-Lab® Software, V10.1x, Biologic-Science Instruments, copyright Feb. 2011, EC-Lab® Software, Technique and Application, V10.1x, Biologic- Science Instruments, copyright Feb. 2011.

[8] K. Karuppasamy, P. A. Reddy, G. Srinivas, A. Tewari, R. Sharma, X. S. Shajan and D. Gupta, *J. Member. Sci.* **514** (2016), p. 350.

[9] S. Ferrari, E. Quartarone, P. Mustarelli, A. Magistris, M. Fagnoni, S. Protti, C. Gerbaldi and A. Spinella, *Journal of Power Sources* **195** (2010), p. 559.

[10] J. Evans, C. A. Vincent and P. G. Bruce, *Polymer* **28** (1987), p. 2324.

CHAPTER 5

CHARACTERIZATION, RESULTS AND DISCUSSION

5.1 Introduction

With the depletion of fossil fuel resources and climate change among other factors, modern society is experiencing an increasingly pressing need for the development of high-performing solid-state electrochemical charge storage devices. Lithium-ion batteries, Electrical double layer (EDL) supercapacitors, and other alternative green energy storage devices have been the focus of research efforts throughout the past few years. EDL supercapacitors and lithium-ion batteries have different charge storage processes for a few fundamental reasons. While lithium-ion batteries store energy via electrochemical reactions, EDL supercapacitors store charge by electrostatic interaction between electrode surfaces and charge carriers of electrolytes. The cycle life of supercapacitors is higher than that of batteries [1], while batteries can store more energy than supercapacitors Due of their wide electrochemical potential window, higher ionic conductivity (<1 mS cm^{-1}) at room temperature, and better electrode-polymer interface stability compared to liquid electrolytes, gel polymer electrolytes (GPEs) have attracted a lot of attention lately for their potential use as an electrolyte/separator in energy storage devices.

A gel polymer electrolyte is a type of electrolyte used in batteries, particularly in solid-state lithium-ion batteries. It consists of a polymer matrix, typically a gel, that contains lithium ions for conduction. This gel matrix provides mechanical support and flexibility while allowing for the movement of ions necessary for the battery's operation. Compared to traditional liquid electrolytes, gel polymer electrolytes offer several advantages, including improved safety, reduced risk of leakage, and enhanced stability. They also have the potential to increase the energy density and cycle life of batteries.

Among various polymer matrices poly (vinylidene fluoride-co-hexafluoropropylene) nowadays[P(VdF-HFP)] copolymer is the most widely studied host polymer matrix used for the preparation of high performance GPEs, because the crystalline part P(VdF) of this polymer supports the mechanical property, amorphous part P(HFP) helps to trap the liquid electrolytes and high dielectric constant which dissolve more ions. Development of high-performance gel polymer electrolytes has been an active research area nowadays. ILs plays dual roles in polymer electrolyte systems such as supplier of additional ions as well as critical role of plasticizers.

The goal of this thesis is to prepare GPEs using copolymer P(VdF-HFP) and 1-Ethyl-3-methylimidazolium bis(trifluoromethylsulfonyl)imide (EMIMTFSI) ionic liquid. The effect of lithium bis(trifluoromethanesulfonyl)imide (LiTFSI) salt. Lithium bis(fluorosulfonyl)imide, often abbreviated as LiTFSI, is a lithium salt commonly used as an electrolyte additive or component in lithium-ion batteries, particularly in advanced electrolyte. Advantages of this salt is it provides improved stability, wide electrochemical window, high conductivity, low volatility and compatibility to all types of electrode materials. COFs are added to one of the samples while preparing the electrolyte and it was then used to fabricate supercapacitors and Li-ion battery. Covalent organic frameworks (COFs) are a class of porous, crystalline materials composed of organic building blocks linked by strong covalent bonds. COFs are designed with specific structures at the molecular level, allowing for precise control over their pore sizes, shapes, and surface functionalities. COFs offer tunable pore sizes and shapes, allowing for the design of materials with tailored properties for various applications like energy storage.[2]

EDL supercapacitors using GPEs are fabricated. Activated Carbon (AC) is used as an electrode material for the process. For the samples prepared physicochemical properties such as structural, thermal properties, ac conductivity, ionic conductivity, lithium-ion transport number, electrochemical potential window of the GPEs is investigated. Comparative study of electrochemical performances of these supercapacitors are studied. Finally, a lithium-ion battery is assembled using the sample containing COFs and electrochemical performance and Li-ion transport of the sample was studied.

5.2 Results and Discussion

The preparation of P(VdF-HFP)-EMIMTFSI ionic liquid based solid-state gel polymer electrolytes are described in Chapter 4. The advantages of this solid-state gel polymer electrolytes were also discussed in Chapter 4 Electrode preparation for Li-ion and Supercapacitor fabrication is also discussed in Chapter 4. Structure, morphological, thermal, electrochemical analysis of the samples are discussed as under:

5.2.1 Crystal Structure Characterization

X Ray Diffraction (XRD)

Crystal structure analysis for the samples prepared were done by X ray Diffraction. XRD patterns of pure P(VdF-HFP), GPE-1, GPE-2 and GPE-3 films are shown as under:

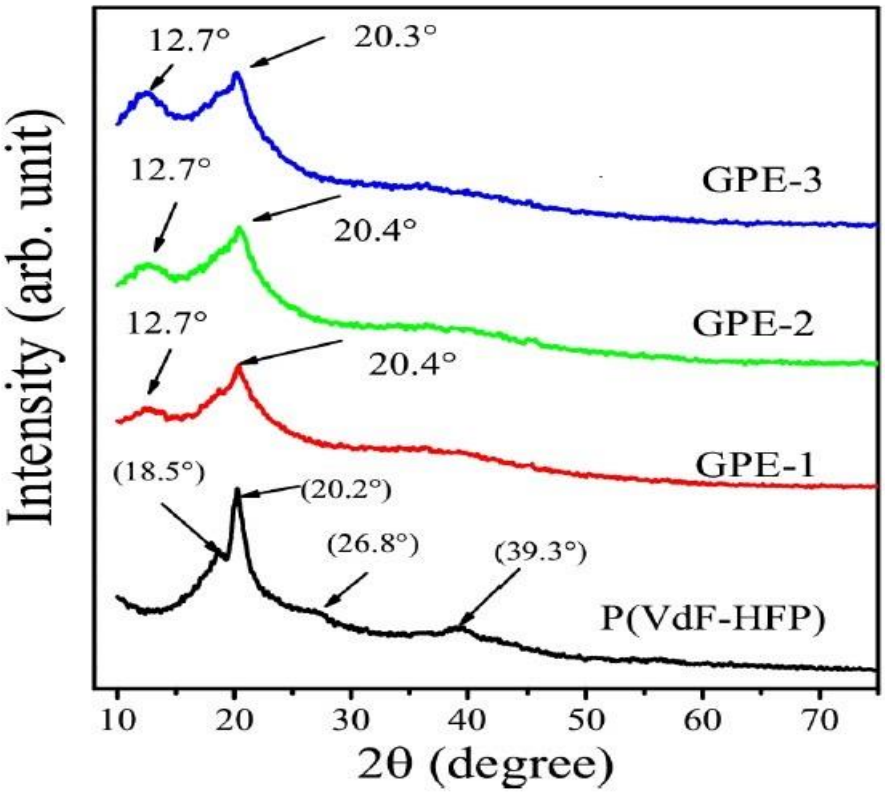


Fig. 5.1 *XRD of pure P(VdF-HFP), GPE-1, GPE-2 and GPE-3 gel polymer electrolytes*

The XRD patterns of P(VdF-HFP) show different crystalline peaks at 2 Θ approximately 18.5^0, 20.2^0, 26.8^0 and 39.3^0. Presence of peaks provide evidence that the P(VdF) units in the copolymer partially contribute to the crystallization property and provide P(VdF-HFP) with an overall semi-crystalline structure. The illustration shows how the injection of ionic liquid into host polymer electrolytes significantly alters the structural property. A few crystalline peaks have disappeared, and the peaks at 18.5°, and 20.2° have widened and became less intense. The peak at $2\theta \approx 20.2°$ is prominent. The results imply that the addition of plasticizers, lithium salt, and ionic liquid increases the amorphous nature of the gel polymer electrolytes.

5.2.2 Morphological Characterization

Scanning Electron Microscopy (SEM)

Morphological Analysis of the samples was done under a scanning electron microscope. The images are shown in Fig 5.2.

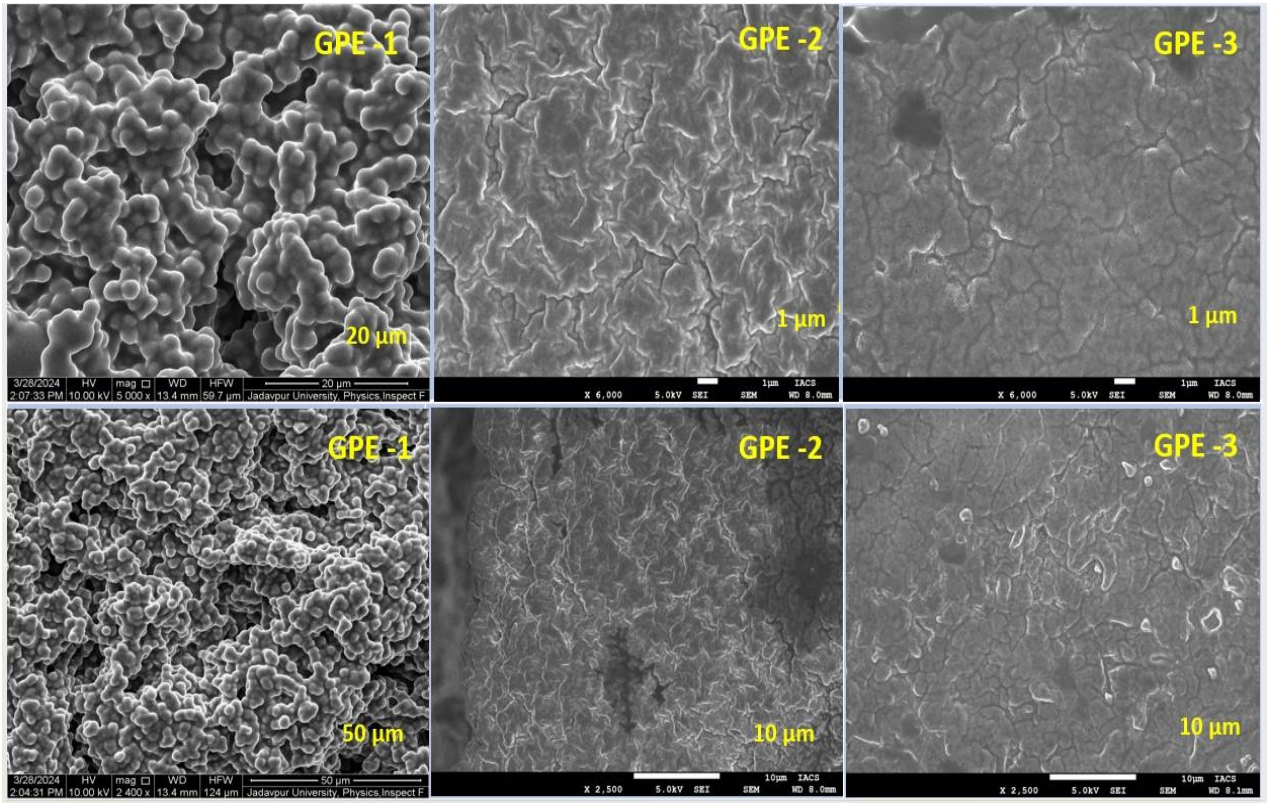


Fig. 5.2 *SEM images of GPE-1, GPE-2 and GPE-3 gel polymer electrolytes*

The haphazardly folded wavelike morphology is observed in case of P(VdF-HFP)-EMIMTFSI (GPE-1) polymer electrolyte under a scanning electron microscope. After the addition of lithium salt (LITFSI) in GPE-1 the morphology has smoothened in P(VdF-HFP)-EMIMTFSI-LITFSI (GPE-2). After further addition of COFs in GPE-2 interconnected granules of the polymer with almost smooth surface have been observed in P(VdF-HFP)-EMIMTFSI-LITFSI-COFs (GPE-3). Also, in GPE-3 porous structure is observed which will be suitable as an electrolyte to fabricate Li-ion batteries to increase lithium-ion transport.

5.2.3 Thermal Characterization

Thermal analysis was done by conducting differential scanning calorimetry (DSC) and thermogravimetric analysis (TGA) on the gel polymer electrolytes.

Differential Scanning Calorimetry (DSC)

DSC traces of P(VdF-HFP) and gel polymer electrolytes are shown as under:

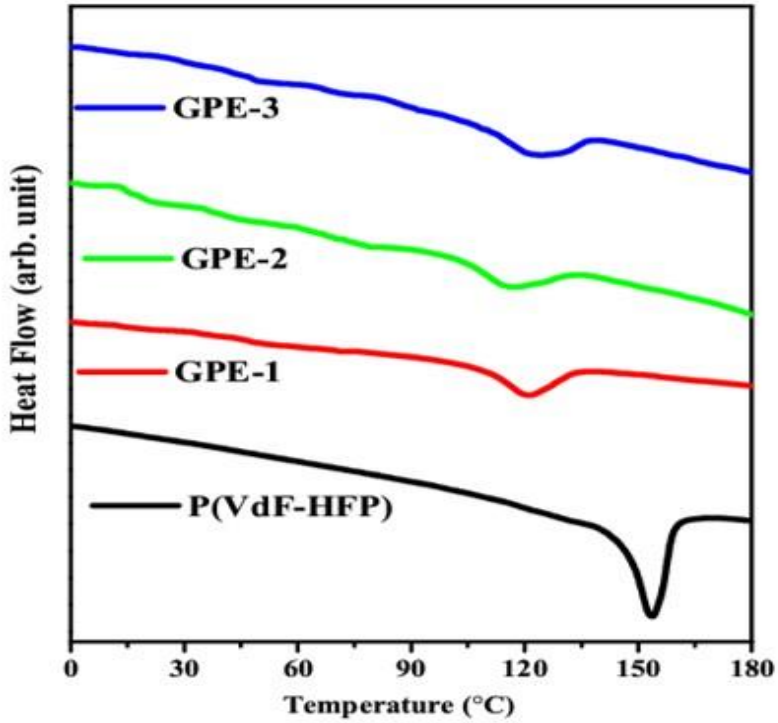


Fig. 5.3 *DSC traces of P(VdF-HFP), GPE-1, GPE-2 and GPE-3 gel polymer electrolytes*

The pure P(VdF-HFP) shows an exothermic peak at around ~154 °C corresponding to the melting temperature of the pure polymer matrix. The melting peak of the polymer matrix is shifted significantly with more flattened and reduced shape with addition of ILs, salts and COFs.It indicates the enhancement of the amorphous phase in the overall polymer electrolytes. The melting enthalpy for 100 % crystalline P(VdF-HFP) is approximately 104.7 Jg^{-1}. It is noted that the melting enthalpy gradually decrease with the addition of ionic liquid EMIMTFSI and lithium salt LiTFSI. It indicates that the degree of crystallinity decreases gradually with the introduction of ionic liquid and lithium salt.

The degree of crystalline fraction (Xc) is calculated from the following relation:

$$X_c = \frac{\Delta H_m}{\Delta H_m^0} \times 100\%,$$

The melting temperature (Tm) and degree of crystallinity (Xc) decrease due to substitution of a fraction of EMIMTFSI. The decrease of degree of crystalline Xc shows an increase of amorphousness of the electrolytes due to plasticization effect. This makes the GPEs more flexible. The amorphousness enhances inter and intra chain hopping of charge carriers and hence ionic conductivity of the polymer electrolytes is expected to increase.

Thermogravimetric Analysis (TGA)

The thermal stability of Gel polymer electrolytes (GPEs) is an important parameter for electrochemical device applications and is investigated by thermogravimetric analysis. TGA was conducted on the gel polymer electrolytes and the results obtained are shown as under.

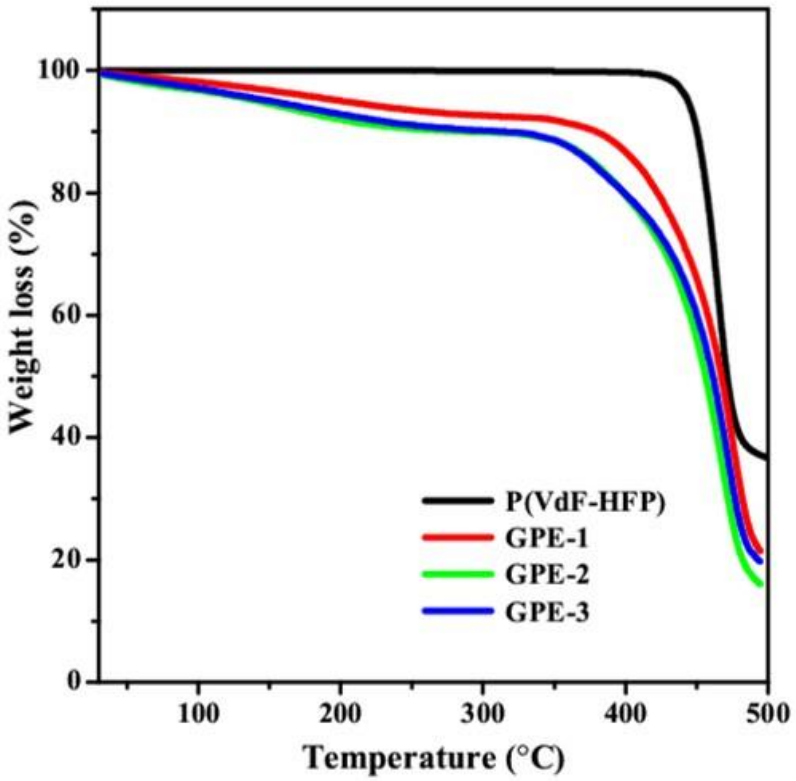


Fig. 5.4 *TGA of P(VdF-HFP), GPE-1, GPE-2 and GPE-3 gel polymer electrolytes*

From the above plot we can see that host polymer P(VdF-HFP) film shows no weight loss up to approximately 419 ^{0} C. After addition of ionic liquid (EMIMTFSI), lithium salt (LiTFSI) and COFs the thermal stability of P(VdF-HFP) is significantly reduced. The weight loss in the samples increases to due to substitution of ionic liquid by the same amount of plasticizers mixture. Thus, the thermal stability of gel polymer electrolytes is reduced due to enhancement of polymer chain flexibility after blending with ionic liquid EMIMTFSI, LITFSI salt and Covalent Organic Frameworks (COFs).

5.2.4 Absorbance Spectra Characterization

The absorbance spectra analysis was done by conducting Fourier Transform Infrared Spectroscopy (FTIR) on the gel polymer electrolytes.

Fourier Transform Infrared Spectroscopy (FTIR)

The FTIR analysis of the samples were done to examine the various possibilities of interactions in the wavenumber range 700−1600 cm^{-1}.

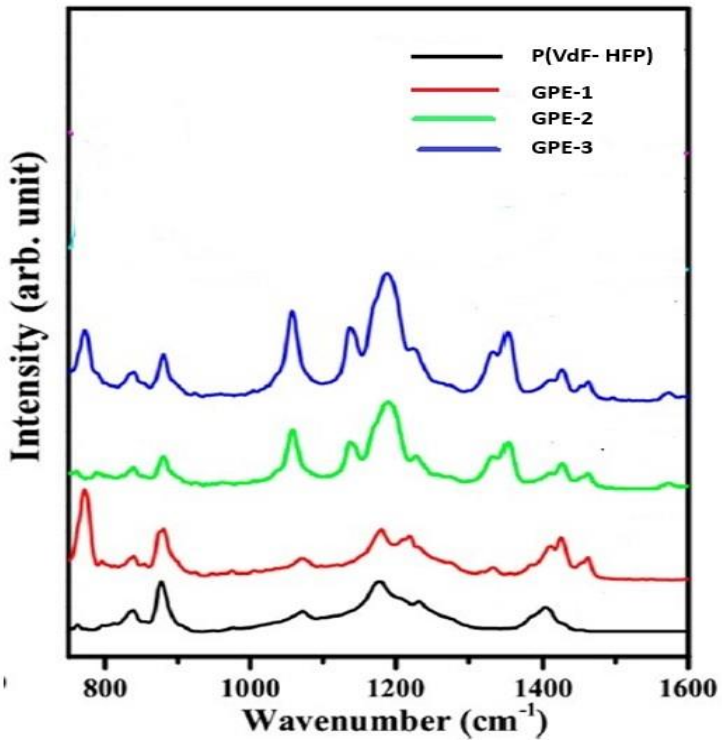


Fig. 5.5 *FTIR of P(VdF-HFP), GPE-1, GPE-2 and GPE-3 gel polymer electrolytes*

From the plot it is observed that the pure P(VdF-HFP) exhibits IR bands at 762, 796, and 976 cm^{-1} corresponding to CH_2 rocking, CF_3 stretching, and C−F stretching, respectively. These three bands represent the crystalline α-phase of the P(VdF-HFP) polymer matrix. In addition, the pure P(VDF-HFP) shows peaks at 837 and 881 cm^{-1}, which correspond to CH_2 rocking and mixed mode and CF_2 and C−C symmetric stretching, respectively, due to amorphous β-phase of P(VDF-HFP). The peaks at 837 and 881 cm^{-1} signify the existence of the amorphous phase in the GPE due to the interaction of the plasticizer with the polymer matrix. The GPE system shows that the peak intensity of the amorphous phase (881 cm^{-1}) increases, and the peak for crystalline phases (773 cm^{-1}) disappear. The above observations signify that the ionic liquid EMIMTFSI and interact with the P(VdF-HFP) polymer matrix.

5.2.5 Electrical Characterization

Electrical Characterization of the samples were done by analysing the ac conductivity, ionic conductivity and electrical potential stability window of the gel polymer electrolytes.

AC Conductivity Spectra

For the gel polymer electrolytes, GPE-1, GPE-2, and GPE-3, the frequency dependence of the real part of the complex conductivity is shown in the figure at various temperatures. From the figure the ac conductivity spectra show three distinct regions associated with mutually correlated phenomena. In the low frequency region, σ′ spectra show a rapid drop due to electrode polarization which depends upon the nature of the metal electrode-polymer interface and thickness of the film Another section shows a frequency independent region long range ion diffusion via hopping and the third section shows high frequency dispersive region, where σ′ increases with increase in frequency.

From the figure it is observed that when temperature rises, the dispersive area moves toward higher frequencies with rise in temperature. The crossover from the frequency independent region to the dispersion region indicates the onset of the conductivity relaxation phenomena.

For different gel polymer electrolytes, it is shown that the frequency and temperature

dependence of the ac conductivity is comparable. Using power law formalism, the frequency dependency of the ac conductivity spectra has been examined.

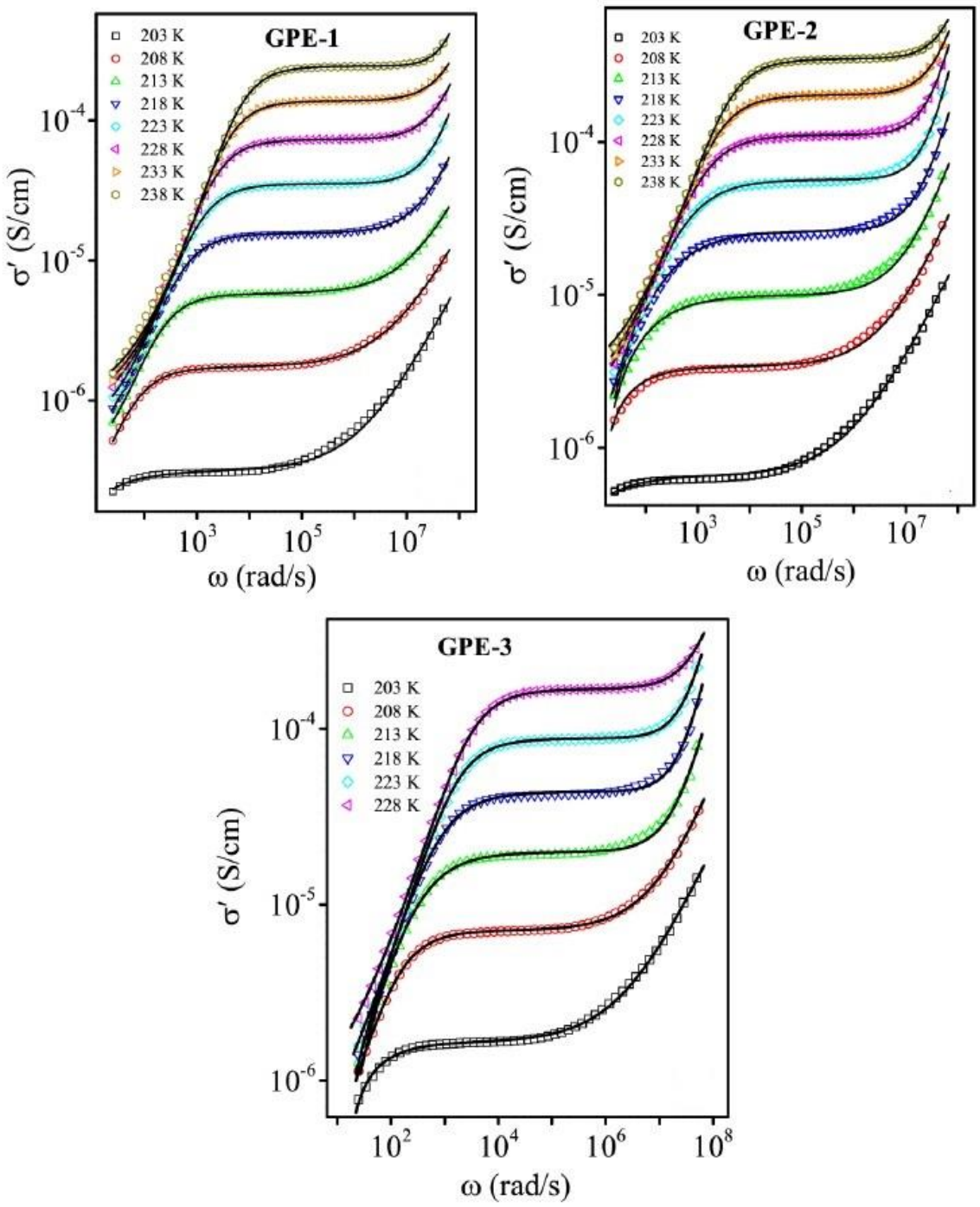


Fig. 5.6 *Conductivity spectra of gel polymer electrolytes at different temperatures*

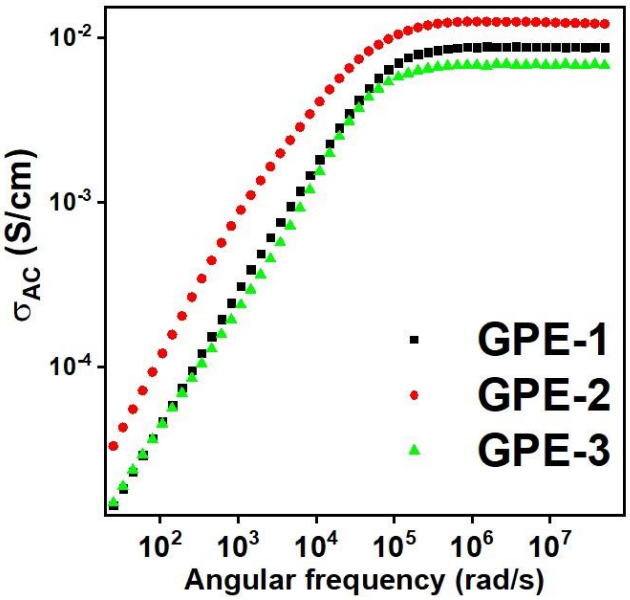


Fig. 5.7 *Comparison from Conductivity spectra for gel polymer electrolytes*

The ionic conductivity for GPE-2 increases on addition of lithium salt (LiTFSI) in GPE-1 due to high mobility of Li^+ ions in gel polymer electrolyte. The ionic conductivity for GPE-3 further decreases when covalent organic frameworks (COFs) are added in GPE-2 due to high dielectric constant which reduces ionic dissociation and ionic mobility by increasing viscosity of the ionic liquid [7]

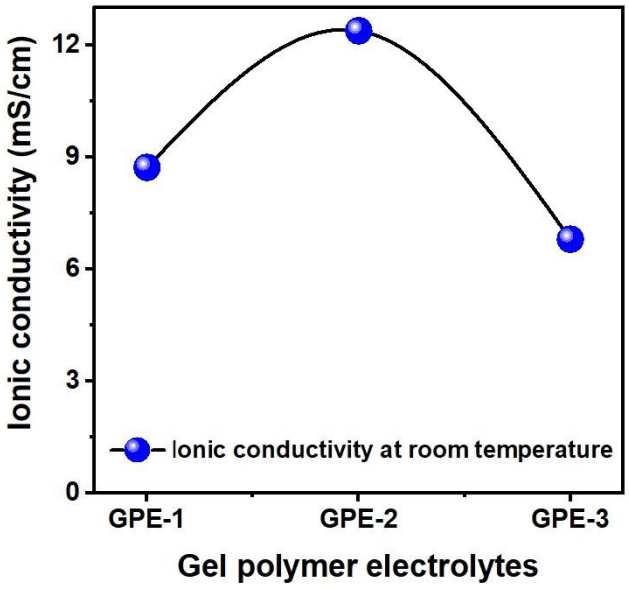


Fig. 5.8 *Ionic conductivity for gel polymer electrolytes*

Fig. 5.7 displays the temperature dependence of the ionic conductivity for all gel polymer electrolytes. It is observed from the analysis that the ionic conductivity increases with increase of temperature.

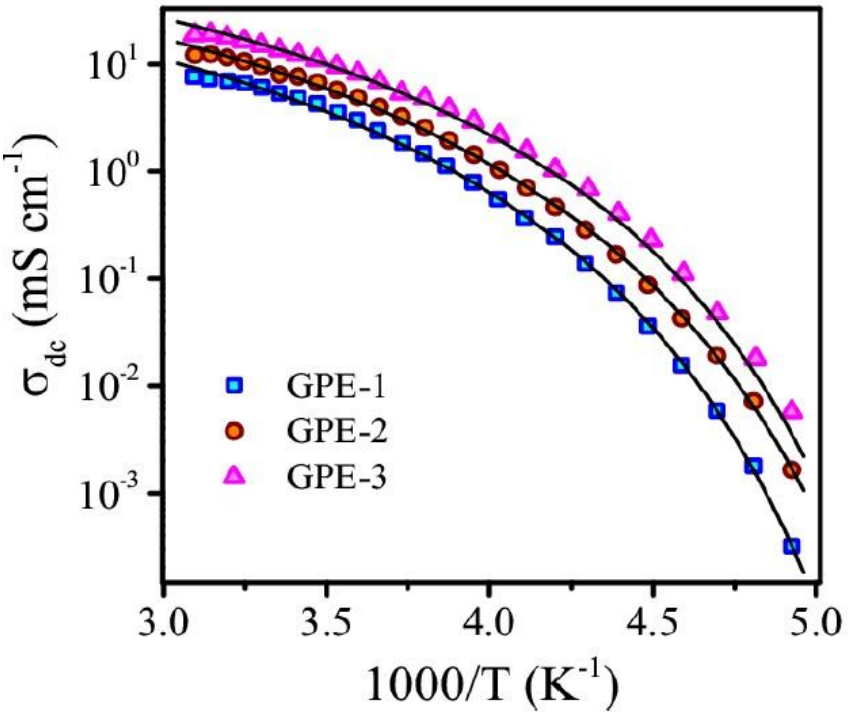


Fig. 5.9 *Temperature dependence ionic conductivity of gel polymer electrolytes*

The ionic conductivity for all gel polymer electrolytes is fitted in this equation given below

$$\sigma_{dc}(T) = \sigma_0 \exp\left[\frac{-E_\sigma}{k_B(T - T_0)}\right],$$

where σ_0 is the pre-exponential constant, k_B is the Boltzmann constant, Eσ is pseudo-activation energy related to the critical free volume for ion transport, T is the absolute temperature and T_0 is the equilibrium Vogel scaling temperature. The ionic conductivity for all gel polymer electrolytes is fitted to the above equation and Fig 5.7 is obtained. The excellent fits to the ionic conductivity data in wide temperature range presented indicates that the charge carrier dynamics is strongly coupled with the segmental motion of polymer chain.

5.2.6 Electrochemical Characterization for Supercapacitors

Electrochemical analysis techniques are widely employed for characterizing the performance and understanding the fundamental mechanisms of supercapacitors. Typical electrochemical techniques for supercapacitor analysis includes Cyclic Voltammetry (CV), Galvanostatic Charge/Discharge (GCD), Electrochemical Impedance Spectroscopy (EIS). These properties directly impact the specific capacity, power density and energy density of the devices. The supercapacitors have been fabricated by sandwiching gel polymer electrolytes between two symmetrical activated carbon (AC) electrodes and are designated as **Cell-1**: AC||GPE-1||AC, **Cell-2**: AC||GPE-2||AC and **Cell-3**: AC||GPE-3||AC. The results of the experiments are summarized below.

Cyclic Voltammetry (CV)

CV is a potentiodynamic technique that involves sweeping the potential between two values at a fixed scan rate. The shape and area of the CV curve are indicative of the capacitance and energy storage capabilities of the supercapacitor. The electrochemical behavior of the supercapacitor cells has been evaluated by cyclic voltammetry (CV). The figure given below shows the cyclic voltammetry data at different scan rates of 10, 30, 50, 80, 100, 150 and 200 mV s^{-1} in the voltage range from -1.0 V to +1.0 V at room temperature. These figures demonstrates that the CV curves for the all cells show almost box-like in shape and correspond to an exceptionally ideal and reversible capacitive characteristic of a double layer at the carbon electrode-polymer electrolyte interface. The specific capacitance of the supercapacitors has been calculated using the following relation

$$C_{sp}^{cv} = \frac{\int idV}{2 \times m \times S \times \Delta V},$$

$\int idV$ is the integrated area of the CV curve, m is the single electrode mass of active material (activated carbon) in g, S is the scan rate, ΔV is cell voltage range. It is observed that the value of C_{sp}^{cv} decreases with increasing scan rate. Actually, the ions have enough time to pass through the pores of activated carbon materials at low-speed scan rates.

while the ions accumulate on the external surface of the carbon materials at the high-speed scan rates. Thus, specific capacitance decreases with the increase of speed of the scan rates.

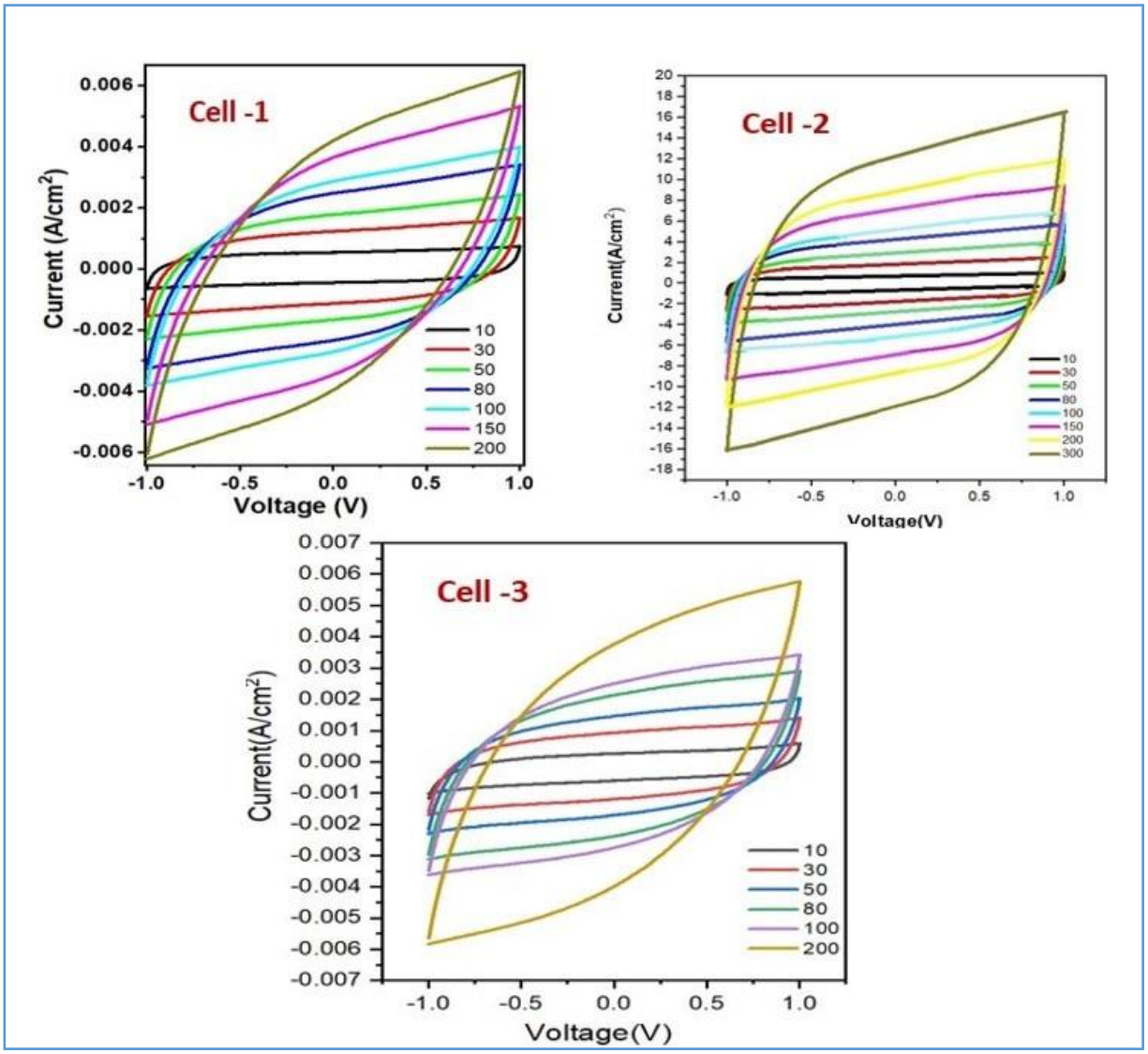


Fig. 5.10 *Cyclic voltammetry (CV) for different Supercapacitor cells.*

The addition of salt into the GPE-1 electrolyte increases the specific capacitance due to enhancement of electrostatic interaction between the activated carbon electrode and charge carriers of gel electrolytes which increases the capacitance.

After addition of COFs, the gel polymer electrolyte shows more flexible and high ionic conductivity. The flexibility of the gel polymer electrolyte GPE-3 provided a very good contact between the electrode-gel electrolyte as a result of which rapid charge carrier adsorption takes place at electrode-electrolytes interface.

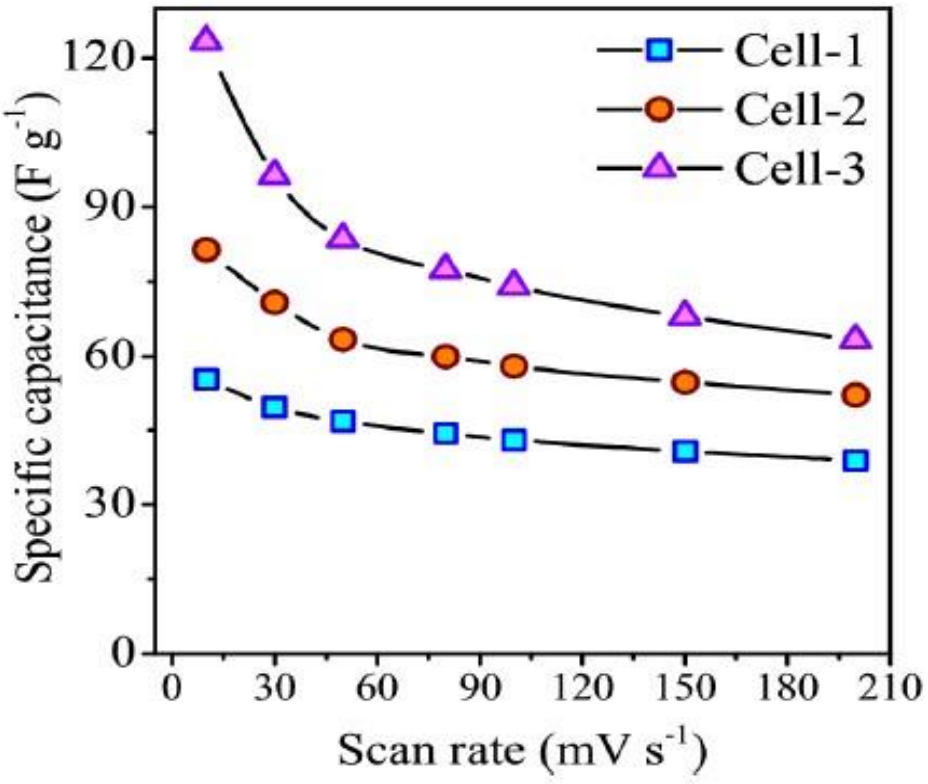


Fig. 5.11 *Specific capacitance obtained from CV with scan rates for different cells.*

Specific capacitance obtained from cyclic voltammetry is a critical parameter that provides valuable insights into the electrochemical performance, charge storage mechanisms, and potential applications of electrode materials in energy storage and conversion systems.

Cyclic voltammetry at a constant scan rate is widely used for various applications, which includes studying the electrochemical behavior of different additives which in this case is EMIMTFSI ionic liquid and LITFSI salt for GPE -2 and EMIMTFSI, salt LITFSI and COFs. Addition of salt, ionic liquids and COFs have significant effect on the electrochemical properties of the fabricated supercapacitors.

The CV patterns have been further recorded to observe the electrochemical voltage window of the gel electrolytes at a constant scan rate 50 mV/s.

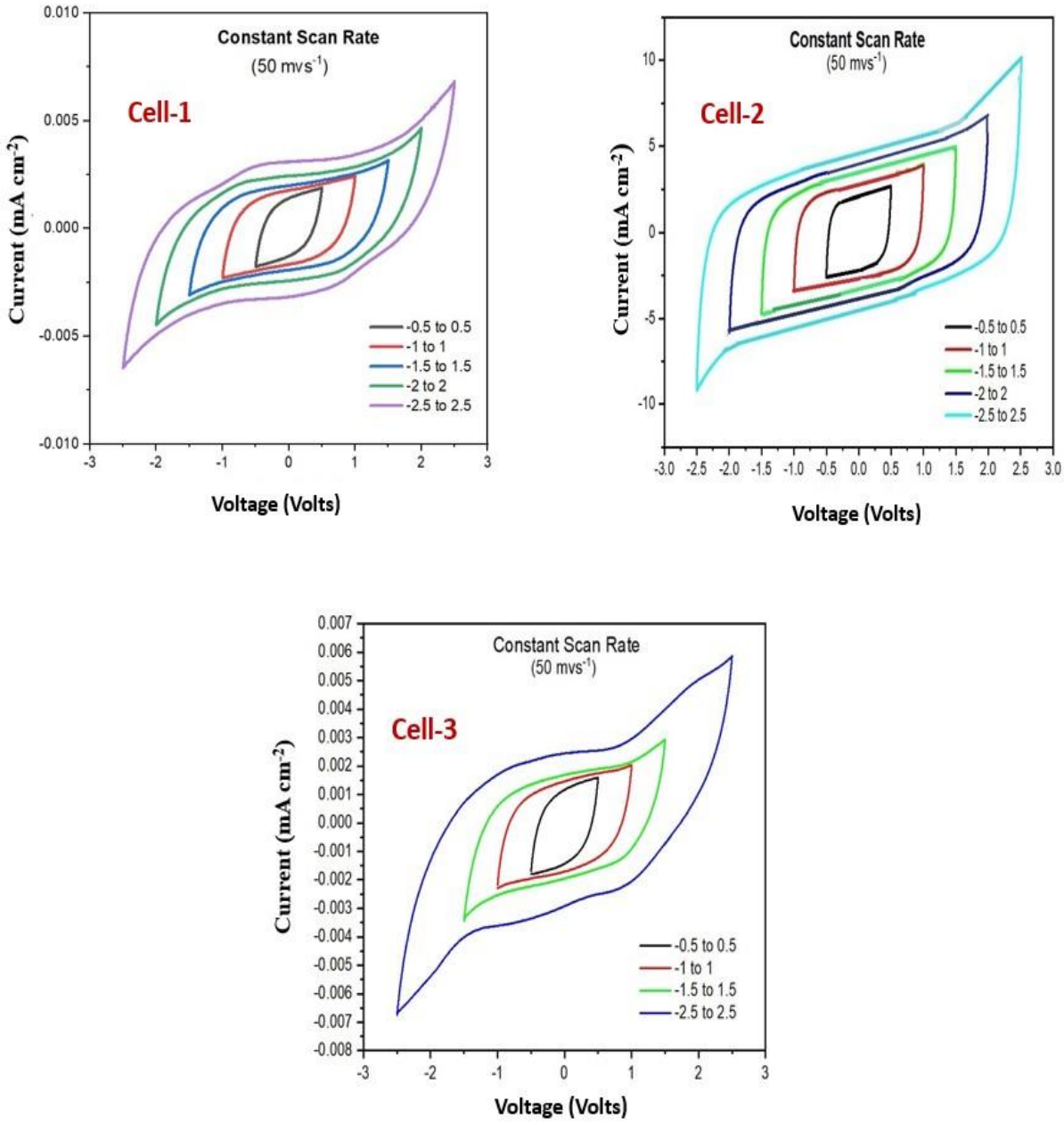


Fig. 5.12 *Cyclic Voltammetry (CV) pattern of the supercapacitors at scan rate 50 mV* s^{-1}.

From the above results it is observed that with gradual increase of voltage range CV patterns remain same in shape (rectangular shape) for all the three cells. This observation indicates that the gel polymer electrolytes show wide range of electrochemical voltage window.

Electrochemical Potential Stability Window (EPSW)

From an application perspective, the electrochemical voltage stability (also known as the working voltage window) of the gel polymer electrolytes is an essential metric for lithium-ion batteries, supercapacitors, and other energy storage devices. The electrochemical potential stability window (EPSW) of gel polymer electrolyte films has been studied by applying cyclic voltammetry (CV) at a constant scan rate.

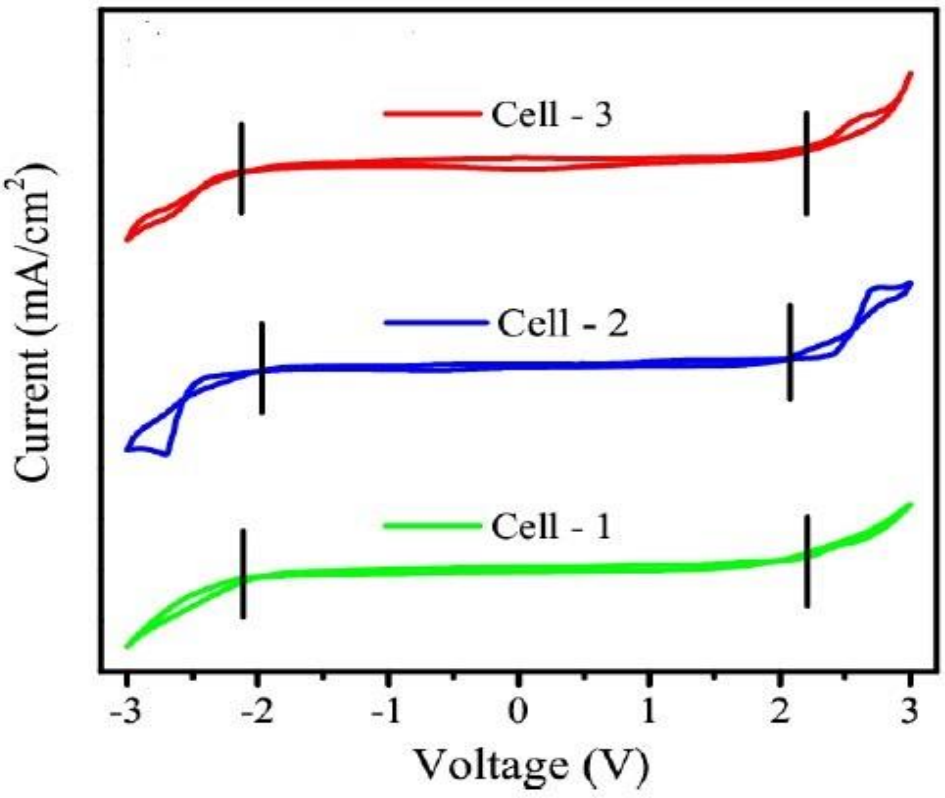


Fig. 5.13 *Cyclic voltammetry (CV) for EPSW for different gel polymer electrolytes*

From the figure it is observed that the working voltage of GPE-1 is in the range from - 2.1 V to + 2.2 V (i.e. 4.3 V). For GPE-2 the voltage range is slightly reduced from – 2.0 V to + 2.1 V (i.e. 4.1 V) due to introduction of LiTFSI salt. In case of GPE-3 the voltage range increases from – 2.1 V to + 2.2 V (i.e. 4.3 V). Addition of covalent organic frameworks (COFs) in sample GPE-3 resulted in increase of EPSW due to plasticization effect as depicted in the figure above.

Galvanostatic Charge-Discharge (GCD)

Galvanostatic charge-discharge is a technique used to study the electrochemical behavior of battery cells, supercapacitors, and other energy storage devices. It involves applying a constant current to the device and monitoring the resulting voltage changes over time during charging and discharging cycles. During the galvanostatic charge process, a constant current is applied to the device, causing it to charge. The voltage of the device increases as it stores energy. The charge process continues until the voltage reaches a predetermined cutoff value, which prevents overcharging and potential damage to the device. Conversely, during the galvanostatic discharge process, a constant current is drawn from the device, causing it to discharge. The voltage of the device decreases as it releases stored energy. The discharge process continues until the voltage reaches a predetermined cutoff value, which prevents over-discharging and potential damage to the device. The galvanostatic charge-discharge technique provides valuable information about the electrochemical properties of the device under test, such as capacity, voltage profile, cycling performance, rate capability.

For this work galvanostatic charge-discharge (GCD) characteristics was recorded from 0.0 - 2.0 V at room temperature for all supercapacitors Cell-1, Cell-2 and Cell-3 respectively at different constant currents. All supercapacitor cells are found to have almost linear discharge characteristics with negligible ohmic drops for all discharge currents, pointing to the cells' non-faradic capacitive nature. Additionally, each discharge curve shows a sharp drop in voltage that is caused by an ohmic internal resistance, commonly known as the cell's equivalent series resistance (ESR). For this work ESR has been calculated from the formula:

$$\mathrm{ESR} = \frac{\Delta V_{IR}}{2 \times i},$$

where i is the discharge current in Ampere, mtam is the total active mass (mass of activated carbon in both electrodes) in supercapacitor in g and $\Delta V/\Delta t$. is slope of the discharge characteristic after internal resistance drop.[10]

The GCD characteristics for Cell 1, Cell 2 and Cell 3 are shown as under.

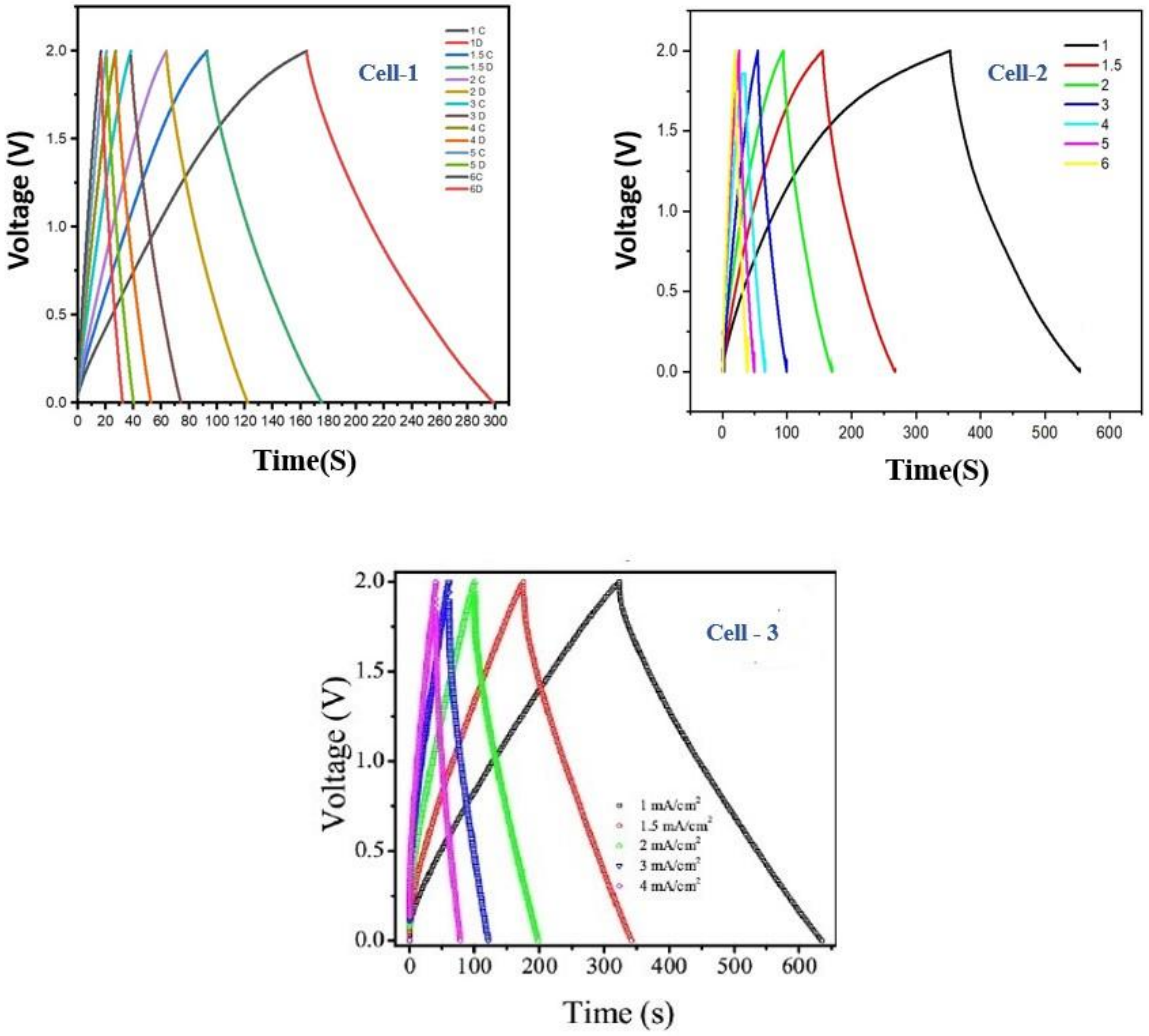


Fig. 5.14 *GCD Characteristics of Cell- 1, Cell-2 and Cell-3 at different constant currents.*

The specific capacitance is a measure of the capacitance of an electrode material per unit mass or volume. It is an important parameter for evaluating the performance of electrode materials used in electrochemical capacitors, also known as supercapacitors. The specific capacitance is typically determined from the discharge curve obtained during a constant current discharge experiment. In this experiment, the electrode material is first charged to a specific voltage and then allowed to discharge at a constant current. The specific capacitance is calculated from the discharge curve using the following equation:

$$C_s = (I \times \Delta t) / (m \times \Delta V)$$

Where C_s is the specific capacitance (in Farads per gram or Farads per cubic centimeter), I is the constant discharge current (in Amperes), Δt is the discharge time (in seconds) is the mass or volume of the electrode material ΔV is the potential window or voltage range over which the discharge occurs (in Volts). The discharge curve is a plot of the voltage (or potential) against time during the constant current discharge process.

The specific capacitance is proportional to the slope of the discharge curve, with a steeper slope indicating higher capacitance. In symmetrical cell system, the specific capacitance referred to a single electrode is related to overall capacitance of the cells by the following relation.[12]

$$C_{sp}^{dis}(Fg^{-1}) = 4 \times C_{cell}^{dis},$$

The variation of specific capacitance with discharge current is shown in Fig 5.13.

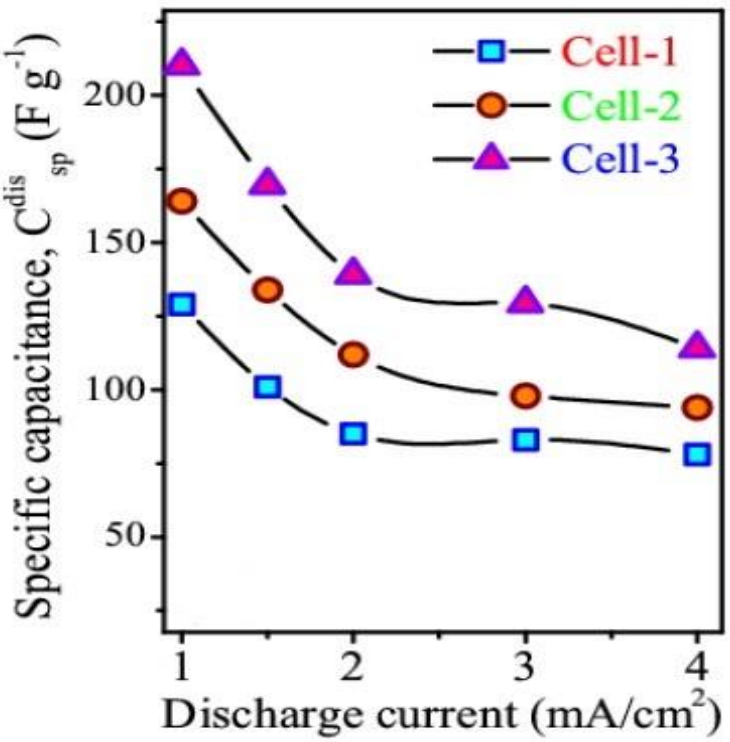


Fig. 5.15 *Variation of specific capacitance obtained from GCD with discharge current.*

From the graph above it is observed that the values of specific capacitances of all cells decrease with increasing number of charge-discharge cycles due to accumulation of ions at the electrode-polymer electrolyte interface coupled with irreversible oxidation/reduction of insecurely bound OH- (most likely) surface groups on the porous activated carbon electrodes [13]. It is observed that after completion of 1200 cycles, specific capacitance values become saturated at 49 %, 57 % and 56 % of the initial value for Cell-1, Cell-2 and Cell-3 respectively. From charge–discharge profiles it can be concluded that both charging and discharging times are almost equal for all supercapacitor cells.

Coulombic efficiency (CE) is a concept used in electrochemistry, particularly in the context of rechargeable batteries and other energy storage devices. It is a measure of the efficiency with which charge is transferred during the charge and discharge processes of a battery or electrochemical cell. The coulombic efficiency is defined as the ratio of the total charge extracted from the battery during discharge (Q_discharge) to the total charge inputted during the charging process (Q_charge). It is expressed as a percentage and can be calculated using the following formula:

$$CE = (Q_{discharge} / Q_{charge}) \times 100\%$$

A coulombic efficiency of 100% would indicate that all the charge put into the battery during charging is recovered during the subsequent discharge cycle. For our work it has been noted that all supercapacitor cells exhibit 100% Coulombic efficiency throughout 4000 cycles.

Energy density refers to the amount of energy that can be stored per unit volume or mass of the supercapacitor. It is typically expressed in units of Wh/L (Watt-hours per liter) or Wh/kg (Watt-hours per kilogram). The energy density of supercapacitors is generally lower than that of batteries but higher than conventional capacitors.

Power density refers to the amount of power that can be delivered per unit volume or mass of the supercapacitor. It is typically expressed in units of W/L (Watts per liter) or W/kg (Watts per kilogram). Supercapacitors have a very high-power density compared to batteries, which

allows them to deliver bursts of energy quickly. Typical power densities for supercapacitors range from 1,000 to 10,000 W/L or 1,000 to 20,000 W/kg. The energy density (E) and power density (P) of the supercapacitor cells have been calculated from charge-discharge characteristics at different current rates using following relations:

$$E = \frac{C_{cell}^{dis} \times (\Delta V)^2}{2} \times \frac{1000}{3600}$$

$$P = \frac{E \times 3600}{\Delta t},$$

Where 'C' is the overall capacitance of the cell, ΔV is the cell voltage and Δt is the discharge time.

Ragone plot shows the relationship between the specific energy (energy density) and the specific power (power density) of an energy storage device. The Ragone plot is useful for several reasons which includes comparison of energy storage devices, design and optimization of energy storage systems, performance evaluation of energy storage systems. The Ragone plot for our system is shown in Fig 5.13 for Cell -1, Cell-2 and Cell-3

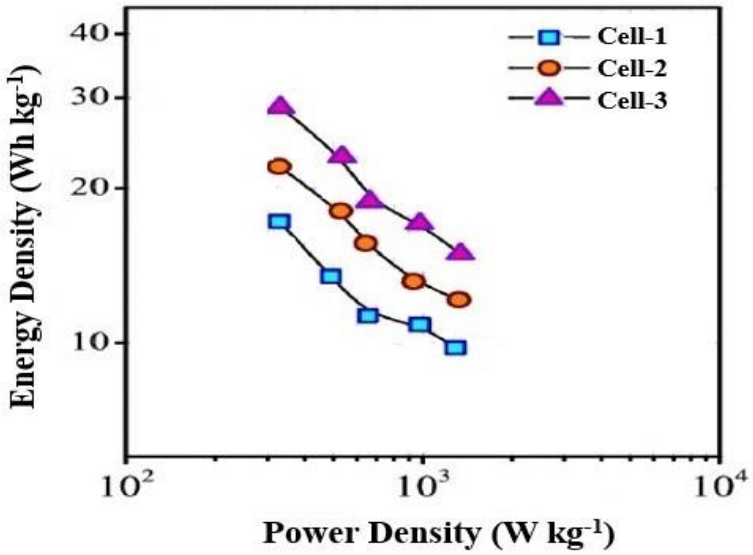


Fig. 5.16 *Ragone Plots for all supercapacitor cells.*

From the plot it is found that adding plasticizers and salt improves the supercapacitor cells' performance and saves energy at high power density. The power density increases due to high ionic conductivity of the gel electrolytes and good contact between electrode and electrolytes which improves the electrostatic interaction between ions of polymer electrolyte and carbon electrode.

The comparative study of GCD characteristics for Cell 1, Cell 2 and Cell 3 is given in Fig 5.14

Cells	ESR (Ω cm^2)	Specific capacitance (Fg^{-1})	Energy Density ($Wh\ kg^{-1}$)	Power Density ($KW\ kg^{-1}$)
Cell -1	12	102	13.49	0.498
Cell -2	11	133	18.05	0.538
Cell -3	6	170	24.01	0.546

Fig. 5.17 *Comparative study for Cell-1, Cell-2, Cell-3 obtained from GCD characteristics.*

From the above table we can observe that specific capacitance has increased as we move from Cell-1 to Cell-3. Energy density and power density values also show an increase. The solid-state supercapacitor containing GPE-3 electrolyte exhibits good capacitance and energy density due to its high ionic conductivity and flexibility which provides good contact between electrode and electrolyte for the supercapacitors fabricated. This is also evident in Ragone plot as shown in Fig 5.13.

Electrochemical Impedance Spectroscopy (EIS)

Electrochemical impedance spectroscopy (EIS) is a powerful technique for characterizing the performance and behavior of supercapacitors. To perform EIS on supercapacitors, a small alternating current (AC) signal is applied over a wide range of frequencies, and the corresponding AC response in the form of voltage or current is measured. The resulting impedance data is then analysed using various techniques, such as Nyquist plots, and equivalent circuit fitting, to extract the relevant information about the supercapacitor's behavior and performance.

For the samples EIS data was obtained and the relevant plots are shown in Fig 5.15 and Fig 5.16.

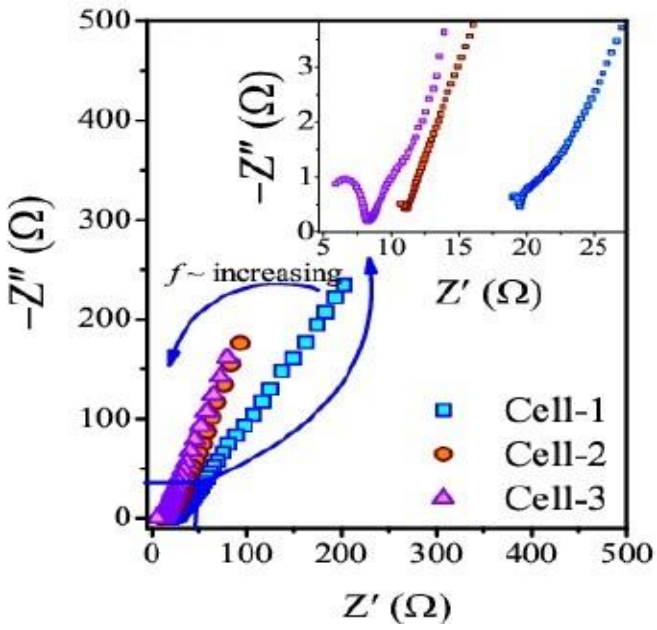


Fig. 5.18 *Complex impedance plots of different supercapacitor cells at room temperature. Inset shows enlarge view of the complex impedance plots*

The Nyquist plots i. e. Z′ (real part) versus – Z" (imaginary part) plots of the supercapacitor cells obtained at room temperature using an ac signal of 1 V is shown in *Fig. 5.15* in the frequency window 10 mHz - 1 MHz.

The variation of specific capacitance with frequency is shown in Fig 5.16.

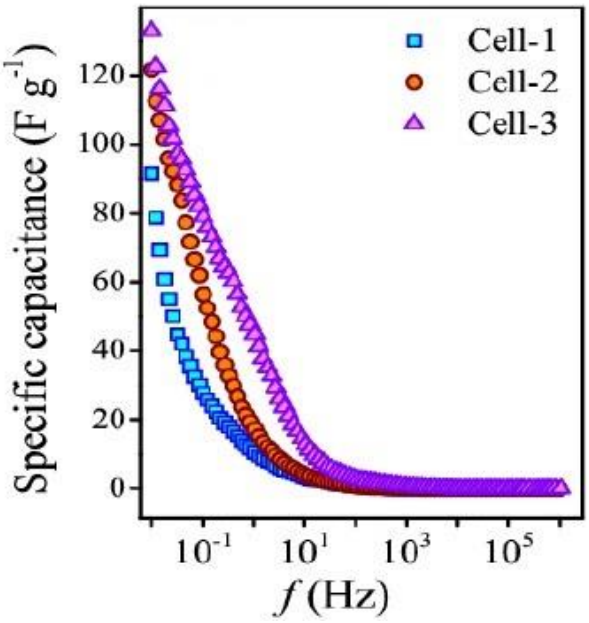


Fig. 5.19 *Variation of specific capacitance with frequency for the supercapacitor cells.*

From the figure it can be observed that at low frequencies the plots for all cells rise steeply indicating capacitive nature of the interface between the activated carbon electrode and the gel polymer electrolyte. In the high frequency region, a small semicircular arc is observed in the impedance spectra. The overall capacitance of the supercapacitor cells can be calculated using the relation.

$$C_{overall}^{EIS} = -\frac{1}{2 \times \pi \times f \times Z''},$$

where *f* is the frequency in Hz and Z" is the imaginary part of the complex impedance in ohm. The single electrode specific capacitance was calculated by multiplying the overall capacitance by a factor of 2 and divided by mass of the active electrode material in gm. From the plots it is also observed that the value of specific capacitance increases with addition of salt and covalent organic frameworks as is evident in the plots shown above.

5.2.7 Functionality of Lithium-ion coin cell

Lithium-ion transference number

The lithium-ion transference number, is a crucial parameter that describes the ionic conduction behavior in lithium-ion battery electrolytes and solid-state electrolytes. It represents the fraction of the total ionic conductivity contributed by the lithium ions relative to the overall ionic conductivity.

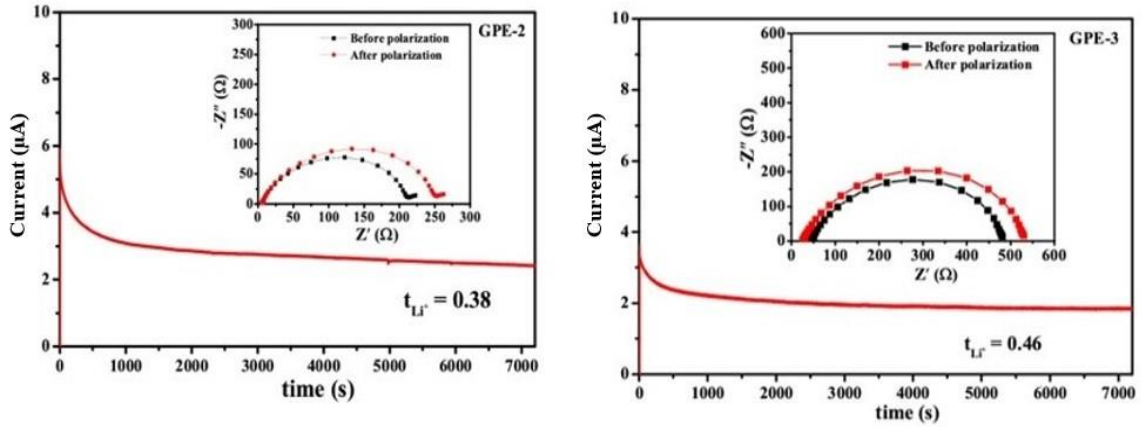


Fig. 5.20 *Plot of current and time with Li-ion transference number for GPE 2 and GPE 3.*

In GPE due to presence of COFs the anion part of the salt gets trapped in porous structure of COFs making way for greater Li ion transport. From the above figure we can conclude as we move from GPE 2 to GPE 3 conductivity decreases as the anion gets trapped in porous COFs making way for more lithium ion to transport to take place hence, we can see that Li ion transference number has increased from 0.38 to 0.46. The electrochemical impedance spectra at 25 ^{0}C of the symmetric cells using GPE-2 and GPE-3 gel electrolytes before and after DC polarization respectively. The time dependence response of current (I-t curves) of DC polarization at 10 mV for the two symmetry cells is shown above. From the figure it is observed that ions are accumulated at the electrode-electrolyte interface when DC polarization voltage is applied across the cells and form a passive layer. From the figure It is observed that the presence of this passive layer reduces the time dependence of the polarization current, and that the passage of Li^+ ions through the gel polymer electrolytes between the electrodes causes the

current to attain a steady-state condition. The Li^+ ion transference number of the GPEs is determined using to Bruce-Vincent-Evans method. where I_0 and I_{ss} are the initial and steady-state current respectively, V is the polarization voltage, R_0 and R_{ss} are the electrode-electrolyte interfacial resistances measured before and after the DC polarization respectively

$$t_{Li^+} = \frac{[I_{ss}(\Delta V - R_0 I_0)]}{[I_0(\Delta V - R_{ss} I_{ss})]},$$

For GPE-2 some Li^+ ions are surrounded by anions and form effectively large ionic species which trap the Li^+ ions, resulting in a low value of transference number. On the other hand, COFs have the property to completely dissociates the large ionic atmosphere into Li^+ cations and anions.

Charge Discharge Characteristics

The supercapacitor cells made with the current gel polymer electrolytes have shown excellent physicochemical characteristics and electrochemical performance hence a lithium-ion full coin cell (Type CR2032) is fabricated using gel polymer electrolyte GPE-3 with the configuration graphite//GPE-3//$LiFePO_4$ and investigated the performance of the coin cell at room temperature (25 ^{0} C). The charge-discharge performance of the coin cell at different current rates in the voltage range of 1.8 V – 3.6 V was performed and the results are shown in figure Fig 5.17.

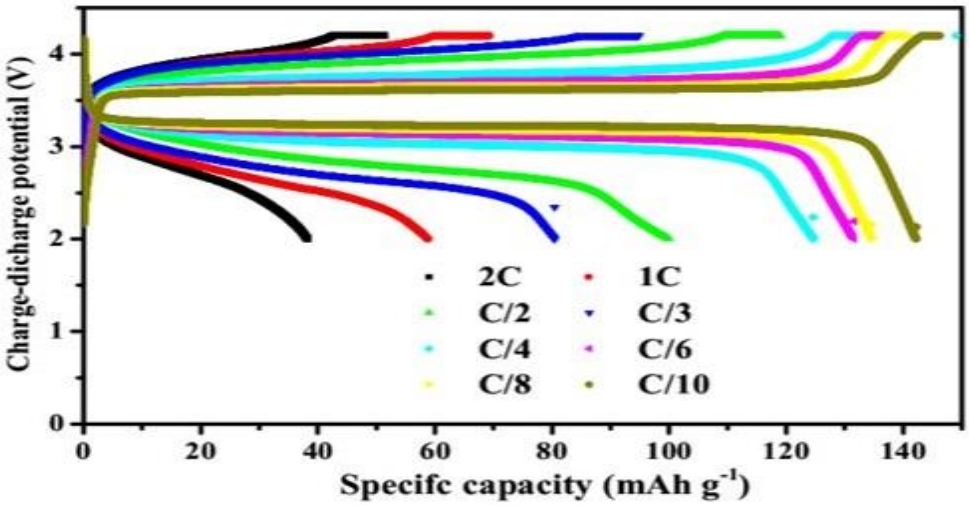


Fig. 5.21 *Rate capability of lithium-ion coin cell (CR2032) at room temperature*

The theoretical capacity of the cathode for the cell was determined as C (mAh) = specific theoretical capacity of $LiFePO_4$ (170 mAh g^{-1}) x weight of the active material (g). From the figure it is observed that that the cell exhibits plateau voltages of 2.75 V and 2.52 V respectively for the 1st charging and discharging cycles at constant current rate C/12. The plateau voltage is nearly 2.80 V for charging and 2.4 V for discharging of 1st cycle at current rate 1C. It is also observed that the ΔV (plateau voltage for charging - plateau voltage for discharge) increases with the increase in charge-discharge current rate. The specific charge capacity of the coin cell is 167.07, 149.12, 110.07, 81.2, 62.9 and 47.2 mAh g^{-1} and specific discharge capacity is 165.8, 143.44, 108.9, 74.35, 57.53 and 45.37 mAh g^{-1} at current rates C/12, C/10, C/8, C/5, C/3 and 1C respectively. This charge- discharge capacity of the coin cell decreases with increasing current rate due to slow diffusion of Li^+ ions within the electrodes and formation of potential barrier at electrode-electrolytes interface. Cycling performance of coin cells can vary depending on several factors, including cell chemistry, depth of discharge, charging and discharging rates, temperature, cell design and construction. For our work cycling performance of the coin cell has been taken at room temperature till 20 th cycle at low current rate C/12 in the voltage range 1.8 V - 3.6 V. The 1st and 20th charge and discharge cycles at constant current rate C/12 while the specific charge/discharge capacity of the coin cell up to 20 cycles. From the analysis it is found that the coin cell delivers specific discharge capacity of 165.8 mAh g^{-1} and 124 mAh g^{-1} for 1st and 20th cycles respectively with respect to the active $LiFePO_4$ cathode material as

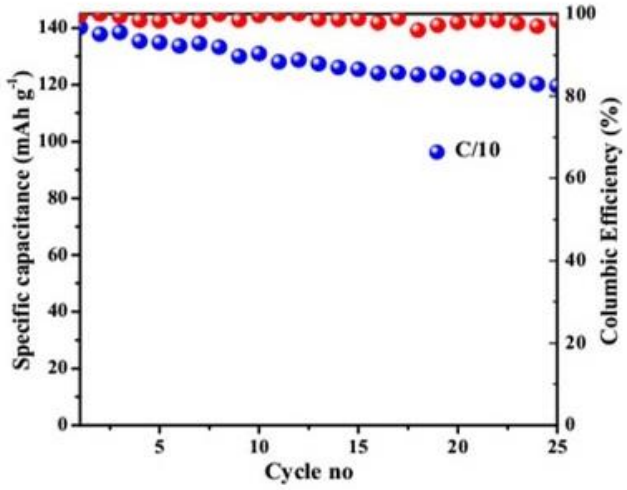


Fig. 5.22 *Cycling performance of specific capacity and Columbic efficiency for the coin cell*

From the plot it can be concluded that the discharge capacity remains 72.9% of the theoretical capacity of the cathode after 20 th cycle. This high-capacity retention and cycling stability of the coin cell arises from the high ionic conductivity and good contacts between gel electrolyte and electrodes However there are several constraints for decay of specific capacity. The most significant obstacles to utilizing these electrolytes in devices are their interfacial stability and electrode compatibility, which result in low cycle-ability of the lithium-ion cell even though the gel electrolytes have good ionic conductivity at ambient temperature. From the figure it can be concluded that capacity for charging and discharging is almost equal, providing nearly 99% Coulomb efficiency of the present lithium-ion cell.

5.3 Bibliography

[1] S. Mitra, A. K. Shukla and S. Sampath, *Journal of Power Sources* **(**2001), p. 213.

[2] C. C. Yang, S. T. Hsu and W. C. Chien, *Journal of Power Sources* **(**2005), p. 303.

[3] X. Yang, F. Zhang, L. Zhang, T. Zhang, Y. Huang and Y. Chen, *Adv. Funct. Mater.* (2013),

[4] P. F. R. Ortega, J. P. C. Trigueiro, G. G. Silva and R. L. Lavall, *Electrochimi. Acta* (2016), p. 809.

[5] V. K. Thakur, G. Ding, J. Ma, P. S. Lee and X. Lu, *Adv. Mater.* (2012),

[6] G. B. Appetecchi, P. Romagnoli and B. Scrosati, *Electrochemist. Commun* (2001), p. 281.

[7] Sellam and S. A. Hashmi, *ACS Applied Materials and Interfaces* **(**2013), p. 3875.

[8] C. Fasciani, S. Panero, J. Hassoun and B. Scrosati, *Journal of Power Sources* **(**2015)

[9] G. P. Pandey and S. A. Hashmi, *J. Mater. Chem. A* (2013), p. 3372.

[10] E. Frackowiak and F. Béguin, *Carbon* **(**2001), p. 937.

[11] M. Que, Y. Tong, G. Wei, K. Yuan, J. Wei, Y. Jiang, H. Zhu and Y. Chen, *J. Mater. Chem. A* (2016), p. 14132.

[12] F. Béguin, V. Presser, A. Balducci and E. Frackowiak, *Adv. Mater.* (2014), p. 2219.

[13] V. L. Martins, A. J. R. Rennie, R. M. Torresi and P. J. Hall, *Phys. Chem. Chem. Phys.* (2017), p. 16867.

[14] H. Y. Sung, Y. Y. Wang and C. C. Wan, *J. Electrochem. Soc.* (1998), p. 1207.

[15] G. P. Pandey, S. A. Hashmi and Y. Kumar, *Energy and Fuels* **(**2010), p. 6644.

[16] M. Egashira, H. Todo, N. Yoshimoto and M. Morita, *Journal of Power Sources* **(**2008),

[17] P. R. Chinnam, V. Chatare, S. Chereddy, R. Mantravadi, M. Gau, J. Schwab and S. L. Wunder, *J. Mater. Chem. A* **(**2016), p. 14380.

[18] P. Pal and A. Ghosh, *Electrochimi. Acta* **(**2018), p. 157.

[19] A. Manuel Stephan, *Eur. Polym. J.* (2006),

[20] B. G. Choi, J. Hong, W. H. Hong, P. T. Hammond and H. Park, *ACS Nano* **(**2011),

[21] Y. Kumar, G. P. Pandey and S. A. Hashmi, *Journal of Physical Chemistry C* **(**2012), p. 26118.

[22] C. Sirisopanaporn, A. Fernicola and B. Scrosati, *Journal of Power Sources* **(**2009), p. 490.

[23] M. Galiński, A. Lewandowski and I. Stepniak, *Electrochimi. Acta* **(**2006), p. 5567.

[24] H. Ohno, M. Yoshizawa and W. Ogihara, *Electrochimi. Acta* **(**2003), p. 2079.

[25] G. A. Tiruye, D. MuÃ±oz-Torrero, J. Palma, M. Anderson and R. Marcilla, *Journal of Power Sources* **(**2016),

[26] K. Ekramul, M. Khatun, L. Nasrin, J. R. Mustafa and M. Rahman, *J. Phys. D: Appl. Phys.* (2017), p. 163002.

[27] K. Karuppasamy, P. A. Reddy, G. Srinivas, A. Tewari, R. Sharma, X. S. Shajan and D. Gupta, *J. Member. Sci.* (2016),

[28] Z. He, Q. Cao, B. Jing, X. Wang and Y. Deng, *RSC Adv.* **7** (2017), p. 3240.

[29] A. Serghei, M. Tress, J. R. Sangoro and F. Kremer, *Phys. Rev. B: Condens. Matter Mater. Phys.* (2009),

[30] B. K. Money, K. Hariharan and J. Swenson, *Journal of Physical Chemistry B* **(**2012),

[31] D. P. Almond and A. R. West, *Nature* **(**1983),.

[32] R. J. Kortschot, A. P. Philipse and B. H. Erné, *Journal of Physical Chemistry C* **(**2014),

[33] J. R. Macdonald, *J. Chem. Phys.* (1971), p. 2026. [

[34] J. K. Kim, A. Matic, J. H. Ahn and P. Jacobsson, *Journal of Power Sources* **(**2010), p. 7639.

[35] A. Fernicola, F. C. Weise, S. G. Greenbaum, J. Kagimoto, B. Scrosati and A. Soleto, *J. Electrochem. Soc.* (2009), p. A514.

[36] H. Vogel, *Z. Phys.* (1921), p. 645.

[37] G. Tammann and W. Hesse, *Z. Anorg. Allg. Chem.* (1926), p. 245.

[38] G. S. Fulcher, *J. Am. Ceram. Soc.* (1925), p. 339.

[39] A. Ghosh and A. Pan, *Phys. Rev. Lett.* (2000), p. 2188.

[40] S. Havriliak and S. Negami, *Polymer* **(**1967), p. 161.

[41] J. Evans, C. A. Vincent and P. G. Bruce, *Polymer* **(**1987), p. 2324.

[42] G. P. Pandey and S. A. Hashmi, *Journal of Power Sources* **(**2013), p. 211.

[43] J. R. Miller, In Proceedings of the Eighth International Seminar on Double Layer Capacitors and Similar Energy Storage Devices; *Deerfield Beach*, Florida Educational Seminars: Boca Raton, FL, 1998 (Dec 7 - 9, 1998).

[44] F. Lufrano, P. Staiti and M. Minutoli, *Journal of Power Sources* **(**2003), p. 314.

[45] A. Yu, I. Roes, A. Davies and Z. Chen, *Appl. Phys. Lett.* (2010), p. 253105.

[46] M. Nasibi, M. A. Golozar and G. Rashed, *Journal of Power Sources* **(**2012), p. 108.

[47] C. W. Liew, S. Ramesh and A. K. Arof, *Energy* **(**2016), p. 546.

[48] R. Kötz and M. Carlen, *Electrochimi. Acta* **(**2000), p. 2483.

[49] W. Lu, K. Henry, C. Turchi and J. Pellegrino, *J. Electrochem. Soc.* (2008), p. A361.

[50] G. P. Pandey, T. Liu, C. Hancock, Y. Li, X. S. Sun and J. Li, *Journal of Power Sources* **(**2016), p. 510.

[51] M. Suleman, Y. Kumar and S. A. Hashmi, *J. Solid State Chem.* (2015), p. 1347.

[52] S. Ferrari, E. Quartarone, P. Mustarelli, A. Magistris, M. Fagnoni, S. Protti, C. Gerbaldi and A. Spinella, *Journal of Power Sources* **(**2010), p. 559.

[53] W. Zhai, Y. W. Zhang, L. Wang, F. Cai, X. M. Liu, Y. J. Shi and H. Yang, *Solid State Ionics* **(**2016), p. 111.

[54] Y. S. Lee, W. K. Shin, J. S. Kim and D. W. Kim, *RSC Adv.* (2015), p. 18359.

[55] H. J. Ha, E. H. Kil, Y. H. Kwon, J. Y. Kim, C. K. Lee and S. Y. Lee, *Energy Environ. Sci.* (2012), p. 6491.

[56] K. Shono, T. Kobayashi, M. Tabuchi, Y. Ohno, H. Miyashiro and Y. Kobayashi, *Journal of Power Sources* **(**2014), p. 1026.

[57] R. E. Sousa, M. Kundu, A. Gören, M. M. Silva, L. Liu, C. M. Costa and S. Lanceros-Mendez, *RSC Adv.* (2015), p. 90428.

[58] A. Roy, B. Dutta and S. Bhattacharya, *RSC Adv.* (2016), p. 6543.

CHAPTER 6

CONCLUSIONS AND FUTURE SCOPE OF WORK

6.1 Conclusions

The above study is based on preparation of supercapacitors using EMIMTFSI as ionic liquid, LITFSI as salt and covalent organic frameworks (COFs) and subsequent fabrication of lithium-ion coin cell with the best possible electrolyte based on different characterization results. In this study P(VdF-HFP) was used as copolymer to make the gel polymer electrolytes.

The gel polymer electrolytes prepared for this study showed high thermal stability up to 340 ^{0} C, high ionic conductivity and electrochemical potential window of approximately 4.0 V, verifying their appropriateness for use in electrochemical devices. The ionic conductivity obtained from ac conductivity analysis for GPE-1, GPE-2 and GPE-3 electrolytes were found to be suitable for to be used for fabricating a supercapacitor. The reciprocal temperature dependence of ionic conductivity shows the Vogel-Tammann-Fulcher(VTF) behavior indicating charge carrier dynamics is strongly coupled with the segmental motion of polymer chain. The ac conductivity spectra show the common ions conduction and relaxation mechanism at different temperatures as well as for different compositions in a limited frequency range. The shape of Cyclic Voltammetry curves for all the fabricated supercapacitors was found to be almost box shaped at room temperature signifying exceptionally ideal and reversible capacitive characteristics of the fabricated supercapacitor cells. Large potential window, small internal resistance, high specific capacitance, and extended cycle stability indicate good electrochemical performance of the fabricated supercapacitor cells at room temperature.

For the lithium-ion coin cell fabricated with GPE -3 it has been observed that the specific capacity of the prepared lithium-ion coin cell for 1st cycle is 165.8 mAh g^{-1} at a constant current rate C/12 at ambient temperature. The discharge capacity for the lithium-ion coin cell remains 72.9% of the theoretical capacity of the cathode material after completion of the 20 th cycle. According to the findings, these gel polymer electrolytes have a great potential for application in various electrochemical devices. Additionally, the fabricated lithium-ion coin cell's performance indicates its suitability to be used in electrical devices.

6.2 Future scope of work

For the current study further research in the areas of dual ion batteries can be done to obtain high voltage and high energy density batteries. In addition, free volume measurement by Positron Annihilation Spectroscopy (PALS) can be conducted to study further which will provide the gateway for further research in the field of gel polymer-based electrolyte. Positron Annihilation Spectroscopy (PAS) is an experimental technique used to study the electronic structure and defects in materials. Gel polymer electrolyte-based supercapacitors, also known as gel polymer supercapacitors, have gained significant attention in recent years due to their potential to address the limitations of conventional supercapacitors. One of the main advantages of gel polymer supercapacitors is their ability to achieve higher energy densities compared to traditional supercapacitors. This is due to the unique properties of the gel polymer electrolyte, which allows for higher operating voltages and better charge storage capabilities. Ongoing research is focused on developing new polymer materials and optimizing the electrode-electrolyte interface to further enhance energy density. Gel polymer electrolytes are non-flammable and have better thermal stability compared to liquid electrolytes used in conventional supercapacitors. This makes gel polymer supercapacitors safer and more reliable, particularly in applications where safety is a critical concern, such as electric vehicles and portable electronics which can be an application of the study as mentioned in this work. The gel-like nature of the polymer electrolyte allows for the fabrication of flexible and even wearable supercapacitors. Researchers are working on developing cost-effective and scalable manufacturing processes for gel polymer supercapacitors. This includes exploring alternative materials, optimizing electrode designs, and improving fabrication techniques. Achieving cost-effectiveness and scalability is crucial for the widespread adoption of gel polymer supercapacitors in various industries. Hybrid energy storage systems combining gel polymer supercapacitors with batteries have the potential to provide high power density and high energy density simultaneously. These hybrid systems can find applications in electric vehicles, renewable energy storage, and other areas where both high power and high energy are required while gel polymer supercapacitors have shown promising results in laboratory settings, further research and development efforts are needed to overcome challenges related to material optimization, manufacturing processes, and system integration before they can be widely commercialized. However, the potential benefits of the sample the material which it is made

of gel polymer supercapacitors, such as improved energy density, safety, and flexibility, make them an attractive area of research for the future of energy storage technologies.

The future of lithium-ion coin cell batteries holds significant importance, particularly in the context of powering various compact electronic devices and applications. Researchers are continuously working on improving the energy density of lithium-ion coin cells, which means higher capacity and longer runtime for the same size or weight. This can be achieved through the development of new electrode materials, advanced electrolytes, and optimized cell designs. Safety is a crucial aspect of lithium-ion batteries, and coin cells are no exception. Future developments may involve the use of solid-state electrolytes or advanced separators that can enhance thermal stability and reduce the risk of short circuits or thermal runaway. Rapid charging is a desirable feature for many applications, and coin cells are expected to benefit from advancements in materials and charging technologies that enable faster charging rates without compromising cycle life or safety. Extending the cycle life of lithium-ion coin cells is an ongoing goal, as it directly impacts the overall lifespan and cost-effectiveness of devices powered by these batteries. Improvements in electrode materials, electrolyte compositions, and cell engineering can contribute to longer cycle life. Coin cells may find applications in emerging fields such as implantable medical devices, wireless sensor networks, or Internet of Things (IoT) devices, where their compact size, long life, and high energy density can be advantageous. In general, the future of lithium-ion coin cell batteries is likely to involve advancements in energy density, safety, charging speed, cycle life, and form factors, along with the exploration of new materials and manufacturing techniques to meet the evolving demands of various industries and applications.